Chemical tools to study NAADP: A novel calcium mobilising intracellular messenger

Brown, Richard Stephen

Award date:
2004

Awarding institution:
University of Bath

Copyright notice

Chemical tools to study NAADP, a novel calcium mobilising intracellular messenger.

Richard Stephen Brown

A thesis submitted for the degree of Doctor of Philosophy

University of Bath,

Department of Pharmacy and Pharmacology

November 2004

Signed.....

Date 24/01/2005

ProQuest LLC
789 East Eisenhower Parkway
P.O. Box 1346
Ann Arbor, MI 48106-1346

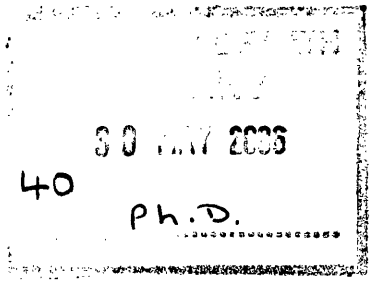
30 MAY 2006
40
Ph.D.

Abstract

Nicotinic acid adenine dinucleotide phosphate (NAADP) **3** has recently emerged as the most potent endogenous calcium mobilising, second messenger. NAADP **3** has been shown to be essential in many different cell types, ranging from mediating fertilisation in sea urchin eggs to the release of insulin from pancreatic β-cells. Therefore, a synthetic route was required to enable the formation of NAADP **3** and its analogues to explore its intracellular chemistry.

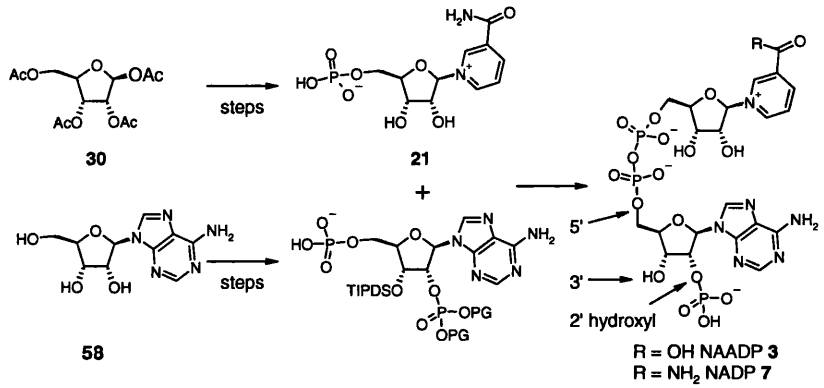

Our aim was to develop a flexible route to NAADP **3** that allowed modifications at key positions, ultimately leading to a range of biological probes. Achieving selective introduction of the 2′-phosphate onto suitably protected adenosine was key. The 5′-hydroxyl was then phosphorylated to afford the protected adenosine diphosphate precursor. Development of a synthetic route towards β-nicotinamide mononucleotide (β-NMN) **21** started from the tetra-protected ribose **30**. Activating the anomeric acetate to allow glycosylation to occur with *in-situ* protecting group cleavage afforded the mononucleoside precursor, which was selectively phosphorylated at the 5′-hydroxyl the afford β-NMN **21**. With the two phosphate precursors synthesised, development of a method towards pyrophosphate formation was undertaken. Reported yields for pyrophosphate formation are generally poor due to apparent purification difficulties, however activation with carbonyl diimidazole and purification on negative ion exchange resin afforded pleasing yields of around 60 %. Global deprotection to afford NADP **7** initially failed due to protecting group incompatibilities; however with protecting group alteration formation of NADP **7** was achieved. Enzymatic base-exchange with *Aplysia* ADP-ribosyl cyclase [E.C. 3.2.2.5] was achieved to afford the synthesis of NAADP **3**, which was proven active by biological assay. Analogues were formed using this scheme and evaluated.

Publications

Brown, R. S.; Dowden, J.; Moreau, C.; Potter, B. V. L. *Tetrahedron. Lett.*, **2002**, *43*, 6561-6562.

Dowden, J.; Moreau, C.; Brown, R. S.; Berridge, G.; Galione, A.; Potter, B. V. L. *Angew. Chem., Int. Ed. Eng.*, **2004**, *43*, 4637-4640.

Acknowledgments

I would like to thank Dr. James Dowden for providing me with the opportunity to undertake this research, and for his continuing energy and enthusiasm throughout the project. I would also like to thank Professor Barry Potter for his support during the course of my PhD.

I would like to express my gratitude to Dr. Christelle Moreau, who worked tirelessly with me on the synthesis and provided me with help and guidance throughout. I would also like the thank Dr. Charles Borissow for helpful discussions and practical guidance on techniques and principles within organic synthesis. Drs. C Moreau, S Bartlett and S Foster are also thanked for constructive criticism and proofreading of this thesis.

For their technical support I would like to thank Dr Steve Black for the NMR spectra, Mr. Chris Cryer for mass spectrometry and Mr. Kevin Smith for his technical support.

For the pharmacological evaluation presented here I would like to thank the group of Professor Antony Galione in the Pharmacology department at the University of Oxford.

Abbreviations

$[a]_D$	specific rotation at 589 nm
AMP	adenosine monophosphate
ATP	adenosine 5′-triphosphate
β-NAD	β-nicotinamide adenine dinucleotide
β-NADP	β-nicotinamide adenine dinucleotide phosphate
β-NaMN	β-nicotinic acid mononucleotide
β-NMN	β-nicotinamide mononucleotide
BSA	*N,O-bis*(trimethylsilyl) acetamide
cADPR	cyclic adenosine 5′-diphosphate ribose
cAMP	cyclic adenosine monophosphate
CDI	carbonyl diimidazole
CICR	calcium induced calcium release
CSO	(1*S*)-(+)-(10-camphorsulphonyl) oxaziridine
d	doublet (spectral)
DAG	diacylglycerol
DBU	1,8-diazabicyclo[5.4.0]undec-7-ene
DCC	N-N′-dicyclohexylcarbodiimide
dd	double doublet (spectral)
DMAP	4-dimethylaminopyridine
ER	endoplasmic reticulum
GDP	guanosine 5′-diphosphate
GPN	glycyl-phenylalanine 2-naphthylamide
GTP	guanosine 5′-triphosphate
HPLC	high performance liquid chromatography
Hz	hertz
$Ins(1,3,4,5)P_4$	inositol-(1,3,4,5)-tetrakisphosphate
$Ins(1,4,5)P_3$	inositol-(1,4,5)-trisphosphate
$Ins(1,4,5)P_3R$	inositol-(1,4,5)-trisphosphate receptor
J	coupling constant (in NMR)

Lit	literature (reference)
m/z	mass to charge ratio (mass spectrometry)
*m*CPBA	*meta* chloroperoxybenzoic acid
mp	melting point
MS	mass spectrometry
NAAD	nicotinic acid adenine dinucleotide
NAADP	nicotinic acid adenine dinucleotide phosphate
NAADPH	reduced nicotinic acid dinucleotide phosphate
NADPH	reduced nicotinamide dinucleotide phosphate
NDC	1-(2,4-dinitrophenyl)-3-carbamoyl-pyridinium chloride
NMR	nuclear magnetic resonance
PI(3)K	phosphatidyl-3-OH kinase
PLCβ	phospholipase C-β
PLCγ	phospholipase C-γ
PM	plasma membrane
PMCA	plasma membrane calcium ATPase
ppm	parts per million (in NMR)
PtdIns(4,5)P_2	phosphatidylinositol-(4,5)-P_2
R_F	retention factor (TLC)
ROC	receptor-operated channels
R_T	retention time (HPLC)
RYR	ryanodine receptor
s	singlet (spectral)
SAR	structure activity relationship
SERCA	sarco endoplasmic reticulum calcium ATPase
SOC	store-operated channels
SR	sarcoplasmic reticulum
t	triplet (spectral)
TBAF	tetrabutylammonium fluoride
TEAB	Tetrabutylammonium bicarbonate
TFA	trifluoroacetic acid
TFAA	trifluoroacetic anhydride

TIPDS	tetraisopropyldisiloxane
TLC	thin layer chromatography
TMG	tetramethylguanidine
TMS	trimethylsilyl
TMSCN	trimethylsilyl cyanide
TMSOTf	trimethylsilyl trifluoromethanesulfonate
UMP	uridine 5'-monophosphate
VOC	voltage-operated channels

Table of contents

Chapter Four

Chapter Five

Chapter Six

Chapter Seven

Chapter One

Introduction

The versatile role of calcium

1.1 Overview of calcium signalling

Calcium is a ubiquitous intracellular messenger that controls a diverse range of cellular functions. Calcium is versatile, playing a pivotal role in cellular processes such as controlling fertilisation, gene transcription, muscle contraction, cell proliferation and secretion of bioactive compounds (Figure 1).[1-4] These processes occur despite the fact that calcium is highly toxic, causing necrosis and programmed cell death (apoptosis).[1,3,5] How calcium orchestrates these specific processes at the cellular level is the subject of intense study, but can be rationalised by the ability of the signal to be modulated in terms of speed, amplitude and spatio-temporal patterning.[3]

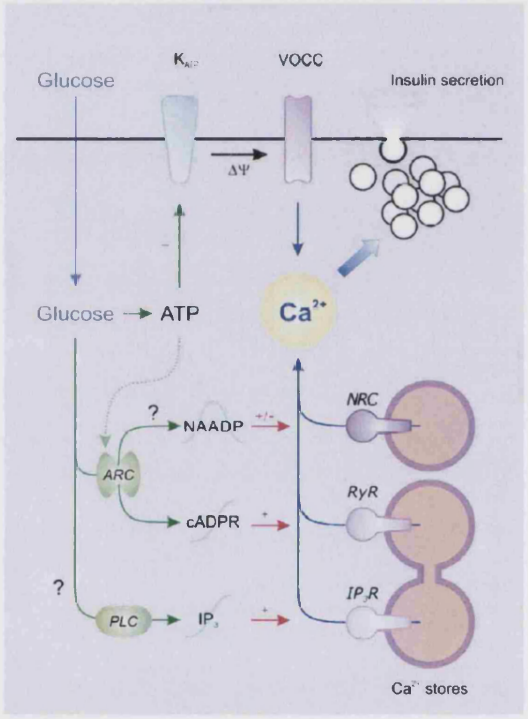

Figure 1: Overview of the effect of insulin release mediated by calcium in response to external stimuli.

Resting cells possess a calcium concentration of 100 nM, however stimulation elevates this level to around 1000 nM.[2,3] The intracellular concentration is finely controlled by an extensive repertoire of signalling components, which when stimulated, activate the 'on' mechanisms, to cause a gradient driven influx of calcium

into the cytoplasm (1-2 mM extracellular concentration). As a messenger, calcium activates a series of dependent processes before finally, the 'off' mechanism re-establishes the resting state by pumping calcium into stores (Figure 2).[3] The 'on' mechanisms include channels located on the plasma membrane (PM) to regulate the supply of calcium from the extracellular space and channels located on the endoplasmic or sarcoplasmic reticulum (ER/SR) to control the internal movement from selected organelles. Calcium can only travel a short distance within the cytoplasm due to rapid binding to various buffers such as parvalbumin, calbindin-D_{28K} and calretinin allowing tight control over movement around the cytoplasm.[5] Release can therefore either be confined to a specific spatial region (*e.g.* the secretory pole of an acinar cell) or can be cell wide, propagating a wave that spreads through the entire cytoplasm (*e.g.* egg fertilisation by sperm). The 'off' mechanism functions to remove calcium from the cytoplasm through either, plasma membrane calcium ATPase (PMCA) pumps and sodium/calcium exchangers to extrude calcium into the extracellular domain or, sarco-endoplasmic reticulum calcium ATPase (SERCA) pumps to internally store calcium in selected organelles. Mitochondria play an important role in this regulation by having a low affinity, yet high capacity, rapid calcium uniporter to significantly reduce the cytosol concentration, while allowing slow release back into the cytosol during the recovery phase. Due to their low sensitivity to calcium, mitochondria function more effectively when closely linked to calcium releasing channels that allow reciprocal interaction with the ER/SR. This diversity enables the huge variability in role and function in the signals recorded within different cell types.

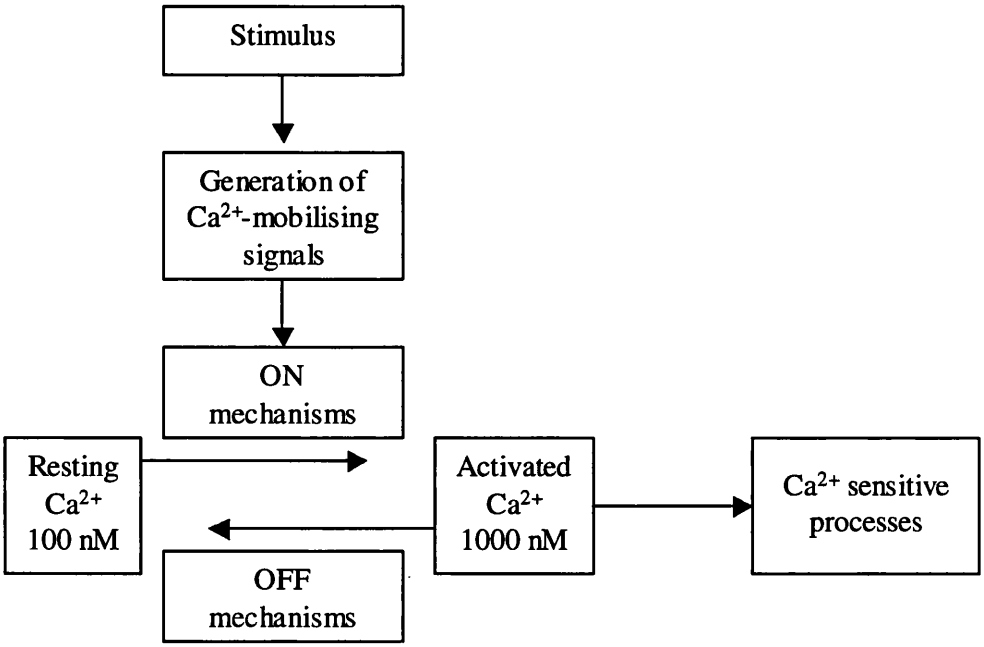

Figure 2: The units of the calcium signalling network to generate the ON signal causing down stream events. The response in terminated by the off signal.

There are three main types of channel responsible for the external influx of calcium into the cell. All produce a local effect due to brief opening times and the action of calcium chelating proteins, but only two of these are well documented.[2,3,5] Most is known about *voltage-operated channels* (VOC's) that respond to transient membrane depolarisation and *receptor-operated channels* (ROC's), that are often coupled to G-proteins. Downstream calcium release in ROC's is normally in response to external stimuli such as, vasopressin, acetylcholine and ATP. There is also a third class, of uncertain identity, that respond to internal store depletion called *store-operated channels* (SOC's).[3]

VOC's are found mainly on excitable cell types including neuronal and muscle cells, where activation is a result of depolarisation of the PM. These channels are comprised of five main subunits, but an array of isoforms of these subunits allows many different possibilities that are conventionally characterised by their different gating properties and pharmacology.[2] VOC's increase calcium concentration in the muscle cytosol, either as a result of direct influx through the channel, or downstream activation of a channel embedded in the SR. Neuronal activation comprises many different sub-types of VOC found either at the synapse to trigger exocytosis of neurotransmitters, or along the dendrite to induce gene transcription leading to memory and learning.[3]

ROC's comprise a wide range of structurally diverse channels, which all rely on the activation by external stimuli. ROC's include the N-methyl-D-aspartame receptor, which in neurons, is responsible for early synaptic modifications that result in learning and memory.[3] These channels either directly allow gradient driven influx of calcium, or are coupled to G-proteins, generating the release of small, water soluble second messengers that rapidly diffuse across the cytosol, bind to receptors on the ER/SR, and thus initiate the calcium release.

SOC's respond to depletion of intracellular stores of calcium, however what is unclear is the manner in which this occurs. The ability of the SOC to 'sense' calcium levels has led speculation towards a coupling between calcium entry channels on the PM and release channels on the ER/SR. Since depleting cell calcium pools has been shown to enhance calcium entry, these SOC's may be the most ubiquitous of the PM calcium channels.[2]

It is at these PM bound receptors where the variety of drugs altering calcium release act. They have been used to treat a variety of conditions such as high blood pressure, cardiac dysrhythmias and angina. By working to inhibit calcium influx into cells they promote the relaxation of the blood vessels (*e.g.* nifedipine), or they reduce the workload of the heart by making it less excitable (*e.g.* verapamil). Both of these drugs provide very effective treatment, yet for the ubiquity of calcium, this is one very small area of medicine.

The calcium signal can also be derived from internal stores mediated by an array of distinct, messenger-activated channels located on either the ER, or, the SR in muscle cells. Release from these internal stores is initially a result of the messenger, but quickly escalates due to calcium induced calcium release (CICR). There are various channels controlled by this mechanism of which the inositol-1,4,5-trisphosphate receptor ($InsP_3R$) and ryanodine receptor (RYR) have been extensively studied.[2-4] This release is initiated by external stimuli binding to cell surface receptors causing the synthesis of second messengers, which diffuse across the cell before binding to their respective receptor on the ER/SR. Two such second messengers are inositol-1,4,5-trisphosphate ($Ins(1,4,5)P_3$) **1** and cyclic ADP-ribose (cADPR) **2** (Figure 3), which act on the $InsP_3R$ and RYR respectively. Although $InsP_3R$'s require $Ins(1,4,5)P_3$ **1** to open, their activity is modulated by the concentration of calcium in the neighbouring cytosol and release is enhanced by a modest cytosolic calcium

concentration (0.5–1 μM) *via* CICR, however large calcium concentrations (>1 μM) inhibit opening.[2] RYR are structurally and functionally similar to $InsP_3R$, however they are activated and inhibited by higher concentrations of calcium (1–10 μM: >10 μM). RYR are located mainly in excitable cells such as muscle or neurons, unlike $InsP_3R$, which are universally expressed throughout mammalian tissues.[2]

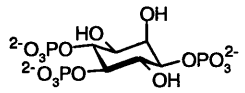

1 - Ins(1,4,5)P_3

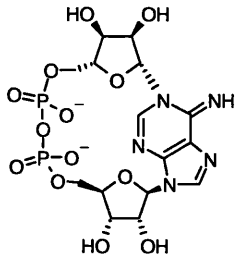

2 - cADPR

Figure 3

The apparent wave of calcium that sweeps across the entire cell has been attributed to CICR, such as that observed during oocytes fertilisation. At low levels of stimulation individual Ins(1,4,5)P_3R's or RYR's open to release calcium characterised as either a 'blip' or a 'quark'. Further stimulation causes clusters of channels to open with the resultant release of either a 'puff' or a 'spark', which can then develop into a self-propagating wave. Gap junctions allow the calcium waves to bridge the space between separate cells to generate *inter*cellular waves, however the exact mechanism of this is unclear. What is apparent is that this allows many cells to function as one, for example, the wave stimulates lung epithelial cells to beat their cilia in tandem to expel inhaled contaminants.[3]

Other messengers have been studied, namely the sphingolipids, cyclic AMP (cAMP), cyclic GMP (cGMP) and nicotinic acid adenine dinucleotide diphosphate (NAADP) **3**. The properties of the sphingolipid receptors bear no similarities to those of Ins(1,4,5)P_3 or RYR and even though they are expressed in many different cell tissues the physiological function of this channel is poorly understood. Upon external stimulation, AMP and GMP are modified by adenyl and guanyl cyclase respectively to form either cAMP or cGMP, which is intimately linked to calcium concentration through its action on channels and pumps. With calcium concentrations initiating both a positive and negative feedback mechanism, depending on which isoform of adenyl cyclase is acted upon, tight regulation of further cAMP/cGMP synthesis can be

achieved. NAADP **3** is emerging as a novel and highly potent mobilising agent of calcium that is only just beginning to be understood. It has been shown to act as a second messenger, but the identity of its receptor is still a topic of huge debate. NAADP **3** will be discussed at far greater depth later in this chapter, however the actions of the sphingolipids, cAMP and cGMP will not be further elaborated.

1.2 Intracellular calcium signalling – Ins(1,4,5)P_3

External stimuli, such as hormones, interact with PM bound, G-protein coupled receptors or tyrosine kinase linked receptors to induce downstream events, mediated by calcium. G-protein coupled receptors allow the activation of a trimeric (α, β and γ) Gq-protein, resulting in the exchange of GDP for GTP in the α subunit and subsequent dissociation of the α subunit from the βγ subunit. This α subunit then activates phospholipase C-β (PLCβ) to cleave membrane bound phosphatidylinositol(4,5)P_2 (PtdIns(4,5)P_2) **4** generating water soluble Ins(1,4,5)P_3 **1** and lipid soluble diacylglycerol (DAG) **5** (Scheme 1).

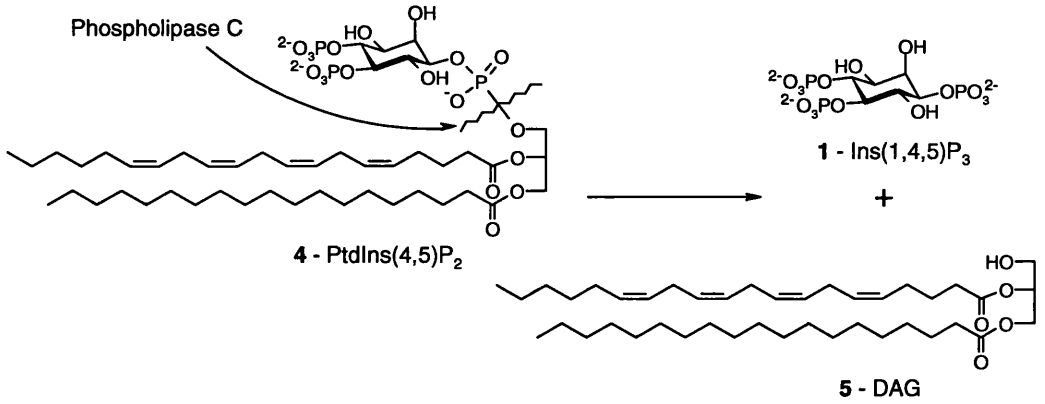

Scheme 1: Hydrolysis of PtdIns(4,5)P_2 **4** to Ins(1,4,5)P_3 **1** and DAG **5**.

Tyrosine kinase linked receptors dimerize in response to stimuli, to allow ATP mediated autophosphorylation of intracellular tyrosine residues. In turn the Src homology region 2 domain of phospholipase C-γ (PLCγ) binds to the receptor, initiating activation of PLCγ *via* phosphorylation. Once activated, cleavage of PtdIns(4,5)P_2 **4** to Ins(1,4,5)P_3 **1** and DAG **5** occurs in the same way as shown in Scheme 1. The pathways then split into two branches, both playing crucial roles. Ins(1,4,5)P_3 **1** rapidly migrates across the cytoplasm of the cell where it binds to

$InsP_3R$'s on the surface of the ER/SR to initiate calcium release. $Ins(1,4,5)P_3$ **1** does however have a short lifespan, in the order of seconds before being either phosphorylated or de-phosphorylated by enzymes. Addition of a phosphate group is mediated by the calcium dependant kinase, phosphatidyl-3-OH kinase (PI(3)K), to generate inositol-1,3,4,5-tetrakisphosphate ($Ins(1,3,4,5)P_4$), which although its exact mechanism is unclear, does bind a specific GTPase-activating protein of the Ras family modulating further calcium release.[2] Some cellular responses initiated as a result of $Ins(1,4,5)P_3$ **1** calcium release are collated in Table 1.

Target Tissue	Signalling Molecule	Major Response
Smooth muscle	Acetylcholine	Contraction
Blood platelets	Thrombin	Aggregation
Hippocampus	Acetylcholine	Memory
Endocrine glands	Acetylcholine	Secretion
Mast cells	Antigen	Histamine secretion

Table 1: Overview of some cellular responses to $Ins(1,4,5)P_3$ **1**.

The second product of the hydrolysis of $PtdIns(4,5)P_2$ **4**, DAG **5** exerts different effects. First, the fatty acid chain can be cleaved, releasing arachidonic acid, which can undergo further modifications to achieve the eicosanoids. Second, and more importantly, a small rise in intracellular calcium associated with $Ins(1,4,5)P_3$ causes C-kinases (serine/threonine protein kinases) to translocate from the cytosol to the cytoplasmic face of the PM. Once achieved, stimulation with DAG **5** and calcium enables these kinases to phosphorylate selected serine or threonine residues on target proteins within the cell. Due to the rapid metabolism of DAG **5** it cannot sustain the required C-kinase activation for long term responses such as cell proliferation, therefore a secondary wave of DAG **5** is generated from the hydrolysis of PM bound phosphatidylcholine.

1.3 Intracellular calcium signalling – cADPR

Although $Ins(1,4,5)P_3$ **1** appears to operate as a universal calcium mobilising agent,[3] it was considered that there may well be other messengers that operate within cells. Experiments using a robust sea urchin egg model showed the presence of other

calcium release mechanisms, which enhance and differentiate the signal, regulated by a family of pyridinium based nucleotide metabolites. By injection of NAD **6** and NADP **7**, calcium release could be observed in microsomal egg fractions that were devoid of $Ins(1,4,5)P_3$ **1**.[6] This calcium efflux was observed from vesicles previously loaded by calcium ATPase's, with the effect of NAD **6** seen as a cellular calcium release after a substantial delay, but NADP **7** appeared to initiate an immediate and potent calcium emmision.[7] Interestingly, calcium release initiated by addition of NAD **6** was only observed in a batch of Percoll purified microsomal fractions, incubated with supernatant or cytosol fractions from the same Percoll gradients, suggesting the requirement for a second soluble factor to enable the calcium release to occur.[7] Two co-factors were in fact isolated to enable NAD **6** to produce calcium release. First was an enzyme responsible for the conversion of NAD **6** into the active metabolite, which was later identified as cADPR **2**,[8] the second, was calmodulin, that confers cADPR **2** sensitivity.[9] The instantaneous effect due to NADP **7** will be discussed in greater detail later in the chapter. These initial experiments lead a challenge to rationalise the exact structure and mechanism of action of this metabolite of NAD **6**. Isolation and mass spectrometry of the product revealed that the structure was smaller than ADP-ribose by one water molecule, and in the same way that cAMP is 18 units lighter than AMP, it was recognised that this structure had in fact cyclised (Scheme 2).[10,11]

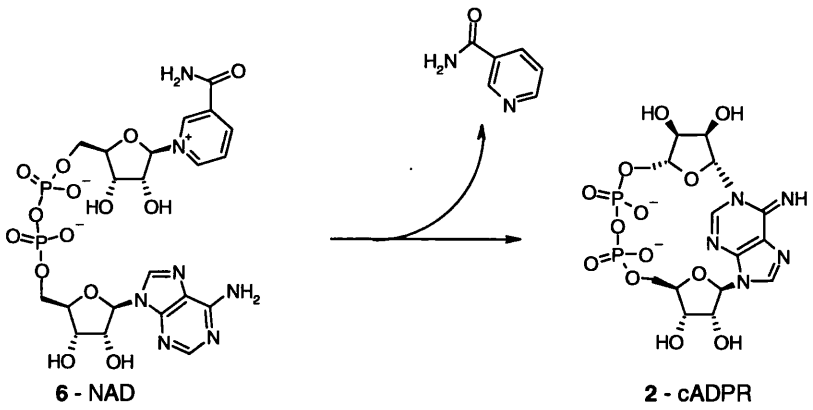

Scheme 2: Cyclisation of NAD **6** into cADPR **2** with NADase.

Clarification of the enzyme responsible for this conversion was then required. An endogenous NADase [E.C. 3.2.2.5] was known to hydrolyse NAD **6** into ADP-ribose, but generating an inactive metabolite from a crucial redox co-enzyme was considered

wasteful and thus not the only role for the enzyme. NADase was shown to catalyse the formation of cADPR **2** from NAD **6** with such efficiency to cause complete exhaustion of the endogenous cADPR calcium stores.[12] As it was clear that this enzyme, purified from *Aplysia* ovotestis, produced cADPR **2** and not ADP-ribose, it was named ADP-ribosyl cyclase. In an effort to identify if there was a homologous enzyme in the mammalian system, searching of the GenBank database revealed two possibilities, CD38 and CD157, both of which are mammalian antigens.[13] They were shown to possess 30 % sequence homology with the *Aplysia* ADP-ribosyl cyclase and are both capable of producing cADPR **2** from NAD **6** and interestingly, CD38 can also hydrolyse cADPR to ADP-ribose. This suggests an inhibitory role of ADP-ribose in channel modulation in eggs and smooth muscle cells,[2,11] which is similar to Ins(1,4,5)P_3 **1** in that the metabolite, Ins(1,3,4,5)P_4 has a cellular function. CD38 was first isolated as a surface antigen on lymphocytes, but has since been shown to be present in many other tissues including the eye and brain. Not only is it found on the cell surface but also within selected organelles. There is however speculation that cADPR **2** is formed in the extracellular space by PM CD38. Transportation of NAD **6** to the extracellular space may be *via* a conexin 43 hemichannel where it can then undergo CD38 (ADP-ribosyl cyclase) catalysed conversion and translocation to the intracellular space.[2,14] Regardless of where cADPR **2** is synthesised, comparison of CD38 knockout mice and wild-type mice has proven that *in-vitro* cADPR **2** synthesis is massively impaired without the enzyme.[15]

Experiments have shown that cADPR **2**, when injected into sea urchin eggs, does release calcium by activation of ryanodine receptors (RYR) located on the endoplasmic reticulum (ER).[2,13] Characterisation of this receptor has shown it to be a large homotetrameric calcium release channel that is widely distributed among many cell types.[7] cADPR **2** induced calcium release is independent to that of Ins(1,4,5)P_3 **1**, because treatment with the Ins(1,4,5)P_3 **1** antagonist heparin does not desensitise the response to cADPR **2**. Antagonism is achieved by high concentrations of ryanodine (~100 μM) with millimolar concentrations of caffeine acting as an agonist.[2] cADPR **2** plays an important role in mediating calcium induced calcium release (CICR) by sensitising the RYR to sub-micromolar levels of calcium, thus increasing the frequency of the 'sparks' leading to formation and propagation of the wave. Many

agonists of the cADPR **2** pathway are found to be cell permeant, such as nitric oxide, glucose and vitamin B_{12}; however, cell impermeant agonists can act through interaction with the surface receptor. This is observed during activation of the T-cell/CD3 complex by the OKT3 antibody and also in longitudinal intestinal muscles by cholecystokinin, both causing calcium influx, stimulating ADP-ribosyl cyclase activity to elevate cADPR **2** levels.[13] Alternative evidence however, suggests that activation of the cyclase may be a result of coupling to a G-protein as stimulation with a cell surface muscarinic agonist induces a 2-to 3-fold increase in cyclase activity that is inhibited with cholera toxin.[13] This is in marked contrast to Ins(1,4,5)P_3 whereby all activation appears to be *via* cell surface stimulation. This would suggest that the cell has employed two separate calcium messengers to distinguish between permeant and impermeant signals. There is however a conflicting report that cADPR **2** may not actually be an intracellular messenger as appreciable levels of cADPR exist in cells that do not express RYR's. This evidence may suggest that cADPR is a general regulator of calcium signalling, or possesses secondary roles discrete from calcium release.[2]

A brief overview of the main functions of cADPR **2** is shown in Table 1.

Stimulus	Receptor	Cell	Response
Acetylcholine	Muscarinic	Tracheal smooth muscle	Contraction
Anti-CD3 mAb	TCR/CD3	Jurkat	T cell activation
Cholecystokinin (CCK)	CCK_A	Pancreas: acinar cell	Secretion
Glucose	Glucose kinase	Pancreas: β cell	Insulin secretion

Table 2: Overview of cADPR **2** activation pathways.

1.4 Intracellular calcium signalling – NAADP

Experiments injecting NADP **7** into sea urchin egg homogenate interestingly caused significant and rapid calcium release. This suggested that unlike NAD **6**, enzymatic modification was not required and once analysed and separated by HPLC it became apparent that the release was in fact caused by a minor contaminant and not by NADP **7**.[6] Difficulties came when trying to decipher the structure, as ^{1}H NMR spectroscopy generated a spectrum for NAADP **3** that was hardly distinguishable from that of NADP **7**. Mass spectrometry did show that the structure was one mass unit heavier,

but it was not until eight years later that the structure of NAADP **3** was published (Scheme 3).[16,17] Amazingly, this single functional group inter-conversion from amide to acid confers total specificity for the system as NADP **7** is completely inactive. Until that time, pyridinium based nucleotides were only thought to be involved in redox biochemistry, whereby the pyridinium ring is reduced to afford NADPH, whose primary role is to reduce fatty acids during their biosynthesis. Exploration was then performed to further understand its biological synthesis and significance.

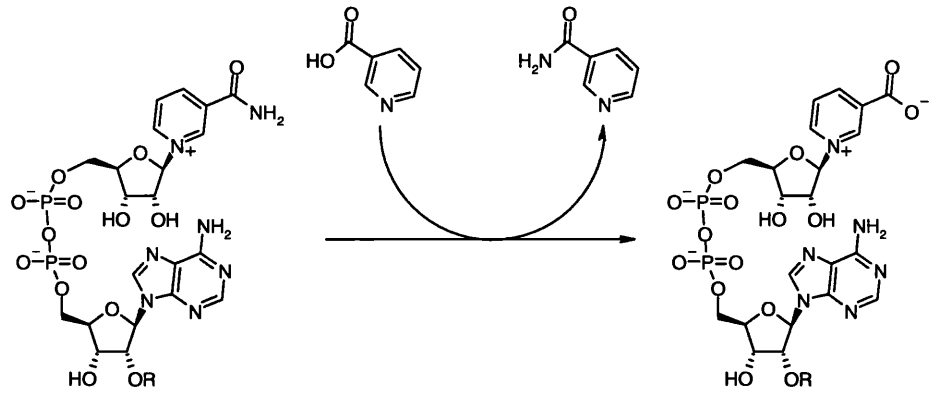

6 - R = H NAD
7 - R = PO_3H^- NADP

8 - R = H NAAD
3 - R = PO_3H^- NAADP

Scheme 3: Published structure and proposed mechanism of synthesis for NAADP **3**.

ADP-ribosyl cyclase [E.C. 3.2.2.5] from *Aplysia california*, homologous with CD38 had already been shown to catalyse the cyclisation of NAD **6**, but it was also able to cyclise NADP **7** to produce cADPR-phosphate **10**.[1] Interestingly, this enzyme is also able to catalyse the replacement of nicotinamide for nicotinic acid at acidic pH. This base-exchange can be used to convert NAD **6** into NAAD **8** and NADP **7** into NAADP **3** (Scheme 3). This enzymatic synthesis of NAADP **3** is the only proposed mechanism for *in-vivo* formation, however *in-vitro* studies require high concentrations (mM) of nicotinic acid to be present with a pH of 4-5, which in cells is normally only observed in the lysosomes. It is also possible to drive the reverse reaction by exposing the cell to large quantities of cell permeable nicotinamide (IC_{50} ~1.5 mM), thus achieving product inhibition by re-generation of β-NADP **7**. Some feel that these reaction conditions are unlikely to exist within the cell and have speculated on the involvement of an NAAD kinase,[14,16,17] or NADP **6** deaminase,[17] although such enzymes are yet to be reported. A recent report using CD38 knockout mice supports the theory that CD38 is responsible for NAADP **3** synthesis. Analysis of brain tissue

homogenate from these animals showed that CD38 -/- tissue was unable to support NAADP **3** synthesis from NADP **7**, although it is recognised that this does not categorically prove that the base-exchange reaction occurs *in-vivo*, it merely proves that CD38 is required for *in-vitro* NAADP **3** synthesis from NADP **7** using brain homogenate.[15] Indeed, in this study, little attention is paid to non-base-exchange reactions.

NAADP **3** appears to interact with receptors that are discrete from those activated by Ins(1,4,5)P_3 **1** and cADPR **2** in sea urchin egg homogenates.[18] It has also been found to be the most potent agonist of calcium channels with ranges of 10-100 nM stimulating the largest calcium signal. Interestingly, high concentrations (> 1-100 μM) fail to cause any detectable calcium release[1] and sub-threshold concentrations totally desensitise sea urchin egg homogenates, such that subsequent challenge with maximal concentrations (10-100 nM) evoke no response.[1,18,19] In other cell types such as rat brain, rat pancreatic acinar cells and T-cells activation occurs at approximately 1 μM, 50 nM and 100 nM (maximum) respectively. Inactivation also occurs with pancreatic cells and T-cells at 1-100 μM and 10 μM respectively, yet no inactivation at sub-threshold concentrations is observed.[20]

Experiments using radiolabelled [^{32}P] NAADP showed that binding, and hence retention of radioactivity was only observed in preparations where calcium release occurred. Once bound it was unaffected by either subsequent exposure to non-labelled NAADP, change in pH, or the presence of high calcium concentrations (10 mM).[19] This corroborates the theory of irreversible binding, which may be linked to the self inactivation[21] allowing speculation that, at least in sea urchin eggs, there is a possible 'one shot' calcium release mechanism, employed during fertilisation.[19] [^{32}P] NAADP binding was inhibited by NaCl in a completely reversible, and concentration dependant manner (0.5-1 M NaCl for a 25-75 % reduction),[19] and NaCl was able to reverse the inhibitory effect caused by sub-threshold NAADP **3** concentrations in sea urchin egg homogenates allowing maximal binding when re-exposed to [^{32}P] NAADP.[22] How this novel pathway interacts in the overall signalling cascade is still under intense scrutiny.

1.5 The synergy of calcium release

It is speculated that there is a close relationship between all three calcium release mechanisms and the term 'channel chatter' has been used to describe this. In pancreatic acinar cells and sea urchin eggs NAADP **3** acts to trigger the calcium response, which is subsequently propagated by $Ins(1,4,5)P_3$ **1**, and cADPR **2**, by CICR. However inhibition of either $Ins(1,4,5)P_3$ **1** or cADPR **2** blocks the NAADP **3** response in acinar cells (Figure 4(a)), yet in urchin eggs both receptors require inhibition suggesting a redundant pathway in that cell line (Figure 4(b)). Interestingly, in sperm cells and T-cell/CD3 complexes it seems to be more complicated whereby the NAADP receptors interlink with $Ins(1,4,5)P_3R$ in sperm and both $Ins(1,4,5)P_3R$ and RYR in T-cells.

Clearly the precise mechanism of coupling is still very poorly understood,[1] but whether NAADP **3** does actually address a discrete calcium pool has still not categorically been proven. Experiments revealed that NAADP **3** can still cause calcium mobilisation after inhibition of calcium ATPase pumps by thapsigargin, which drains the ER calcium stores sensitive to $Ins(1,4,5)P_3$ **1** and cADPR **2**. This shows that NAADP **3** does not mobilise calcium from the ER[21,23] and later studies suggest that calcium is released from lysosome related organelles in sea urchin eggs, which will be discussed later.[1,24] However a type 2 RYR from dog heart incorporated into a lipid bilayer showed a response to NAADP **3**, although it should be acknowledged that the concentration was 100 times higher than previously reported for other systems. These findings may indicate that the NAADP receptor is an accessory protein, which binds to a known channel on the ER rather than an actual novel intracellular channel.[14]

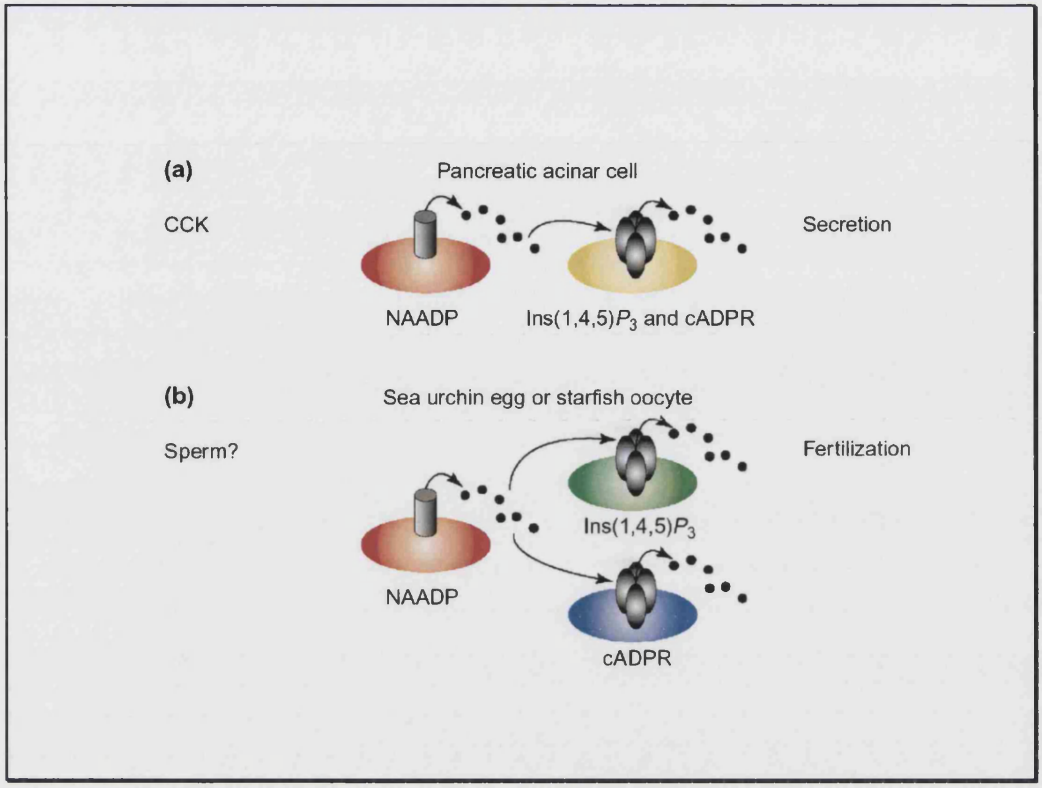

Figure 4: The effect of channel chatter in pancreatic acinar cells and sea urchin egg oocytes.

There is evidence of spatial separation between stores activated by NAADP **3** and those by Ins(1,4,5)P_3 **1** and cADPR **2** found in starfish oocytes. Uniform photolysis of oocytes and pancreatic acinar cells preloaded with caged NAADP **3** showed a highly localised release of calcium in the region of the cortex and apical pole respectively, which would suggest a fine-tuned signal for a specific function. However, localised photolysis of caged NAADP **3** in sea urchin eggs produced a wave that propagated across the entire cell.[13,25] There are however differences noted in starfish oocytes with a fluorescent halo, restricted to the cytosol, which rapidly decays when the NAADP is locally uncaged in *Astropecten aurantiacus* cells.[12] However, the wave initiated by activation of Ins(1,4,5)P_3R, does eventually spread across the cell it just requires a longer time.

1.6 Tissues responsive to NAADP

Not as many cell systems have been identified as being responsive to NAADP **3** compared to those of cADPR **2**. Table 3 lists a large selection of the systems where NAADP **3** has been shown to be required.

Cell or tissue	NAADP effect	Effective concentration
Cauliflower	Inactivation Activation	3 nM 1 μM
Sea urchin egg	Inactivation Activation	<1 nM (IC_{50} = 200 pM) >3 nM (EC_{50} = 25 nM)
Starfish oocytes	Activation	< ~1 μM
Frog neuromuscular junction	Activation	10 μM – 1 mM; liposomal delivery
Rat brain	Activation	EC_{50} = 1 μM
Rat pancreatic acinar cells	Inactivation Activation	1-100 μM 50 nM
Rabbit heart	Activation	320 nM
Human T-lymphocytes (Jurkat)	Inactivation Activation	10 μM EC_{50} = 50 nM
Pancreatic β cells	Activation	~ 100 nM

Table 3: Overview of cells responsive to NAADP **3**.[20]

The mechanism of calcium release mediated by NAADP **3** has been extensively studied in a variety of cell types. NAADP **3** was first shown to mobilise calcium from sea urchin eggs[16,17] and has since been shown to initiate and co-ordinate calcium signalling pathways.[1]

Sea urchin eggs

Sea urchin eggs have become widely used as a tool for the investigation of calcium release as they can be produced in relatively large batches and possess multiple signalling mechanisms for calcium release, that are easily manipulated.[26] In this way using caged compounds in combination with confocal microscopy, identification of the organelles targeted by NAADP **3** was obtained.[24] It was shown that organelles disrupted *via* osmotic lysis using glycyl-phenylalanine 2-naphthylamide (GPN, 100 μM), a substrate of the lysosomal exopeptidase cathepsin C, produced a significantly smaller rise in calcium when subjected to photo-activated NAADP **3**.[24] Lysosomes were fluorescence labelled with the targeted dye LysoTracker Red, whereupon introduction of GPN caused dissipation of the fluorescence, confirming their lysis. In contrast to this, GPN did not reduce the amount of calcium released by either

Ins(1,4,5)P_3 **1** or cADPR **2**, suggesting that GPN-mediated disruption of lysosomes selectively reduces the response to NAADP **3**.[24] It is known that protons are actively pumped into lysosomes through ATPase pumps and it is this gradient which drives the influx of calcium *via* a proton/calcium exchange pumps.[24] Bafilomycin A1 is a useful tool as it disrupts calcium storage through inhibition of the proton ATPase pump, which manifests itself as a reduced calcium release in response to NAADP **3** activation, for example, during fertilisation.[25]

Fertilisation of the egg elicits a cell wide calcium wave, stimulating the initiation of cell division and eventual maturation.[13] This can be visualised in Figure 5 by the localised photorelease of caged NAADP **3**.

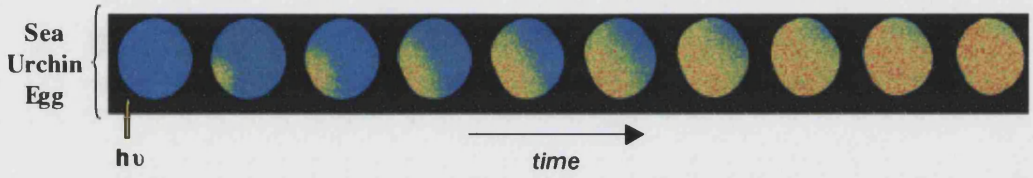

Figure 5: Propagation of the calcium wave in a sea urchin egg upon localised photorelease of NAADP **3**. The calcium released is visualised by its chelation to the fluorescent dye, Fluo-3.

Until recently it was believed that immediately after fertilisation, the egg synthesised NAADP **3** or released it from a store to initiate the initial calcium release that eventually propagated across the entire cell as a wave by CICR.[1,21] A recent study using the eggs of *Lytechinus pictus* (a sea urchin) showed binding of the spermatozoa to the egg plasma membrane (PM), may present a separate compartment containing NAADP **3**. As a result, it was postulated that release of the sperm cytosol into the egg donated not only nuclear material, but also a locally high concentration of NAADP **3**, which initiated the wave.[22] There is however some contradictory evidence to suggest that the spermatozoa interacts with a NAADP receptor at the PM to initiate the synthesis of NAADP **3**, however no such receptor has been isolated, yet NAADP **3** has been characterised in spermatozoa.[22] Experiments revealed that egg homogenates pre-treated with sperm extract, or with an inhibitory concentration of NAADP **3** did not bind radiolabelled [^{32}P] NAADP. Furthermore, NAADP **3** and sperm extract were unable to displace radiolabelled [^{32}P] NAADP, but high salt concentration could displace both.[22] These findings are consistent with the theory that spermatozoa

contain NAADP **3**. It was also speculated that the base-exchange reaction was responsible in the spermatozoa for the conversion of NADP **7** to NAADP **3** (Scheme 3) as the absence of nicotinic acid inhibited its formation. The base-exchange reaction was time and pH dependent with maximal production after one hour and at pH 5, consistent with enzymatic formation.[22] This evidence strongly suggests a role for NAADP **3** as an initiator of a cell wide calcium wave, once it is released into the cytosol of the egg during fertilisation. This in turn initiates downstream events leading to maturation of the cell.

T-cells

T-cell proliferation in response to an antigen has been attributed to activation of the T-cell/CD3 complex. This complex has been shown to elicit a fast increase in calcium caused by Ins(1,4,5)P_3 **1**, followed by a sustained response mediated by cADPR **2**.[13,27] It is now emerging that NAADP **3** is closely linked to this activation pathway, but unlike sea urchin eggs, NAADP **3** at sub-threshold concentrations (10 nM) does not cause inactivation, but instead initiates low-amplitude calcium spikes.[27] Stimulation with optimal concentrations (50 – 100 nM) triggered CICR from Ins(1,4,5)P_3 **1** and cADPR **2** stores. Interestingly, high concentrations (>10 μM) were self-inactivating, abolishing the calcium release arising from subsequent stimulation *via* the activated T-cell/CD3 complex, or Ins(1,4,5)P_3 **1** and cADPR **2** pathways.[27]

Pancreatic β-cells

Calcium release and subsequent downstream insulin secretion has been studied in pancreatic β-cells. It has been shown that acetylcholine acts to stimulate Ins(1,4,5)P_3 **1** and cADPR **2** pathways through interaction with the ER and that glucose stimulates the NAADP **3** pathway mediated by lysosomal related organelles (Figure 6).[25] This work showed that NAADP **3** mobilised calcium from a store independent from those stimulated by Ins(1,4,5)P_3 **1** and cADPR **2** on the ER. Using whole cells it was possible to demonstrate that glucose initiated calcium release lead to subsequent insulin secretion *via* an acidic lysosomal NAADP **3** store that was sensitive to bafilomycin A1.[25] It is less clear how NAADP **3** elicits the influx of extracellular calcium into β-cells, however a possible mechanism may be linked to voltage operated channels similar to those observed in sea urchins. In response to external

stimuli, this direct release of calcium from internal stores, independent from those of other specific second messengers, confirms NAADP **3** as a second messenger for the first time. This rise in calcium has thus been shown to cause a downstream event and in this example causes the release of insulin to directly reduce the blood glucose concentration.

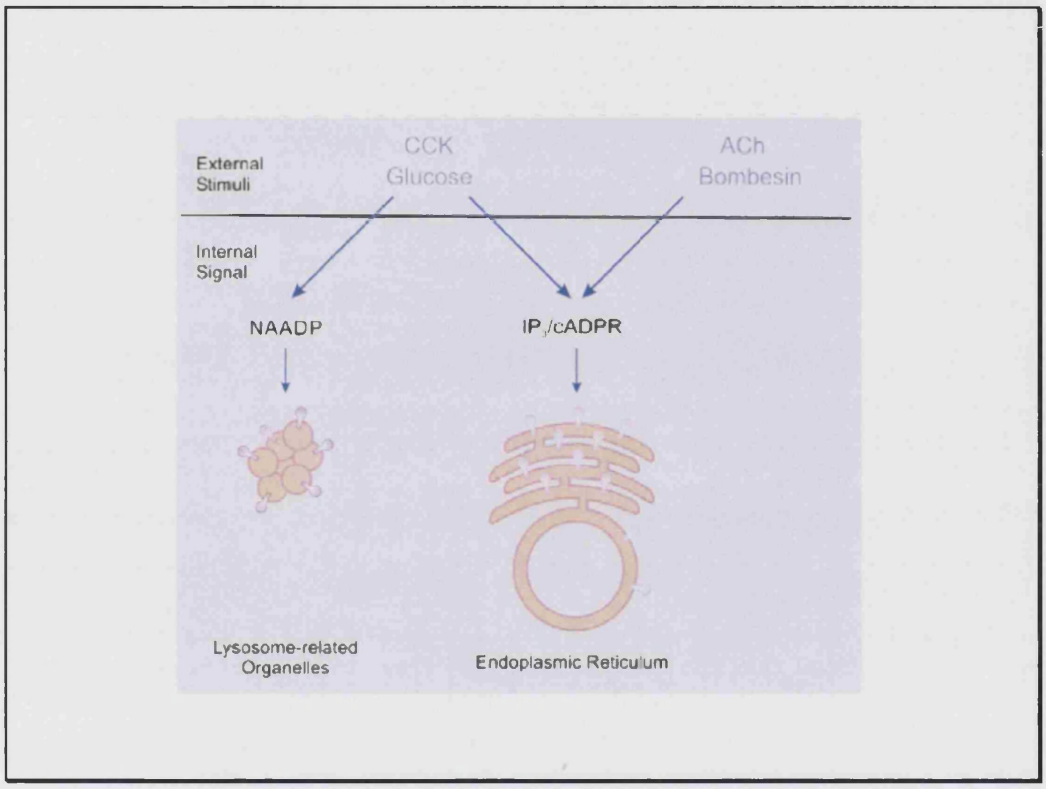

Figure 6: Effect of glucose causing NAADP **3** mediated calcium release from an organelle discrete from that acted on by cADPR **2** and Ins(1,4,5)P_3 **1**.

1.7 Inactivation of NAADP

NAADP **3** has been shown to be highly active in a range of cell types, so there must be a highly selective mechanism of inactivation in order to switch off the signal (Scheme 4).

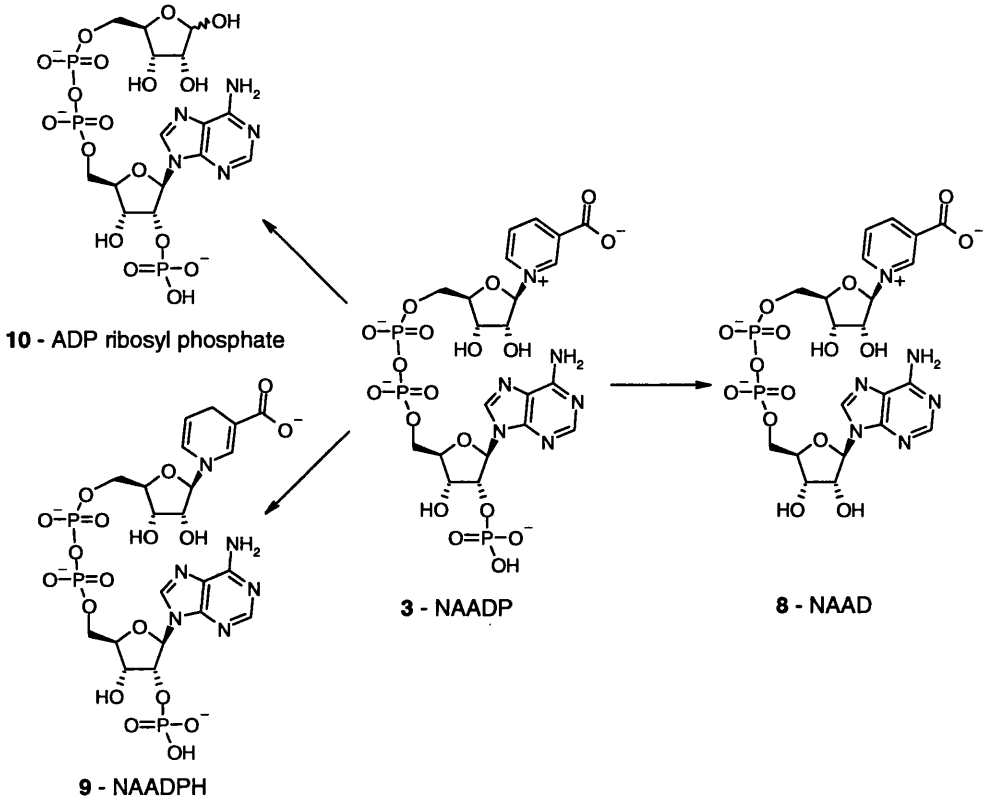

Scheme 4: Proposed mechanism of inactivation of NAADP **3**

It has been shown in brain tissue that NAADP **3** is metabolised predominantly to NAAD **8** by dephosphorylation.[28] This is in contrast to NADP **7** which mainly undergoes metabolism to ADP-ribose.[28] Addition of the calcium chelator, EDTA showed attenuation of this metabolic pathway to form NAAD **8**, revealing the intimate relationship between this feedback mechanism and cytosolic calcium concentration. These results also suggest that metabolism does not proceed *via* base-exchange as NAADP **3** is not converted to the NADP **7** metabolite ADP-ribosyl phosphate **10**.[28] Recently emerging data suggest that NAADP **3** might also be inactivated by reduction to NAADPH **9**, catalysed by glucose-6-phosphate dehydrogenase [E.C. 1.1.1.49] with a small amount of ADP-ribose phosphate **10** also produced.[29] NAADPH **9** had virtually no calcium release properties with

concentrations above 400 nM required to observe release. This result seems remarkable because one might expect some contamination or degradation of NAADPH **9** to NAADP **3** and concentrations as low as 3 nM (of **3**) will cause calcium release. It was also shown that sub-threshold NAADPH **9** concentrations, incubated for 5 minutes, serve to inhibit subsequent NAADP **3** stimulation. However, in 5 minutes it would be reasonable to expect that the unstable NAADPH **9** could undergo oxidation to NAADP **3**, in sufficient concentration to cause the receptor inactivation, which would invalidate this result. It was speculated that NAADPH **9** could either then be used as a precursor molecule to NAADP **3** by undergoing oxidation before instigating calcium release, or as a metabolite that can efficiently inactivate the calcium signal allowing storage of this molecule in an inert state.[29] Work undertaken within our group found that unlike NADPH, it was very difficult to produce NAADPH **9** by either chemical or enzymatic methods, and even harder to purify due to decomposition to ADP-ribose phosphate **10**, or re-oxidation to NAADP **3**.

1.8 Summary of NAADP

NAADP **3** has been shown to be active in a number of cell types producing an array of responses that have been characterised to varying degrees. It has now been firmly established as an endogenous molecule responsible primarily for the initiation and co-ordination of calcium release. Its release from stores independent of Ins(1,4,5)P_3 **1** and cADPR **2** suggest that NAADP **3** is a second messenger of immense interest. However, the exact mechanism for *in-vivo* synthesis and metabolism still remain a topic of huge debate. Unfortunately, studies are currently restricted due to the limited array of chemical probes available to interrogate this system. As the total synthesis of NAADP **3** has not been previously published, analogues have been limited to direct alteration of NAADP **3** or NADP **7** modifications that still remain substrates for ADP-ribosyl cyclase. A disadvantage of this approach is potential contamination with very potent NAADP **3** in the product. Total chemical synthesis of NAADP **3** would provide a much more feasible route toward structurally relevant analogues. It is hoped that these analogues will help isolate the NAADP **3** receptor protein and allow the *in-vivo* chemical pathway to be elucidated.

Chapter Two

Aims and objectives

2.1 Synthesis of chemical analogues

A small structure-activity relationship (SAR) of NAADP **3** (Figure 7) involving readily accessible modifications of NADP **7** such as substitution of nicotinic acid for analogues using *Aplysia* ADP-ribosyl cyclase had previously been investigated.[18]

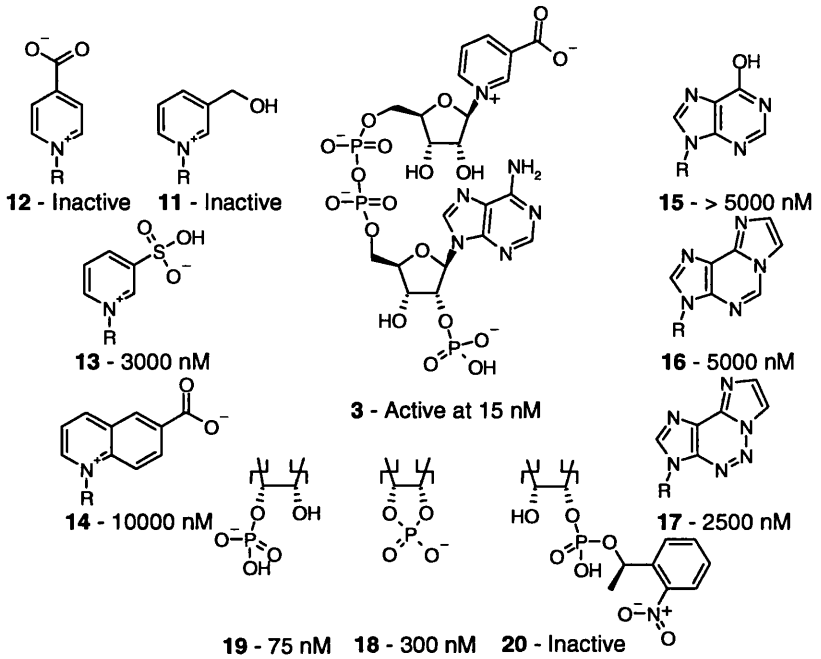

Figure 7: Activity of NAADP **3** and closely related analogues.

Installation of the alcohol equivalent **11** generated an inactive compound, which provided evidence that the carboxylate negative charge was essential for activity. This is confirmed by the fact that NADP **7** is totally inactive in the mobilisation of calcium. Altering the position of the carboxylic acid from the *meta* to the *para* position **12** also resulted in total loss of activity, suggesting that the active site of the receptor is very tightly controlled. There is however a small degree of tolerance of the negative charge or aromatic group as both the sulphonic acid **13** and quinoline 3-carboxylate **14** remain partially active. Pyridines substituted at the 2-position were not substrates for the cyclase enzyme inhibiting their inclusion into the SAR scheme (Figure 7).[18]

Other analogues were obtained by conversion of the adenine base. Replacement of the adenine ring for a hypoxanthine (purinyl amine replaced by a hydroxyl) resulted in desamino NAADP **15** after base-exchange.[18] Two fluorescent analogues were

synthesised by manipulation of commercially available etheno NADP. Replacement of the nicotinamide for nicotinic acid resulted in the formation of etheno NAADP **16** that with further modification led to etheno-aza NAADP **17** (Figure 7).[30] Both were partially active but highly fluorescent, potentially enabling *in-vivo* detection. Both of these analogues retained the nitrogen at the 6-position, suggesting that it may contribute to activity.[30]

NAAD **8** was completely inactive in mobilising calcium, while the 2′,3′-cyclic **18** and the 3′-regio-isomers **19** were found to be less active, proving that the 2′-phosphate **3** is essential for activity.[18] Formation of a phosphate ester at the 2′-position renders the molecule inactive, however the nitrophenyl ester **20** was synthesised to provide caged NAADP which could be activated *in-vivo* upon flash photolysis (Figure 7).[31]

All of the analogues that confer activity are agonists and also retain the self-inactivation observed for NAADP **3**. Despite this intriguing effect there has been no reported antagonists, even though agonists may be used as pseudo-antagonists *via* the self-inactivation mechanism.[17,32]

This small study provided an invaluable insight into the chemical biology of NAADP **3**; however the range is seriously limited by requiring substrates that can still be turned over by enzymes. This is emphasised by the lack of knowledge regarding other positions such as the positive charge and substitution at the 2-position of the pyridinium. Total chemical synthesis therefore offers the most practical approach to a wider range of analogues without the potential complication of trace NAADP contamination skewing observed result. Therefore formation of analogues, devoid of any potential trace of NAADP **3** would be of great value.

2.2 Project aims

The aim for this project is the development of a synthetic route that would be sufficiently flexible to allow modifications at key positions. Initially, these could focus on the pyridinium ring, but later targets include the adenosine-2′-phosphate and the pyrophosphate (Figure 8).

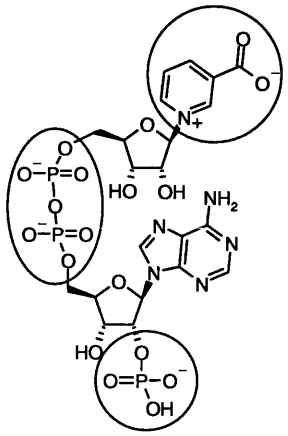

Figure 8: Target areas for NAADP **3** analogue synthesis.

2.3 Synthetic strategy

Late stage pyrophosphate bond formation would enable the two halves of the molecule to be linked through a convergent synthesis, which should enable modifications to be installed in the initial stages of the synthesis and reduce potential problems that may be associated with late stage alterations. Chemical synthesis of the 2′-phosphate moiety would be required as biological studies have shown that the 3′-phosphate **19** is distinctly less active.[18] To achieve this, an efficient synthetic scheme, incorporating minimal protecting groups would ideally be employed, thus avoiding potentially problematic late stage cleavage (Scheme 5).

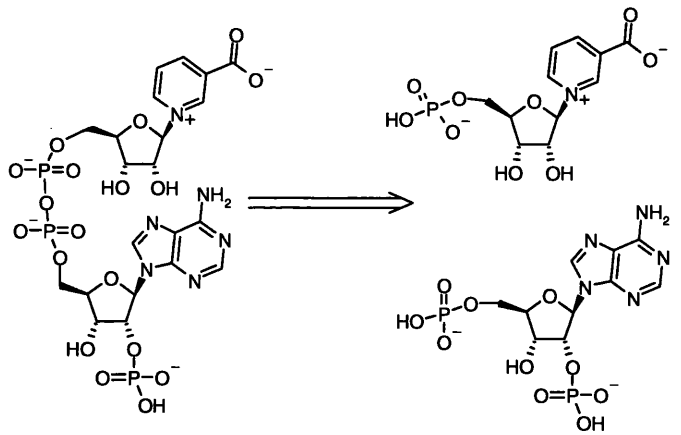

Scheme 5: Retrosynthetic approach to the synthesis of NAADP.

The formation of nicotinic acid ribonucleotide will provide a number of synthetic challenges. Initially, glycosidic bond formation will be required, with a suitably protected pyridinium ester moiety that can be cleaved to afford the carboxylate during

the later stages of the synthesis and secondly, selective phosphorylation at the 5′-ribose hydroxyl will be required. To facilitate efficient synthesis, work will be carried out to achieve this without the use of ribose protecting groups, however, it may become necessary to incorporate these to afford the desired ribonucleotide.

Synthesis of the adenosine moiety will require manipulation of protecting groups as the 2′-ribose hydroxyl will need to be either selectively unveiled or activated to allow regio-specific phosphorylation to ensure purity of the final compound. Protected phosphates will also be required to increase the lipophilicity of the compound to enable reactions and purification to be carried out with organic solvents for a large proportion of the synthesis.

Once the 5′-hydroxyl has been phosphorylated, pyrophosphate bond formation will be required to link the two halves together. This will entail challenging chemistry as there is a limited pool of reported methods for this reaction and the yields are often poor. A method will need to be developed that offers high yields, as this is the critical step in the synthesis.

Once a synthetic route has been developed, the emphasis can shift towards analogue formation. Initially, modification to the pyridinium ring will enable further understanding of the importance of the positively charged nitrogen along with the necessity for the base labile glycosidic linkage. Once formed this analogue will be tested for its ability to release calcium in sea urchin egg homogenates to further develop the SAR surrounding NAADP **3**.

Chapter Three

Synthesis of β-Nicotinamide Mononucleotide

3.1 Introduction

Development of a flexible route towards enantiomerically pure pyridinium ribosides was sought to enable the total chemical synthesis of NADP **7**, NAADP **3** and an array of analogues. Phosphorylation at the 5′-position would then provide access to linkage with the adenosine moiety *via* a pyrophosphate bond, providing a late stage, convergent synthetic route. A flexible synthesis is required to enable the generation of analogues to investigate the biochemistry of NAADP **3**.

β-Nicotinamide mononucleotide (β-NMN) **21** is a key portion of co-enzymes NAD **6** and NADP **7**, allowing the transfer of hydrogen during redox reactions.[33] *In-vivo* synthesis of NAD **6** proceeds by reaction of the vitamin niacin (nicotinate) **22**, which is added to phosphoribosylpyrophosphate (PRPP) **23** to form β-nicotinic acid mononucleotide (β-NaMN) **24**. Linkage to adenosine monophosphate (AMP), from adenosine triphosphate (ATP) **25**, catalysed by nicotinamide/nicotinate mononucleotide adenylyltransferase (NMNAT) [E.C. 2.7.7.1], gives $NAAD^+$ **8**, which is finally converted to NAD **6** upon transfer of the amide group by exchanging glutamine into glutamate (Scheme 6).[34]

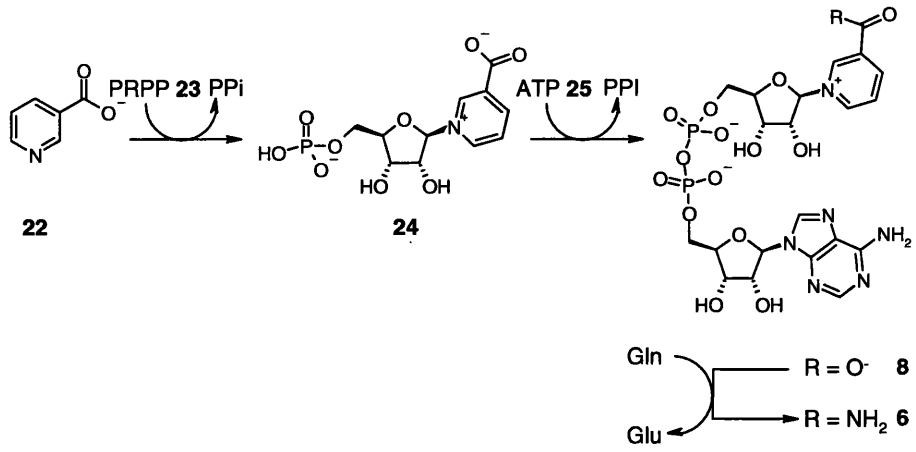

Scheme 6: Biosynthetic pathway for synthesis of NAD **6**.

In-vitro synthesis of *N*-1-pyridinium ribose compounds requires β-stereoselective glycosidic bond formation. Use of protecting groups is limited by requirement for subsequent cleavage in the presence of the newly formed labile pyridinium bond. Consequently, there have only been four main approaches reported over the past forty years.

β-NMN **21** has been produced by the enzymatic degradation of NAD **6**, using NAD-pyrophosphatase.[33] Reaction in the presence of enzyme adsorbed on buffered P-cellulose at 37°C provided 2.9 g of β-NMN **21** in 82 % yield based on NAD **6**. This presents an attractive route to large-scale β-NMN **21** production, however it is impractical as a flexible route for the production of structural analogues.

Previous work used adenosine monophosphate (AMP) **26** as the starting material in the chemical synthesis of enantiomerically pure β-NMN **21** (Scheme 7).[35] AMP **26** was degraded to ribose 5-phosphate **27** by refluxing in an aqueous solution of acidic Dowex resin. Subsequent treatment with dry ammonia gas afforded the 1-amino ribose 5-phosphate **28**, which was followed by the *in situ* Zinke reaction with 1-(2,4-dinitrophenyl)-3-carbamoyl-pyridinium chloride (NDC) **29**. This provided diastereotopic NMN **21** in quantitative yield from ribose-5-phosphate **27** in an isomeric ratio of 4:6 (α:β). Even though this route provides an efficient synthesis of β-NMN **21**, it is not generated as the single diastereoisomer. However, as the next step required enzymatic coupling with NAD pyrophosphorylase [NADPP, EC 2.7.5.1] to ATP **25**, resolution was not required due to the specificity of the enzyme for only the β-isomer.[35]

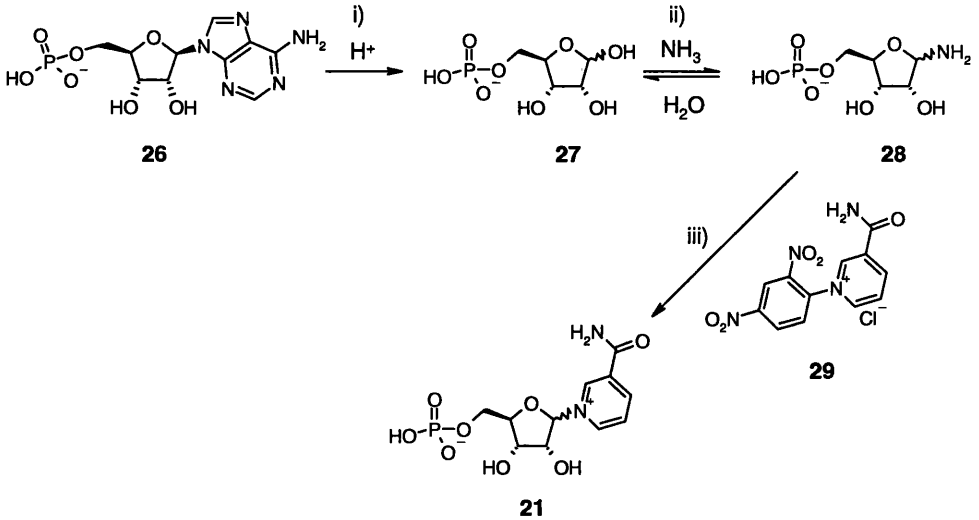

Scheme 7: *Reagents and conditions*: i) Dowex H^+, water, 100 °C, 6 mins; ii) ethylene glycol, ammonia gas, 0 °C, 30 mins, then **27**, 5 °C, 15 h; iii) NDC, CH_3OH, 5 °C, 14 h.

A recent synthesis of NAD **6** involved bromination of commercially available tetra-*O*-acetyl-β-D-ribose **30** using HBr to afford **31** (Scheme 8), prior to glycosylation with nicotinamide **32** to afford **33** in a 1:25 α:β ratio after re-crystallization. The reported deacetylation using methanolic ammonia caused substantial nucleoside cleavage. Low temperature conditions (-5 °C) solved this problem leading to pure β-nicotinamide nucleoside **34**. Phosphorylation using an excess of $POCl_3$ and trimethylphosphate led to the formation of β-NMN **21** after isolation on Dowex resin.

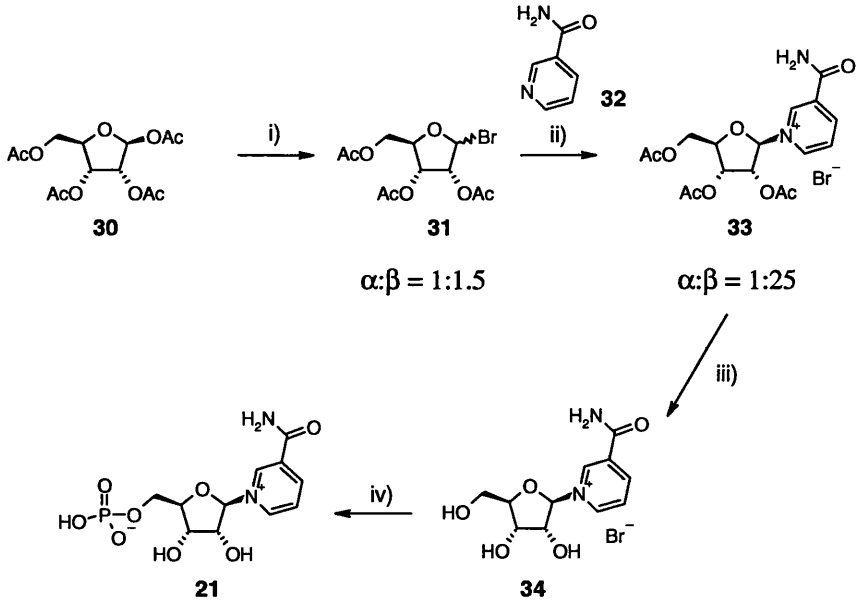

Scheme 8: *Reagents and conditions*: i) HBr, CH_2Cl_2; ii) nicotinamide **32**, SO_2, -10 °C; iii) 3 equiv. of NH_3, 1 M in CH_3OH, -3 to –5 °C, 20 h; iv) $POCl_3$, $PO(OMe)_3$, -5 to 0 °C, 7 h.

Commercially available tetra-acetyl ribose **30** has also been activated with the Lewis acid trimethylsilyltrifluorosulphonate (TMSOTf) and reacted with nicotinamide **32** to afford the protected nicotinamide ribose **38**.[36] This reaction proceeded *via* the following mechanism. The anomeric acetate was eliminated *via* the formation of the oxonium ion **35**, which underwent *intra*molecular ring closure initiated by the neighbouring 2-acetyl **36** to afford the α-oxonium cation **37**. Subsequent reaction with nicotinamide **32** therefore provided the β-isomer **38** (Scheme 9). *In situ* transesterification was achieved by the addition of CH_3OH, which afforded nicotinamide nucleoside **39** as the β isomer, in >95 % yield as characterised by ^1H

NMR spectroscopy, whilst avoiding basic protecting group removal, thus making it attractive and flexible synthetic route for β-NMN **21** and analogues.

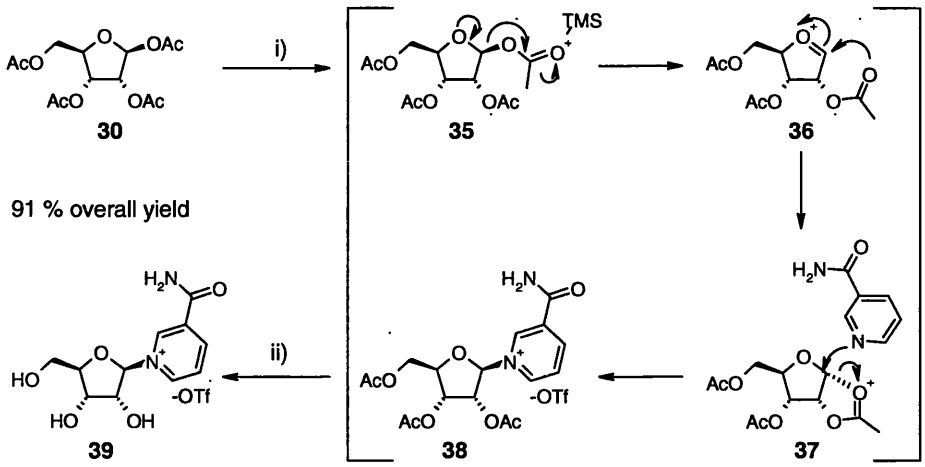

Scheme 9: *Reagents and conditions*: i) Nicotinamide **32**, TMSOTf, CH_3CN, 1 h; ii) CH_3OH, 30 mins.

3.2 Synthesis of nicotinamide riboside and its analogues

This efficient production of β-nicotinamide nucleoside **39** with mild acetate cleavage encouraged us to explore the Lewis acid activated route further. The formation of the *tri*-acetyl intermediate **38** was observed by TLC, but never isolated; instead the mixture was treated with CH_3OH to allow the *in-situ* transesterification to afford **39**. Purification of the product on an activated charcoal column, as described in the literature,[36] was unsuccessful due to the loss of material on the column. An alternative method of purification was thus sought. Partitioning of the reaction material between water and *n*-butanol, followed by silica flash chromatography of the concentrated aqueous phase, afforded the nucleoside triflate salt **39** in 91 % yield as an oil (Scheme 9). Formation of the glycosidic bond was confirmed by analysis of the ^1H NMR spectrum, which showed a downfield shift for the pyridinium protons suggesting that they were in the electron deficient environment of a positively charged nitrogen. By structural examination of the dihedral angle between the anomeric proton and the 2′ proton it was possible to assign the stereochemistry from the ^1H NMR spectrum. In ribose, the angle exists at approximately 130 to 140° when the anomeric proton is α (hence substitution is β) (Figure 9). By substituting this angle into the Karplus equation it equates to a vicinal coupling of 4 to 5 Hz. The

corresponding value for α substitution would be approximately 8 Hz. Analysis of the anomeric proton indicated that the product had formed the single β-isomer with a coupling constant to the 2′-proton of 4.2 Hz. This successful result led us to explore how other pyridinium bases react under these conditions.

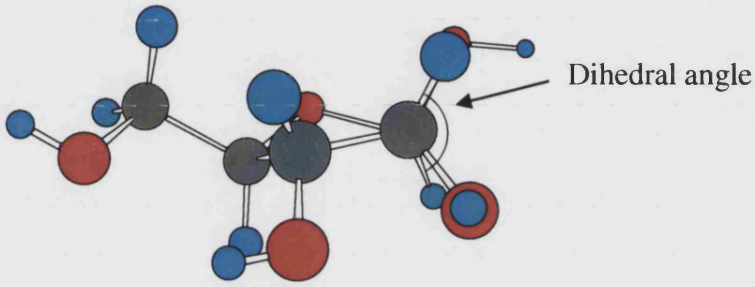

Figure 9: The dihedral angle between the anomeric proton and the 2′ proton of β-D-ribose. Black = carbon; red = oxygen; blue = hydrogen.

The glycosylation was carried out using different pyridinium bases, initially methyl nicotinate and nicotinic acid, to ascertain the flexibility of the route (Scheme 10). Under the same conditions the desired methyl nicotinate riboside **40** was synthesised in 81 % yield after partition between water and *n*-butanol followed by flash chromatography of the concentrated aqueous phase. Using nicotinic acid, however the reaction failed and the only material purified from the reaction was nicotinic acid and deacetylated ribose.

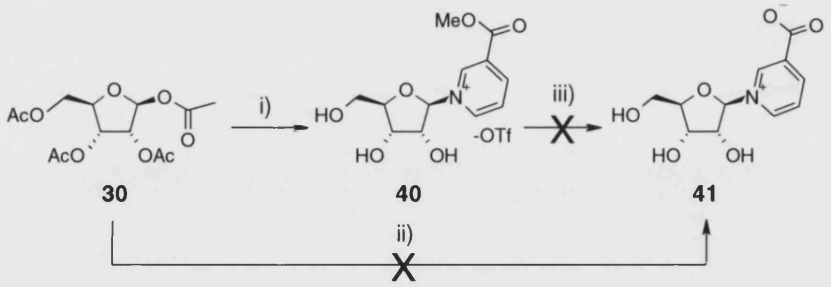

Scheme 10: *Reagents and conditions*: i) a) Methyl nicotinate, TMSOTf, CH_3CN, 1 h; b) CH_3OH, 30 mins; ii) nicotinic acid, TMSOTf, CH_3CN, 2 h; b) CH_3OH, 30 mins; iii) PSL, 60 °C, 24 h, or 1 M HCl, 18 h.

Analysis of the ^1H NMR spectrum for the methyl ester **40** proved that glycosylation had occurred, as shown by a downfield shift of the pyridinium protons, while the β-stereochemistry was confirmed by examination of the anomeric coupling constant

(4.4 Hz). Even though hydrolysis to the carboxylic acid **41** at this stage in the synthesis is not required, trial reactions would ascertain whether hydrolysis may be possible and if so, highlight any potential problems that could be encountered later in the synthesis (Scheme 10). Basic hydrolysis was avoided though, due to possible epimerisation to **42** or cleavage of the glycosidic link (**43** and **22**), as previously reported (Scheme 11).[37]

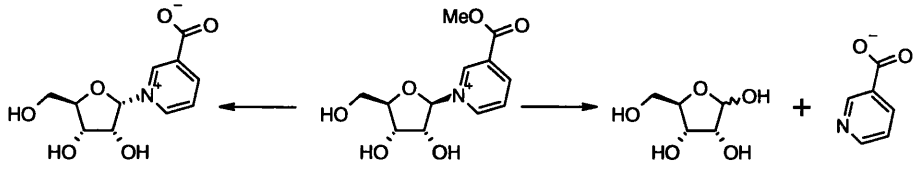

42 **40** **43** **22**

Scheme 11: Possible results of using aqueous base to perform the ester hydrolysis.

A method utilising an enzyme was investigated using *Pseudomonas cepacia* lipase [E.C. 3.1.1.3] at 60 °C over 24 hours,[38] but unfortunately this proved to be unsuccessful. Analysis of the ^{1}H NMR spectrum showed that both the anomeric and pyridinium protons had shifted upfield, presumably due to glycosidic bond cleavage, leaving an impure mixture of ribose **43** and nicotinate **22**. Acid catalysed ester hydrolysis using 1 M HCl was also evaluated, but this failed to show that a reaction occurred in all but one instance, when the ^{1}H NMR spectrum did show the presence of a second anomeric peak further upfield at 6.27 ppm. It was not possible to isolate this product to obtain any reliable data from this reaction and the focus was therefore shifted towards a protecting group, such as a benzyl ester that could undergo late stage neutral cleavage using H_2, without causing glycosidic bond hydrolysis or other side reactions.

Initially nicotinic acid was protected using 0.9 equivalents of benzyl alcohol in the presence of DCC and DMAP to afford the ester **44** as a clear colourless oil in 67 % yield. The ester **44** was then reacted with *tetra*acetyl-ribose **30** under the established protocol (Scheme 12). As the product was soluble in both water and *n*-butanol, separation was accomplished using H_2O and EtOAc, and the concentrated aqueous phase later analysed by ^{1}H NMR spectroscopy. An anomeric peak at 5.9 ppm (J=3.9 Hz, characteristic of the β-isomer), and the pyridinium protons confirmed that

glycosylation had occurred. However, no signals were observed for the benzylic ester protons. Mass spectrometry analysis showed a peak at 256 establishing that the nicotinic acid riboside **41** had indeed been formed (Scheme 12) presumably *via in situ* TMS catalysed debenzylation in 87 % yield. For the complete synthesis of NAADP the carboxylic acid is required, but it must remain protected until the final stages to prevent unwanted side reactions. Avoiding an aqueous workup and subjecting the crude material to silica flash chromatography, afforded the benzyl protected material **45** in 82 % yield, although, it still remained extremely water sensitive, and hence unusable in the synthetic scheme.

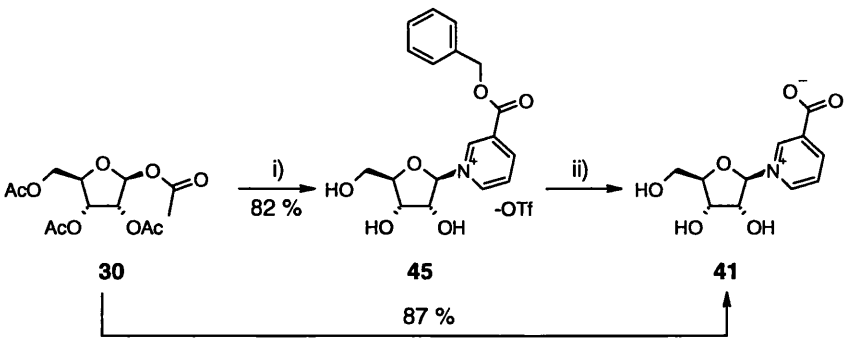

Scheme 12: *Reagents and conditions*: i) a) Benzyl nicotinate **44**, TMSOTf, CH_3CN, 2 h; b) CH_3OH, 1 h; ii) aqueous work up.

3.3 Phosphorylation of nicotinamide riboside and its analogues

Conditions were sought to achieve phosphorylation of the nicotinamide ribose 5′-alcohol **39**. Methods utilising either trimethyl or triethyl phosphate should allow the selective phosphorylation without the need for protecting groups based on precedence for phosphorylation of guanosine **46**.[39] For guanosine, the 5′-hydroxyl group is believed to form a hydrogen bond with the P=O group, which acts as a Lewis base, while the N^9 interacts with the phosphorus atom (Figure 10). It was speculated that nicotinamide riboside **39** would behave in a similar manner to enable the selective phosphorylation, but several attempts to treat nicotinamide riboside with stoichiometric quantities phosphorus oxychloride ($POCl_3$) in triethylphosphate produced no visible results.

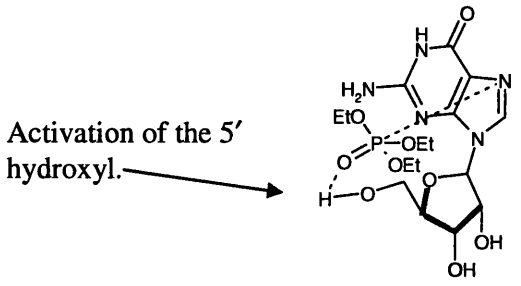

46

Figure 10: The complex formed between guanosine and triethylphosphate causing the activation of the 5′ hydroxyl.

The addition of 0.5 equivalents of H_2O to $POCl_3$ was explored as this produces a more reactive species that may provide better yields (Scheme 13).[39] Monitoring of the reaction was difficult due to the high polarity of both the starting material and product. Conditions for reverse phase HPLC were found, enabling a change in retention time to be detected (Method B: R_T 8 minutes (**39**) to 3 minutes (**21**)). Purification of the β-NMN **21** from this reaction mixture proved difficult due to the polarity of the products. Reverse phase chromatography failed to separate the compounds as they eluted on the solvent front when loaded in H_2O. Ion exchange chromatography was also difficult using positively charged resin, such as AG-MP1 as neither the neutral product **21**, nor cationic starting material **39**, was retained. Previous literature purifications of β-NMN **21** utilised two successive negatively charged resins, Dowex 1X2 formate and 50 WX8 H^+ respectively.[37] Unfortunately, attempts at this method only yielded triethylphosphate.

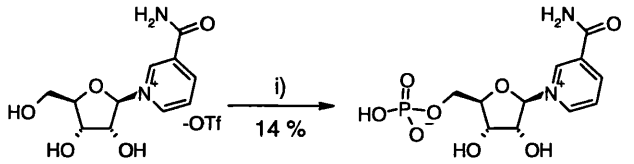

39 **21**

Scheme 13: *Reagents and conditions*: i) Trimethylphosphate, $POCl_3$, H_2O, 5 h, 0 °C.

Ultimately, it was found that using trimethylphosphate provided better yields, perhaps enabling formation of the complex as shown in Figure 10. Precipitation of the product from CH_3CN:diethylether (1:3), followed by elution through the same negatively charged resins provided β-NMN **21** in 14 % yield. This yield does not correlate with the conversion observed by HPLC analysis, leading us to believe that

loss during purification had occurred. Even though this yield is low, it does enable the synthesis to continue to attempt the formation of protected acid ribonucleotides. Improvements to the yield could be achieved by the development of a negatively charged resin purification method that would retain the starting material **39** allowing separation from the neutral product **21**.

Phosphorylation of the benzyl and methyl nicotinate (**45**, **40**) riboside led to a complex mixture of products (as shown by both ^{1}H and ^{13}C NMR), which could not be purified. Attempts to precipitate the products *via* a variety of conditions only led to product degradation. Phosphorylation of the nicotinic acid riboside **41** gave a product that proved just as difficult to purify even though a precipitate was obtained (Scheme 14). This method was therefore abandoned as a route to install the 5′-phosphate on protected nicotinic acid ribosides.

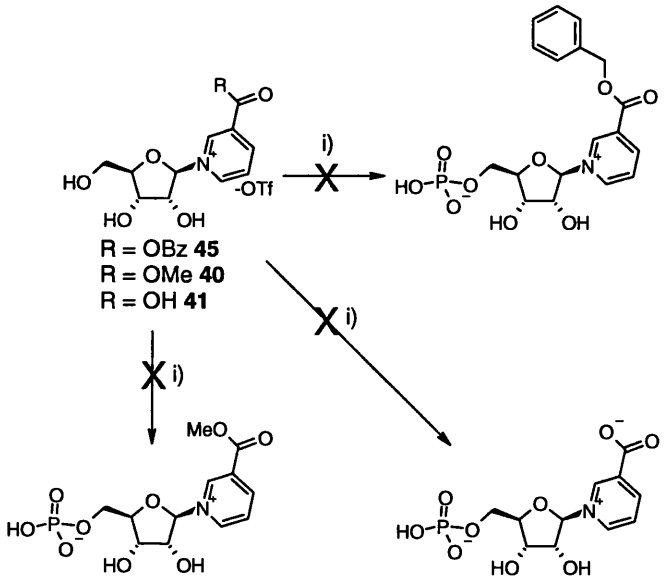

Scheme 14: *Reagents and conditions*: i) Trimethylphosphate, $POCl_3$, H_2O, 5 h, 0 °C.

An alternative route could involve synthesis of ribose 5-phosphate, followed by formation of the glycosidic bond, to afford either β-NMN **21**, or protected carboxylate analogues. $POCl_3$ could be utilised to install the 5′ phosphate, but phosphoramidite chemistry may provide a more efficient method of producing a protected phosphate that may be easier to purify using silica flash chromatography. Protecting groups on the three secondary alcohols would ensure regio-selectivity and may further increase lipophilicity, thus aiding organic solubility and purification.

3.4 Formation of β-D-ribose 5-phosphate

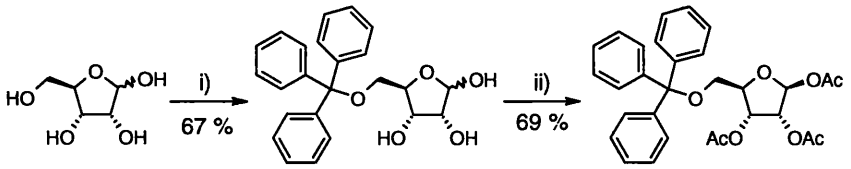

43 **47** **48**

Scheme 15: *Reagents and conditions*: i) Triphenylchloromethane, pyridine, 45 °C, 1 h; ii) Ac_2O, Et_3N, toluene, 18 h.

D-Ribose **43** was selectively protected using trityl chloride and pyridine exploiting the higher reactivity of the 5′-alcohol leading to **47** in 67 % yield, after purification (Scheme 15).[40] Mass spectrometry analysis only showed a peak at 243 due to cleavage of the labile trityl group. Acetylation with acetic anhydride and Et_3N provided *tri*-acetyl ribose **48** in 69 % yield (Scheme 15).[40] The coupling constant of the anomeric proton (1.0 Hz) in the ^1H NMR spectrum indicated the acetate protection had adopted the β-conformation, even though the dihedral angle must be strained to approximately 110°. This is further supported in the literature,[40] which confirms that Et_3N does afford primarily the β-isomer at 6.22 ppm. When pyridine is used as a catalyst both isomers are produced in a 1:1 ratio and the α isomer is further downfield at 6.53 ppm. As no peak is observed in that region, it was concluded that the β-isomer had been selectively formed. Trityl deprotection using a 2 % solution of TFA in CH_2Cl_2 (Scheme 16) initially led to only partial cleavage of the trityl group due to the rapid back reaction with the reactive carbocation species. 2 % H_2O was added to scavenge this species leading to the improved yield of 76 % of triacetyl-ribose **49** after purification.

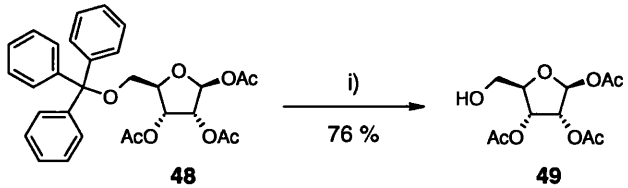

48 **49**

Scheme 16: *Reagents and conditions*: i) 2 % TFA, 2 % H_2O, CH_2Cl_2, 3 h.

The *tri*-acetyl ribose **49** was then reacted with $POCl_3$ under the standard protocol to phosphorylate the primary hydroxyl (Scheme 17).

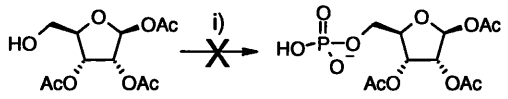

49 50

Scheme 17: *Reagents and conditions*: i) Trimethylphosphate, $POCl_3$, H_2O, 0 °C, 5 h.

As the *tri*acetyl-ribose **49** no longer possessed a chromophore, TLC visualisation by UV light was difficult, but staining with PMA or $KMnO_4$, revelaed the disappearance of starting material **49** and the appearance of a new spot on the baseline. Extraction of the product **50** into water afforded a mixture that was difficult to resolve. Purification by AG-MP1 chromatography was thought possible as the product was negatively charged. However, the poor UV absorbance meant that each fraction required staining with PMA, but isolation only afforded trimethyl phosphate. As the remaining hydroxyls were protected, phosphoramidite chemistry was employed to provide the desired di-benzyl protected 5′-phosphate, which contained a UV active chromophore that also aided in detection and purification. Reaction of the primary alcohol **49** with the benzyl phosphitylating agent **52** and imidazolium triflate **51** catalyst afforded, after *m*CPBA oxidation, the desired protected phosphate **53** in 85 % yield following silica flash chromatography (Scheme 18).

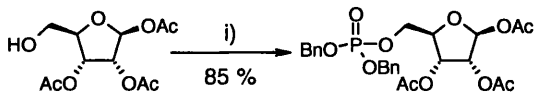

49 53

Scheme 18: *Reagents and conditions*: i) a) *Bis*(benzyloxy)diisopropyl aminophosphine **52**, imidazolium triflate **51**, CH_2Cl_2, 3 h; b) *m*CPBA, -78 °C, 30 mins.

Attempts to remove both benzyl protecting groups under hydrogenation conditions in the presence of 20 % $Pd(OH)_2/C$ and cyclohexene proved difficult. Despite both TLC analysis and ^{31}P NMR spectroscopy (δ 0.69 ppm) showing complete reaction within three hours a complicated mixture of products was obtained after purification. A peak at 355 by mass spectrometry confirmed that the free phosphate **50** had indeed been formed (Scheme 19), so this material was therefore used crude in the following steps.

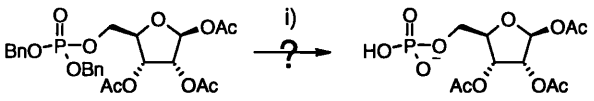

53 **50**

Scheme 19: *Reagents and conditions*: i) 20 % $Pd(OH)_2/C$, cyclohexene, CH_3OH, H_2O, 80 °C, 3 h.

Both the benzyl protected **53** and crude free phosphate **50**, were subjected to glycosylation with nicotinamide **32** using the established protocol. It was speculated that if CH_3OH, in the presence of TMSOTf cleaved the acetyl protection, it may replace the benzyl groups with methyl esters **54** (Scheme 20).

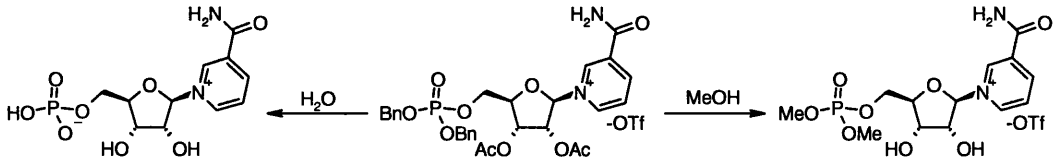

21 **55** **54**

Scheme 20: The hypothesised result of using CH_3OH or H_2O to perform the protecting group cleavage.

With this in mind both CH_3OH and water were used in two separate reactions to perform the *in-situ* acetyl cleavage for the benzyl protected material **55**. As there was no risk of forming the methyl ester in the reaction with the free phosphate **50** only CH_3OH was used to perform the deacetylation.

In all three cases ^1H NMR spectroscopy showed the reaction had failed as no anomeric and downfield nicotinamide protons were observed. After work up, neither ribose moieties could be recovered or adequately characterised to establish the result of the reaction (Scheme 21).

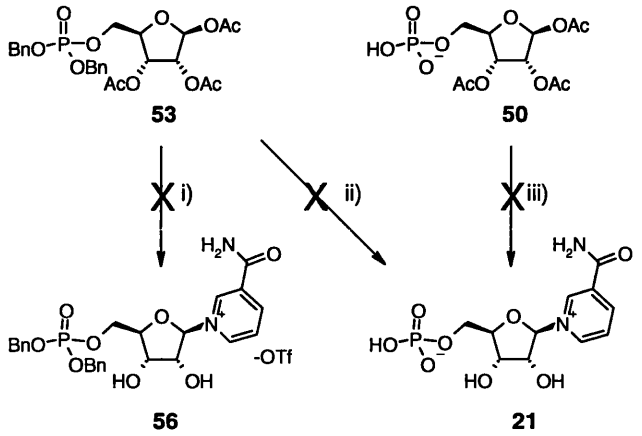

Scheme 21: *Reagents and conditions*: i) a) Nicotinamide, TMSOTf, CH_3CN, 2 h; b) CH_3OH, 1 h; ii) a) nicotinamide, TMSOTf, CH_3CN, 2 h; b) H_2O, 1 h; iii) a) nicotinamide, TMSOTf, CH_3CN, 2 h; b) CH_3OH, 1 h.

3.5 Summary

Overall, the Lewis acid catalysed route enabled the synthesis of nicotinamide ribosides, but further experimentation is required to develop structural analogues and to explore the phosphorylation. An alternative strategy toward late stage installation of the nicotinamide led to a synthesis of pyridinium ribose 5′-phosphate, but further work will be required to progress the *N*-glycosylation. Glycosylation could be carried out on tetra-protected ribose **48** (Scheme 22), as the product formation could be easily monitored by TLC with purification on silica flash chromatography possible. The material could then be selectively deprotected to provide the 5′-alcohol **57**, followed by phosphitylation and hydrogenation of the resulting dibenzyl phosphate to afford β-NMN **21**. Purification of these types of compound is still a problem and to further this area of work development of an adequate purification protocol, such as using a negatively charged resin needs to be undertaken.

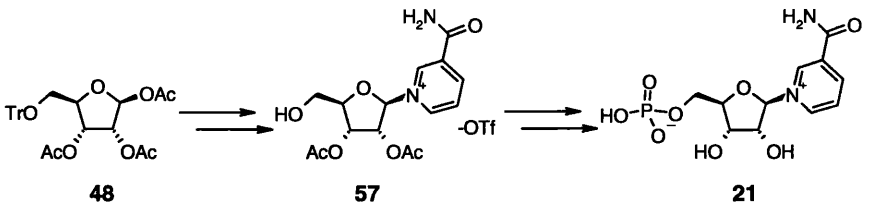

Scheme 22: Representation of the overall synthetic route to β-NMN **21**.

Chapter Four

Selective adenosine phosphorylation and pyrophosphate formation

4.1 Selective diphosphate adenosine formation

4.1.1 Introduction

The synthesis of NADP **7** and NAADP **3** could be achieved by pyrophosphate bond formation between a suitably protected 2′,5′-adenosine *bis*phosphate and β-NMN **21** or β-NaMN **24**. This approach required the development of a method to selectively install phosphates onto the 2′-and 5′-hydroxyls of adenosine without cyclisation, or subsequent migration to the 3′-hydroxyl.

Methods to selectively modify the 2′-position of adenosine **58** include routes to either selectively activate one hydroxyl (Scheme 23), or achieve protection of the remaining hydroxyls (Scheme 24 and Scheme 25).

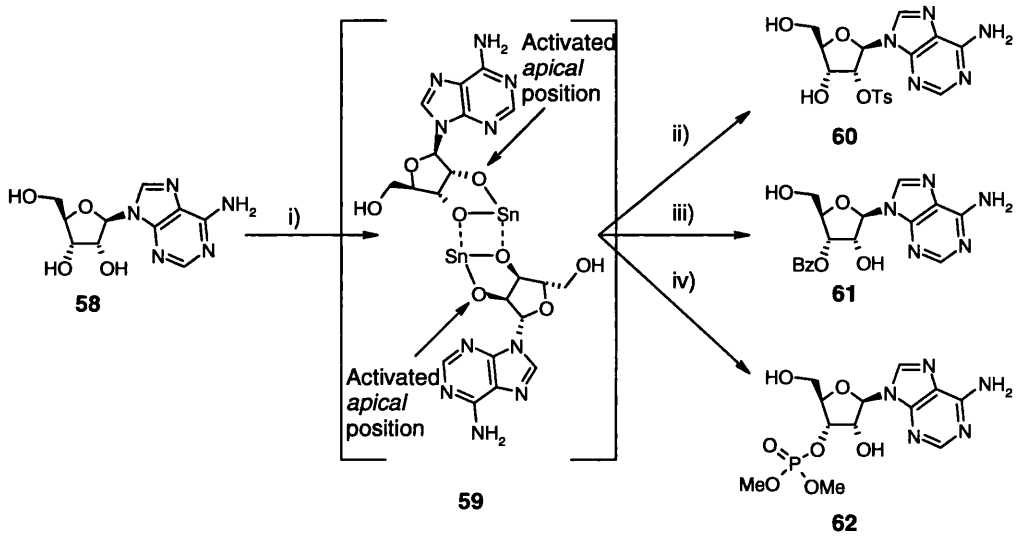

Scheme 23: *Reagents and conditions*: i) Dibutyltin oxide, CH_3OH, reflux, 30 mins; ii) tosyl chloride, Et_3N, 5 mins; iii) benzoyl chloride, Et_3N, 15 mins; iv) hexabutyldistannoxane, $POCl_3$, 20 mins.

Formation of the stannylene acetal **59** has been investigated as a method to selectively functionalise the 2′-hydroxyl.[41] Reaction with tosyl chloride led to the single regio-isomer **60**. The observed regioselectivity was attributed to the formation of the dimeric structure **59**,[42] which forces the oxygen atoms to adopt either an *apical* or *equatorial* position. The *apical* oxygen is more reactive, since the *equatorial* position is deactivated by coordination to the tin atom. However, benzoylation afforded a mixture of regio-isomers, which when crystallised yielded primarily the 3′-product **61**. Whether this was due to ring opening of the acetal at the 3′ position or that the 3′

regio-isomer was thermodynamically more stable was unclear. Subsequent attempts to selectively install a protected phosphate also produced a mixture of 2′-and 3′-products **62** (1:9) (Scheme 23).

This method of selective activation was attempted but as a result of failed tosylation later abandoned. As a result subsequent phosphorylation was never attempted. However, on reflection this approach could have been revisited had time permitted as it provides a fast and efficient synthesis of phosphorylated adenosine.

Regioselective deprotection of benzoyl protected adenosine **63** has been explored to selectively release the 2′-hydroxyl (Scheme 24). Previous work utilised either hydrazine hydrate to afford pure 2′-hydroxyl **64** in 64 % yield,[43] or KO^{t}Bu to achieve a mixture, whereby the prominent species was the exposed 2′-hydroxyl **64** (96 %, 5:1; 2′:3′-hydroxyl).[44] The regioselectivity was attributed to the greater acidity of the 2′-hydroxyl group,[43] and X-ray crystallography of purine ribosides showed the *C*(2′)–*O*(2′) to be shorter than the other two hydroxyl *C-O* bonds, suggesting it may behave as the most active towards nucleophiles such as hydrazine hydrate and KO^{t}Bu.[43]

Tri-*O*-benzoyl adenosine **63** was synthesised to explore the selective cleavage of the 2′-benzoyl protection (**64**). Unfortunately, our attempts only led to a mixture of products that were inseparable by flash chromatography. This caused us to explore a further method that avoided a two-step protocol, and would allow unambiguous exposure of the 2′-hydroxyl.

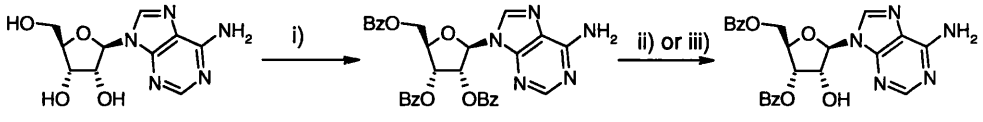

58 **63** **64**

Scheme 24: *Reagents and conditions*: i) Benzoic anhydride, DMAP, pyridine, 2 h; ii) hydrazine hydrate, glacial acetic acid/pyridine (1:4) 2 days; iii) KO^{t}Bu, THF, 1 min.

A protecting group that simultaneously tethers the 3′ and 5′-hydroxyls of adenosine **58** that leaves the 2′ hydroxyl free for unambiguous modification has been established (**65**).[45] Introduction of the 1,3-dichloro-1,1,3,3-tetraisopropyl disiloxane protecting group allowed selective formation of 2′-thioadenosine **66**[46] and 2′-deoxynucleotides

67,[47] which has since become an established route for the synthesis of DNA (Scheme 25).

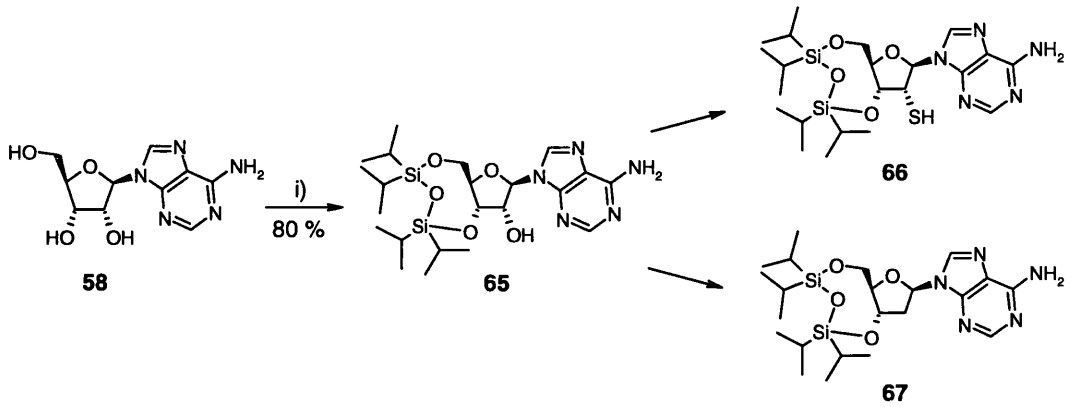

Scheme 25: *Reagents and conditions*: i) 1,3-Dichloro-1,1,3,3-tetraisopropyl disiloxane, pyridine, 3 h.

4.1.2 Synthesis of 2′, 5′ phosphorylated adenosine

Adenosine **58** was reacted with one equivalent of 1,3-dichloro-1,1,3,3-tetraisopropyldisiloxane in pyridine for three hours to afford the tetraisopropyldisiloxane (TIPDS) adenosine **65** in an 80 % yield (Scheme 25).[45] Synthesis of a suitably protected phosphitylating reagent was required to install the protected phosphate at the 2′-hydroxyl. Diisopropylamine and phosphorus trichloride (PCl_3) were reacted to afford the chlorophosphine **68** in 71 % yield.[48] Substitution with two equivalents of hydroxypropionitrile afforded the phosphitylating reagent **69**, in 74 % yield after flash chromatography on silica gel, pre-treated with Et_3N (Scheme 26).[49] It was important to ensure that the excess Et_3N was completely eluted to prevent unwanted base-induced cyanoethyl elimination.

Activation of the phosphitylating reagent required displacement of the diisopropylamine with a suitable azole catalyst. If tetrazole is used (pK_a ~ 5), phosphitylation would also occur on the purinyl amine.[50,51] However, the analogous imidazolium phosphane **70** (imidazole pK_a ~ 7) is less reactive enabling phosphitylation solely at the free hydroxyl.[50] Therefore, the phosphoramidite **69** was treated with imidazolium triflate **51** to yield the imidazolium phosphine **70**, which was reacted with protected adenosine **65**, and subsequently oxidised with *m*CPBA to

afford the 2′-di(2-cyanoethyloxy) phosphate adenosine derivative **71** in 98 % yield (Scheme 26).

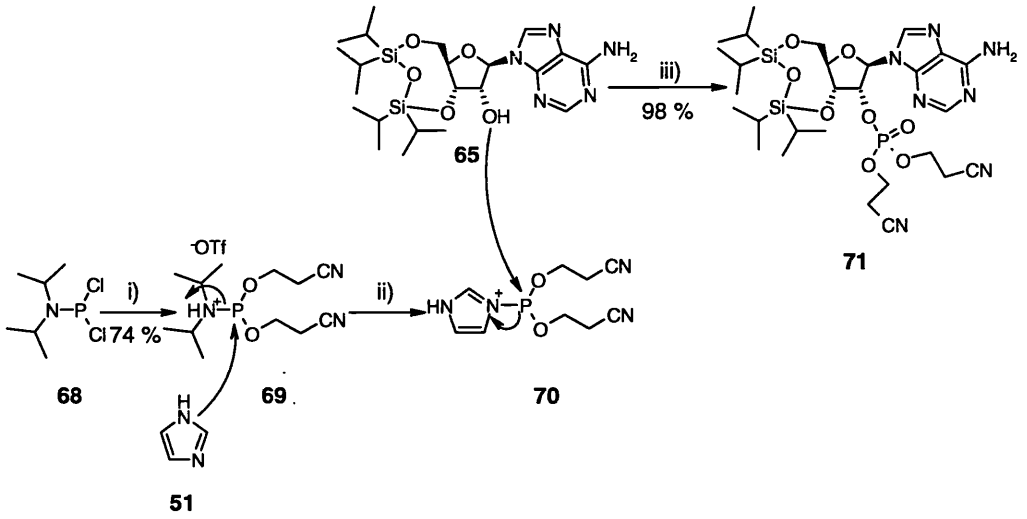

Scheme 26: *Reagents and conditions*: i) Hydroxypropionitrile, Et_3N, CH_2Cl_2, -78 °C to RT, 2 h; ii) imidazolium triflate; iii) a) *bis*(2-cyanoethoxy) diisopropylamino phosphine, CH_2Cl_2, 3 h; b) *m*CPBA, –78 °C, 30 mins.

Selective protodesilylation of the TIPDS protecting group had previously been explored using 0.2 M HCl in dioxane–H_2O, 1 M HCl in dioxane or HF–pyridine. However, under these conditions, total deprotection also occurs and yields are moderate.[52] With dilute TFA (TFA–H_2O–THF (1:1:4; *v/v/v*)) however, ring opening occurs exclusively at the less hindered 5′-silyl-ether in high yield.[52] Reaction of **71** for three hours at 0 °C under these acidic conditions afforded the adenosine derivative with a free primary hydroxyl **72** in quantitative yield (Scheme 27).

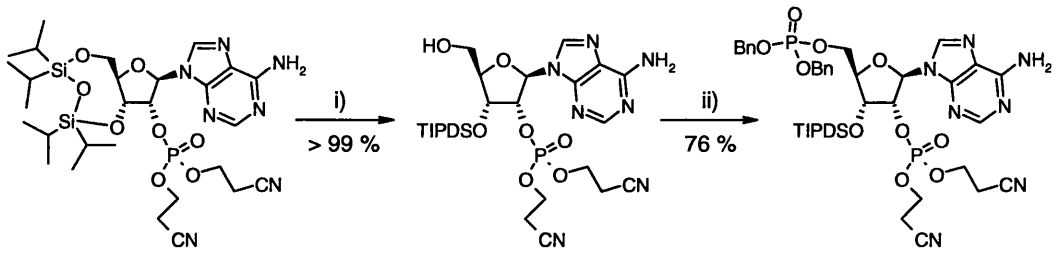

Scheme 27: *Reagents and conditions*: i) TFA–H_2O–THF (1:1:4; *v/v/v*), 0 °C, 3 h; ii) a) *bis*(benzyl)diisopropylaminophosphine, imidazolium triflate, CH_2Cl_2, 18 h; b) *m*CPBA, –78 °C.

Phosphoramidite chemistry was again used to install the second phosphate. However, a second phosphitylating reagent possessing orthogonal protecting groups to the rest of the molecule was required to enable later selective cleavage. *Bis*benzylphosphine **52** was synthesised in 79 % yield following the standard protocol.[53] Subsequent activation with imidazolium triflate **51** and reaction with the deprotected primary hydroxyl **72** led to the formation of the phosphite, but this required a greater reaction time than the 2′-phosphitylation, presumably due to increased steric hindrance. Overnight reaction followed by *m*CPBA oxidation, afforded the *bis*-phosphate **73** in a satisfactory 76 % yield after flash chromatography (Scheme 27).

The final synthetic step, in the preparation of the pyrophosphate bond formation, was to selectively remove the 5′-phosphate benzyl groups to afford the free phosphate **74**. Retention of 3′-and 2′-phosphate protecting groups was desirable in order to reduce the risk of phosphate migration, or spurious pyrophosphate formation at the 2′-phosphate.

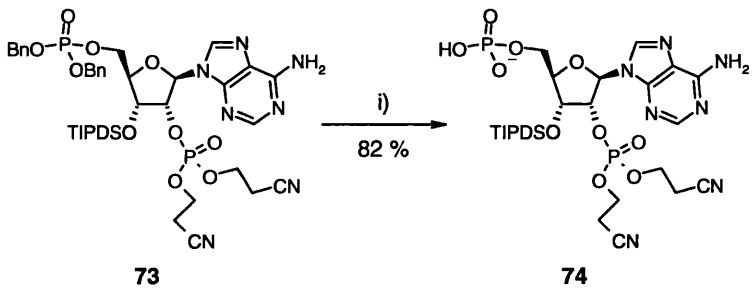

73 **74**

Scheme 28: *Reagents and conditions*: i) 20 % $Pd(OH)_2/C$, cyclohexene, CH_3OH, H_2O, 80 °C, 3 h.

Reductive deprotection using 10 % Pd/C and hydrogen at 50 °C proved to be successful for the removal of the benzyl protection and was accompanied by a downfield shift in the ^{31}P NMR spectrum (-0.42 ppm to 1.5 ppm). However, difficulties were encountered in the removal of the catalyst. Initially the compound adhered to celite, but this problem was overcome using a membrane filter. However, the resulting product was black, suggesting palladium contamination. Subsequent treatment with chelex resin sought to remove any remaining metal ions, but analysis by ^1H NMR spectroscopy indicated a complex mixture, betrayed by a second anomeric peak δ 0.06 ppm upfield of the major peak. Exploration of the literature

revealed that adenosine compounds had been cleanly deprotected previously using 20 % $Pd(OH)_2/C$ and cyclohexene as a source of hydrogen.[54] Reaction in CH_3OH and water at 80 °C for three hours, followed by membrane filtration, afforded clean, deprotected phosphate **74** in 82 % yield without the need for flash chromatography (Scheme 28).

With this final step completed, a high yielding (49 % yield, over five steps) and robust, synthetic route to a protected 2′,5′-adenosine diphosphate **74** in had been developed. This could be carried forward to investigate the formation of the pyrophosphate bond and subsequent protecting group removal.

4.2 Pyrophosphate bond formation

4.2.1 Introduction

Pyrophosphate bond formation is often difficult to achieve because of slow reaction times and the challenging purification of the water-soluble products leading to poor yields. Current literature procedures for pyrophosphate bond formation activate one of the phosphates to enhance its electrophilic properties, and the common methods are described below.

An early synthesis of NAD **6** utilised a vast excess of di*cyclo*hexylcarbodi-imide to condense racemic NMN **21** and AMP **26**. Isolation was achieved by selective enzyme reduction of the β-form by alcohol dehydrogenase, followed by alkaline destruction of the α-form and subsequent enzymatic oxidation to afford the correct β-isomer of NAD **6**.[55,56] By using mixed 2′,5′-and 3′,5′-adenosine diphosphates, prepared from adenosine, they also tried to synthesise NADP. Unfortunately the material was contaminated with β-NMN **21** and adenosine diphosphate after purification. It was believed that this was due the apparent instability of NADP when the phosphate is carried at the 3′-position.[55] This would however have provided a method for the synthesis of regio-selective NADP **7**, if they could separated the two regio-ismoers.

Previous NAD **6** syntheses have activated adenosine monophosphate (AMP) **26** as an electrophile using the phospho-imidazolide, triazolide or tetrazolide.[37] Activation of β-NMN **21** *via* the phospho-imidazolide was also explored, but all these routes

yielded NAD **6** in less than 5 %.[37] It was reasoned that the low reactivity of β-NMN **21** was a consequence of inner salt formation, making it less nucleophilic.[37] Accordingly, activation of AMP-imidazolidate and β-NMN **21** using the Lewis acid $MnCl_2$-$4H_2O$ afforded NAD **6** in an improved, 25 % yield. With further fine-tuning, using AMP-morpholidate **75**, a respectable 58 % yield was achieved. Interestingly, the authors claim that $MnCl_2$ was most active when stored in formamide, over 4Å molecular sieves for three days. Anhydrous $MnCl_2$ was found to be inferior and the identity of the active species remains unclear.

Alternative literature examples explore the production of various sugar-base pyrophosphate couplings using acid catalysts to accelerate the phosphomorpholidate chemistry.[57] Kinetic investigations of various different acids such as 1,2,4-triazole, acetic acid, *N*-hydroxysuccinimide and 1*H*-tetrazole, showed that 1*H*-tetrazole was the most efficient catalyst providing pyrophosphate synthesis in 76-91 % isolated yields, with reactions complete after two days. It was concluded that 1*H*-tetrazole not only acted as an acid, protonating the morpholine nitrogen **76**, but also as a nucleophilic catalyst. This allowed nucleophilic substitution to the more reactive phosphotetrazolide **77**, which underwent coupling to the second free phosphate **78**, forming the pyrophosphate **79** in 76 % yield (Scheme 29).

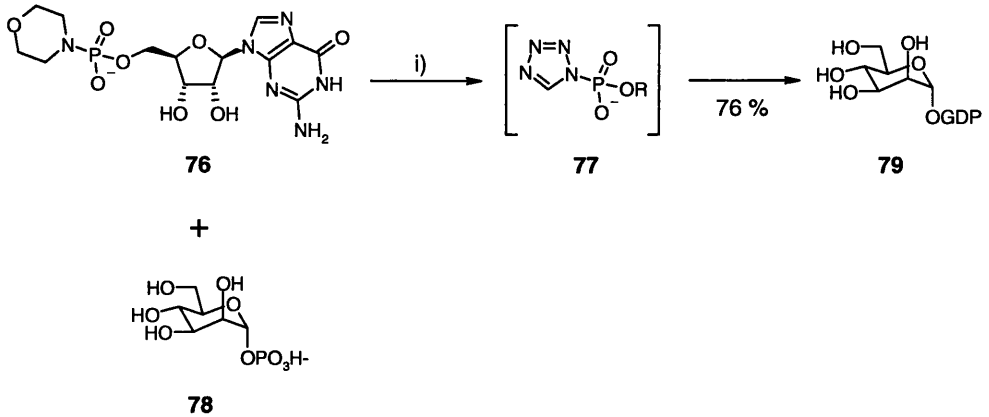

76 + **78** → **77** → **79**

Scheme 29: Formation of the phosphotetrazolide. *Reagents and conditions*: i) 1*H*-tetrazole, pyridine, **78** 2 days.

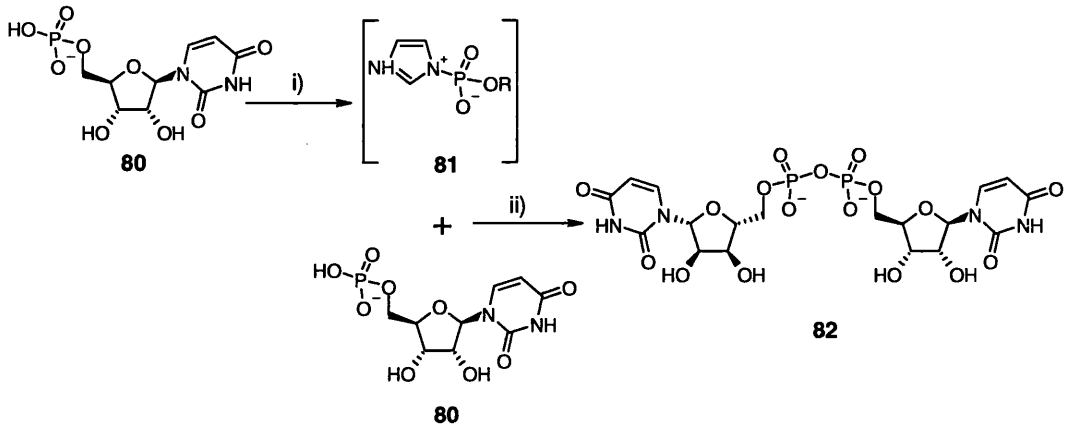

Scheme 30: Activation of a phosphate using CDI. *Reagents and conditions*: i) CDI, Et_3N, DMF, 3 h; ii) 50 °C.

Phosphate activation *via* the formation of the imidazolide represents an alternative strategy that has been incorporated into the syntheses of a uridine dinucleotide **82**[58] and an oestrogen sulphotransferase inhibitor.[59] Addition of carbonyl diimidazole (CDI) to uridine monophosphate (UMP) **80** generated the activated imidazolium phosphite **81**, which when treated with a second phosphate **80** formed the pyrophosphate bond **82** (Scheme 30) in acceptable 63 % yield.[58] The oestrogen sulphotransferase inhibitor was synthesised in 43 % yield[59] (not shown).

Further work examined the formation of a pyrophosphate bond between UMP morpholidate and imidazolide with galactofuranose to form the anti-microbial UDP-α-D-galactofuranose **86**. Unfortunately, reaction times were modest (1-2 days) and the observed completion, poor (50 %) with corresponding low yields (19-23 %).[60] UMP **80** was activated using trifluoroacetic anhydride (TFAA) towards a more efficient route leading to the mixed anhydride and simultaneous esterification of the remaining hydroxyls **83**, providing an intermediate that was soluble in DMF (Scheme 31). Subsequent addition of 1-methylimidazole afforded the highly reactive methylimidazolide-phosphine **84**, which could then be coupled to a second free phosphate **85** to generate the pyrophosphate **86** in an apparently quantitative conversion as observed by ^{31}P NMR spectroscopy. Reaction times were very short (2h, 0 °C), but purification proved difficult and isolated yields were only 30-40 %.

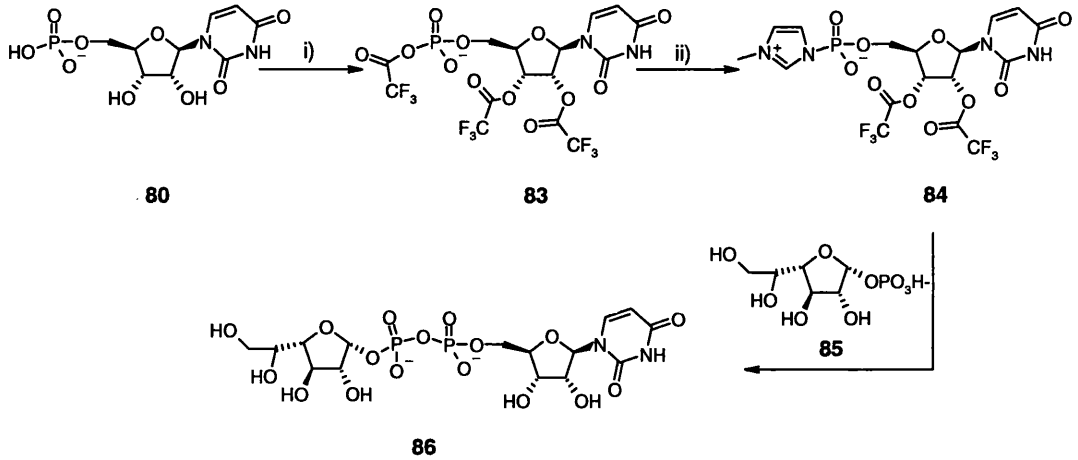

Scheme 31: Formation of the methylimidazolide. *Reagents and conditions*: i) a) Dimethylaniline, Et_3N, CH_3CN, 0 °C; b) added dropwise, TFAA, CH_3CN, 0 °C, 5 mins; ii) 1-methylimidazole, Et_3N, CH_3CN, 0 °C, 5-10 mins

4.2.2 Pyrophosphate synthesis

We initially explored the well established morpholidate chemistry, which lead us to revisit, the reported synthesis of NAD **6**.[37] We chose to generate commercially available AMP-morpholidate **75** from the free acid of AMP **26**.[61] Once formed, (δ_P 8.77), the AMP-morpholidate **75** was precipitated by the addition 0.1 M NaI in acetone in quantitative yield. This was then reacted with β-NMN **21** using 0.2 M $MnCl_2$ in formamide to afford NAD **6** in 27 % yield after ion exchange chromatography (Scheme 32).

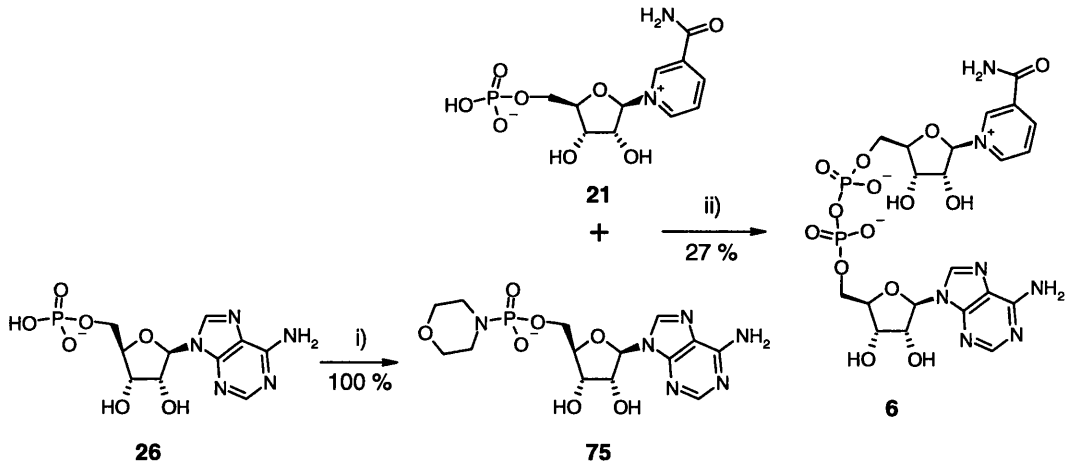

Scheme 32: *Reagents and conditions*: i) Powdered triphenylphosphine, 2,2′-dipyridyldisulphide, morpholine, DMSO, 4 h; ii) 0.2 M $MnCl_2$ in formamide (stored over 4 Å molecular sieves for three days), $MgSO_4$:$7H_2O$, 18 h.

This methodology was transferred directly to the modified adenosine phosphate **74** and synthesis of the activated morpholidate was attempted. *In-situ* analysis by ^{31}P NMR spectroscopy (δ 8.0 ppm) showed the reaction proceeding as expected, but purification proved difficult. Eventually, crude material was used to form the pyrophosphate bond, but analysis by HPLC and ^{31}P NMR spectroscopy showed that no reaction had taken place. This was reasoned to be a result of the poor nucleophilicity of β-NMN **21**. Previous work circumvented this poor reactivity by employing a Lewis acid, [37] but this did not work for our target. We considered that activation of β-NMN **21** as the electrophile component would provide a more reactive, organic soluble starting material.

Using the method reported for the synthesis of UDP-α-D-galactofuranose **86**, generation the β-NMN methylimidazolide, *via* formation of the trifluoroacetyl mixed anhydride was explored.[60] Initial phospho-methylimidazolide activation proceeded with the observation of a singlet at δ –10 ppm in ^{31}P NMR spectrum. Disappointingly, addition of the adenosine analogue **74** did not result in the characteristic pyrophosphate signal in the ^{31}P NMR spectrum and no product was obtained. This reaction was repeated using a variety of model reactants, including coupling between adenosine and cytosine monophosphate, but a pyrophosphate was never isolated from these mixtures. This method was therefore abandoned, although activation of β-NMN **21** was still regarded as essential.

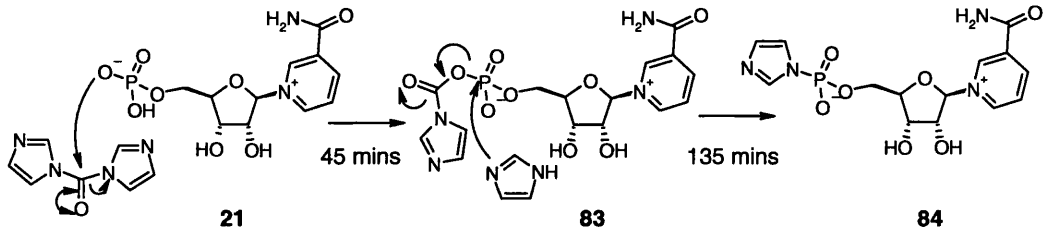

Scheme 33: Formation of the activated β-NMN via the mixed anhydride to the imidazolide with ^{31}P NMR spectra values.

We turned our attention to potentially more simple phosphate activation using carbonyl diimidazole (CDI). Activation of β-NMN **21** occurs in two stages; first the

mixed anhydride is formed **83**, followed by subsequent substitution to the imidazolide **84** (Scheme 33). Initial mixed anhydride **83** formation occurred within forty-five minutes and was accompanied by solubilization of β-NMN **21** in DMF and a shift in the ^{31}P NMR spectrum from approximately 1 ppm to -9 ppm. The second stage was harder to detect by ^{31}P NMR spectroscopy as the chemical shift is only about 0.8 ppm upfield, but after three hours phospho-imidazolide **84** formation was complete (Figure 11). CH_3OH was introduced to quench any remaining carbonyl diimidazole, before the addition of the protected adenosine **74** (Scheme 34).

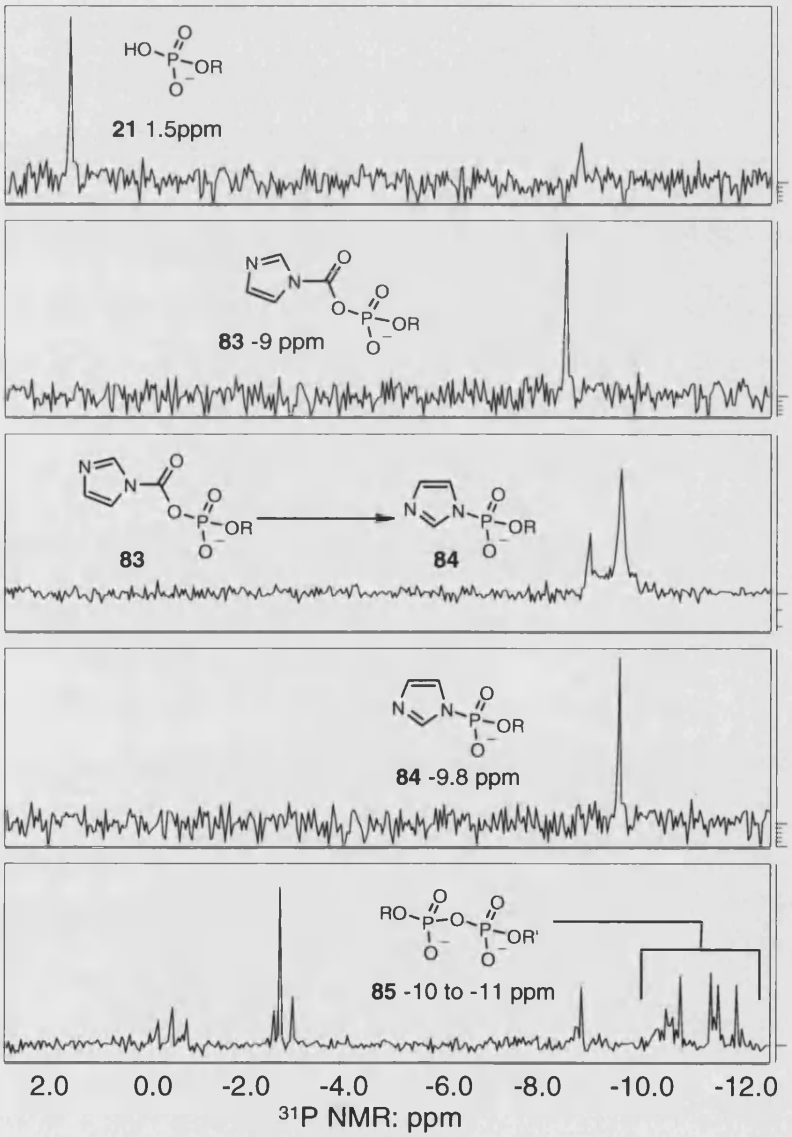

Chemical shift of β-NMN **21**.

After 45 mins the transition to the mixed anhydride **83** can be observed.

After two hours the reactive imidazolide **84** is partially formed.

After three hours the imidazolide **84** is formed and the second phosphate can be added.

The pyro-phosphate signal was observed after 18 h. (The second peak is the 2′ adenosine phosphate at –2.7 ppm).

Figure 11: NMR spectra to show the chemical shift during the pyrophosphate bond formation. Shows reaction drawn in Scheme 34.

The ^{31}P NMR spectrum showed consumption of both the 5′-adenosine phosphate **74** and the activated β-NMN **84** through the production of the characteristic pyrophosphate multiplet at -10 to -11 ppm (Figure 11). Analysis using ion exchange HPLC (AG-MP1) showed the appearance of a new peak at 11 minutes with good separation from any impurities. This retention time was longer than expected and analysis of the crude mixture by mass spectrometry provided a peak at 1055, which suggested Et_3N promoted *β*-elimination of one of the cyanoethyl protecting groups **85** (Scheme 34).

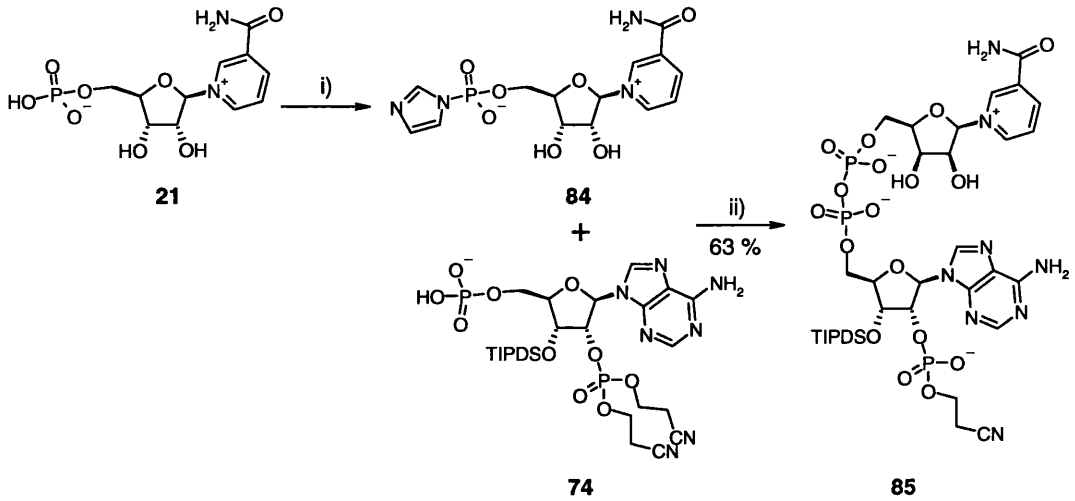

Scheme 34: *Reagents and conditions*: i) a) Carbonyl diimidazole, Et_3N, DMF, 3 h; b) CH_3OH, 10 mins; ii) **74**, DMF, 18 h.

4.2.3 Pyrophosphate purification

As ion exchange HPLC analysis showed distinct peaks, initial purification was carried out on the same quaternary ammonium AG-MP1 resin (Bio-Rad). However, eluting with a gradient of 150 mM aq. TFA apparently caused the gradual cleavage of the 3′-TIPDS group and the only material obtained from this column was disappointing quantities of the desilylated compound **86**. More controlled TIPDS deprotection was attempted by reacting the crude pyrophosphate **85** with a 10 % aqueous solution of TFA. This was monitored by reverse phase TLC and once complete, neutralised with 1 M NaOH and purified on a column of AG-MP1 resin, to afford a 10 % yield (from adenosine analogue **74**) of pyrophosphate **86** (Scheme 35). This was a dissatisfying yield as the HPLC analysis and ^{31}P NMR spectrum both showed a high conversion to the pyrophosphate.

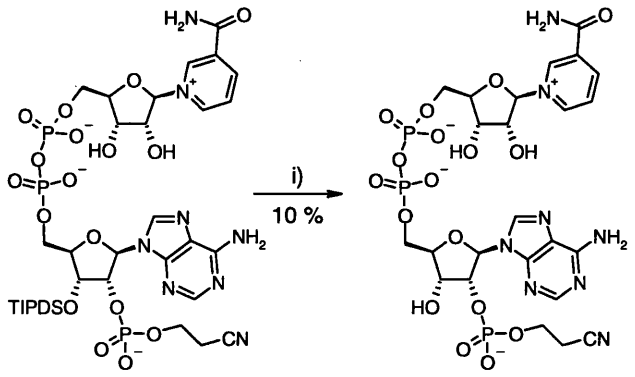

Scheme 35: *Reagents and conditions*: i) 10% aq. TFA, 2 h.

It was suspected that residual sodium trifluoroacetate from the neutralisation increased the conductivity of the solution causing poor adhesion of the compound to the resin. Analysis showed that a 1 % solution of 150 mM aq. TFA possessed a conductivity greater than 400 μS; therefore, to ensure correct adhesion of the products to the stationary phase a conductivity of less than 400 μS was required for loading. Unfortunately, this did not have a dramatic effect on the yield, therefore it was necessary to find a better purification technique.

Size exclusion chromatography was investigated as the product had a molecular weight larger than the two starting materials.[57] Crude pyrophosphate mixture was applied to Biogel P2 beads (1.5 x 70 cm) and eluted using 250 mM NH_4OAc, but this failed to provide any separation. Reverse phase column chromatography was also explored, but co-elution of product and starting material was repeatedly observed. Ion exchange chromatography still offered the best separation due to the negatively charged product, so a different quaternary ammonium resin was sought that avoided the use of TFA.

Q-Sepharose ion exchange resin offers similar characteristics to AG-MP1, and was identified as a purification method incorporating a quaternary ammonium stationary phase. Instead of using 150 mM aq. TFA, this resin required 1 M triethylammonium bicarbonate (TEAB) (pH 7) as the counter ion. The conductivity of the solution still needed to be adjusted to less than 400 μS, but once loaded and eluted, this method produced pure pyrophosphate **85** as the triethylammonium salt, in 63% yield from starting adenosine **74**, with the silyl ether still in place (Scheme 34). Excess Et_3N

needed to be removed, but this was accomplished with repeated co-evaporation with CH_3OH. Isolation and characterisation of this material confirmed that the removal of one cyanoethyl group had indeed occurred, with four cyanoethyl protons being observed in the ^1H NMR spectrum, instead of eight (Figure 12).

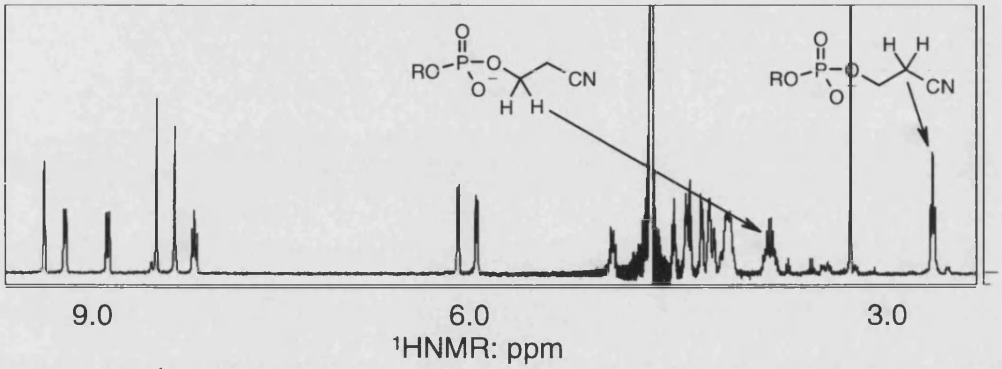

Figure 12: ^1H NMR spectrum showing the signals for the residual cyanoethyl protecting group on **85**.

4.2.4 Protecting group removal

The base labile cyanoethyl and fluoride labile TIPDS protection were selected because of their potential to undergo global deprotection with the addition of tetrabutyl-ammonium fluoride (TBAF).[62]

Initial cleavage conditions were evaluated using the protected diphosphate adenosine precursor **74**. After three hours treatment with 1 M TBAF in THF buffered with AcOH, an increase in the HPLC retention time was observed from 13 to 15 minutes. Purification on Q-Sepharose resin and ^1H and ^{31}P NMR spectroscopy of the isolated material revealed that both the cyanoethyl group and silyl protecting group had indeed been cleaved, but the 2′ phosphate had undergone cyclisation to afford 2′,3′-cyclic phosphate **87** (Scheme 36) characterised by ^{31}P NMR spectroscopy (δ 20 ppm). This was confirmed in the ^1H NMR spectrum by a downfield shift for the 3′-proton to 5.04 ppm together with an increased complexity due to phosphorus coupling.

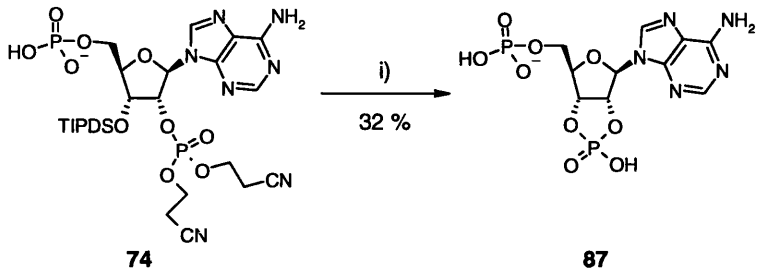

74 87

Scheme 36: *Reagents and conditions*: i) 1 M TBAF, AcOH, THF, 0 °C.

It was suspected that cyclisation was the result of Et_3N catalysed attack on the free 2′-phosphate by the deprotected 3′-hydroxyl, during TEAB evaporation. While, deprotection appeared possible under these conditions, purification would need to be carried out using acidic AG-MP1. Repeating these reaction conditions with the protected pyrophosphate **85** afforded TIPDS cleavage, but removal the second cyanoethyl group did not occur leading to monoprotected NADP **86** in 75 % yield (Scheme 37). It may be that the deprotection observed in the model was due to nucleophilic substitution by the 3′-hydroxyl to afford the cyclic phosphate **87**. To enhance the reaction the pH of the solution was increased by the removal of the acetic acid. As there was no longer a buffer present, any hydroxide ions formed by water contamination reacting with fluoride ions, would accelerate the β-elimination. Upon reaction with **85**, phosphate deprotection was still elusive, with only the desilylated material **86** produced. However, this revealed the glycosidic linkage had a greater stability than previously expected.

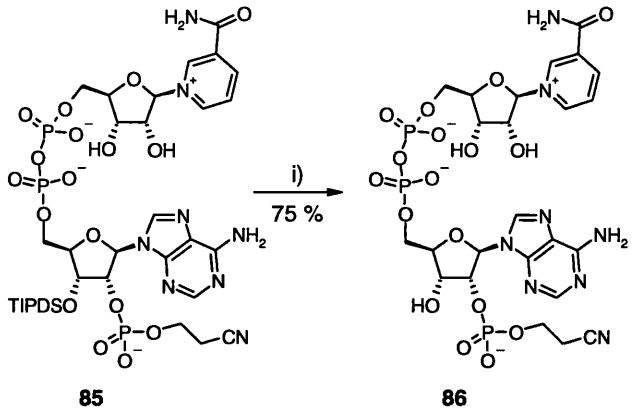

85 86

Scheme 37: *Reagents and conditions*: i) 1 M TBAF, AcOH, THF, 0 °C.

Even though the global deprotection failed, it was satisfying to achieve the NADP **86** precursor in high yield that enabled further exploration into the removal of the final

protecting group. It was speculated that the negative oxygen on the mono-deprotected 2′ phosphate repelled the TBAF, thus hampering β elimination (Scheme 38).

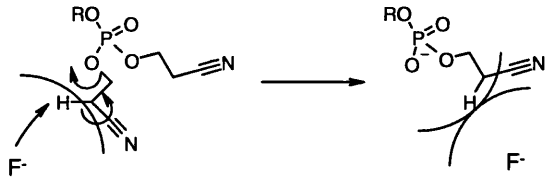

Scheme 38: The repulsion of the negative oxygen and fluoride ion.

Different methods were sought to try to remove the cyanoethyl group using stronger basic conditions.[63,64] A number of literature methods including methanolic ammonia, $^{t}BuNH_2$, Me_2NH and diisopropylethylamine were attempted but were all unsuccessful. All of these conditions only returned starting material, which although unsuccessful, indicated the pyridinium bond to be more stable than initially expected.

Methods were then sought to chemically neutralise the negatively charged oxygen atom to enable base cleavage of the remaining 2′-phosphate protecting group. Previous work during the synthesis of Calyculin A required the removal of *bis*cyanoethyl protecting groups to unveil a free phosphate late in the synthesis. The first protecting group was removed under basic conditions by the addition of DBU, but difficulties in removing the second protecting group were observed. This problem was solved by quenching the newly generated negative charge by silylation of the oxygen **89** using TMSCl. Complete deprotection of the second protecting group was achieved *in-situ* with DBU (**90**), allowing the formation of the free phosphate **91** under mild conditions in excellent yield. However, no reference was made to the deprotection of the TMS groups.[65] A further development used TMSCl with tetramethylguanidine (TMG) as base, to perform the *β*-elimination of the cyanoethyl groups **90**.[66] Methanolic ammonia was then added before the TMS groups were cleaved using mild hydrolysis with AcOH and water to afford the free phosphate **91** (Scheme 39).

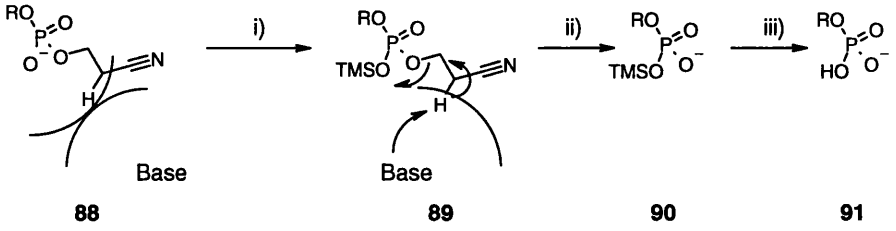

Scheme 39: i) TMS protection; ii) protecting group cleavage; iii) TMS cleavage.

TMSCl and TMG were explored in a trial reaction using fully protected 2′,5′-adenosine *bis*phosphate **74**. The methanolic ammonia step was removed, due to the potential hydrolysis of the pyridinium. The acid hydrolysis was also replaced by TBAF, with the aim of simultaneously cleaving both fluoride labile silicon groups (Scheme 40).

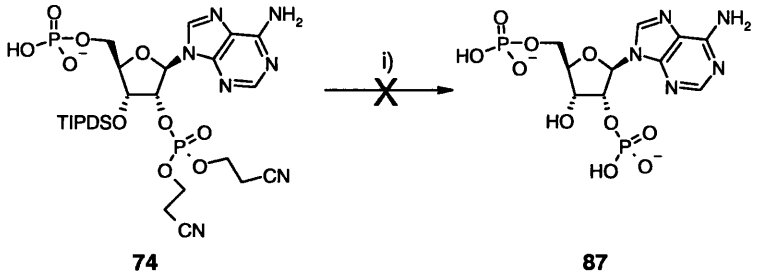

Scheme 40: *Reagents and conditions*: i) a) TMSCl, TMG, CH_3CN, 16 h; b) 1 M TBAF, THF, 3 h, 0 °C.

Unfortunately, there were difficulties in observing even monocyanoethyl cleavage by HPLC analysis and isolation of any materials proved impossible. Due to poor reactivity an alternative TMS donor was used instead TMSCl. Again, a trial reaction was undertaken using 2′-protected *bis*phosphate adenosine **74** to initially cleave the first cyanoethyl group, followed by *in-situ* TMS protection using *N,O-bis*(trimethylsilyl) acetamide (BSA).[67] Subsequent cleavage of the second cyanoethyl with DBU and simultaneous silyl deprotection with TBAF generated a new peak by HPLC analysis at 14 minutes. Purification on AG-MP1 afforded 2′,5′-ADP **87** in an unoptimised, 36 % yield, as confirmed by ^{1}H and ^{31}P NMR spectroscopy (Scheme 41).

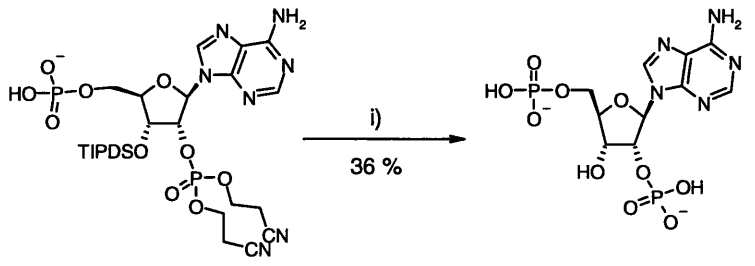

74 87

Scheme 41: *Reagents and conditions*: i) a) BSA / DBU, 90 mins; b) TBAF, THF, 3 h, 0 °C.

This method was transferred directly to the 2′,3′-protected pyrophosphate **85**, and the reaction monitored by HPLC. It was expected that the retention time of the product would be similar at 11 minutes, as the overall charge on the molecule should remain the same. This is because the pK_a of the second phosphate hydroxyl is around 8-9 so only one 2′ phosphate hydroxyl would be ionised during analysis. Upon addition of the BSA / DBU there was no visible change, but after treatment with TBAF the retention time surprisingly increased to 14 minutes. Purification on ion exchange chromatography afforded only the hydrolysed 2′,5′-ADP **87** (Scheme 42).

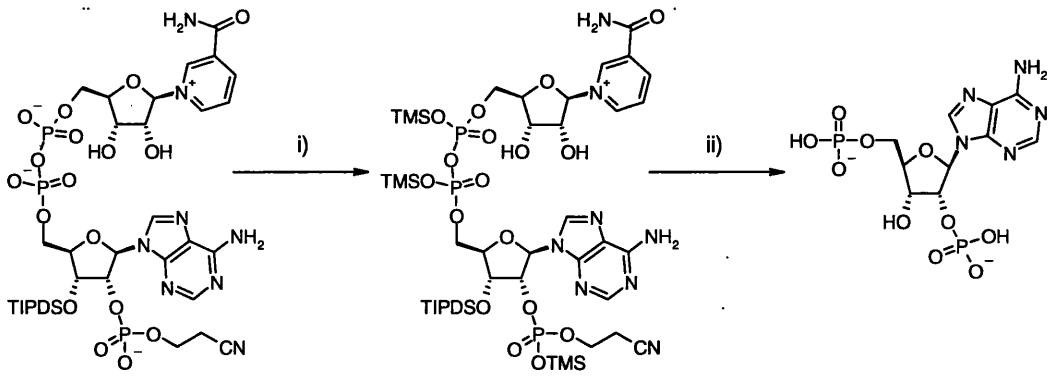

85 92 87

Scheme 42: *Reagents and conditions*: i) BSA / DBU, 90 mins; ii) TBAF, THF, 3 h, 0 °C.

It was suspected that silylation not only occurred at the 2′-phosphate, but also on the pyrophosphate backbone (Scheme 42) and once silylated, the pyrophosphate underwent hydrolysis. Milder conditions were therefore sought to cleave the TMS groups in the hope of avoiding pyrophosphate hydrolysis. TBAF was therefore replaced with an aqueous solution of TFA or AcOH, but both of these afforded 2′,5′-ADP **87**. Material, pre-treated with TBAF to cleave the monoprotected NADP **86**, was subjected to BSA / DBU treatment, followed by, overnight stirring in H_2O to

hydrolyse the TMS groups. This did provide a poor yield, of a product that closely resembled NADP **7**, but careful examination using mass spectrometry revealed a discrete peak at 765, possibly corresponding to the single sodium salt of NADP **7**. Unfortunately, the ^{1}H and ^{13}C NMR spectra provided conflicting results, as no signal was detected for $2_{N}H$ and $6_{A}C$. When this reaction was repeated, the de-purinated product was isolated, as characterised by the absence of the two purine protons in the ^{1}H NMR spectrum. Further work will be required to understand what has taken place, especially as the changes observed relate to different parts of the molecule.

As treatment with BSA / DBU resulted in the total deprotection of the 2′-phosphate, a further method was sought to cleave the TMS groups, whilst avoiding pyrophosphate hydrolysis. Literature TMS deprotection has been performed using HF as the source of fluoride.[67] It was hoped that the 3′-TIPDS along with all the TMS groups could finally be simultaneously removed with anhydrous acidic HF / pyridine to afford NADP **7**. Purification of the result of this reaction on AG-MP1 resin unfortunately only provided nicotinamide adenine dinucleotide (2′-cyanoethoxy) phosphate **86**. It remains unclear why the second cyanoethyl group remained intact as the initial reaction conditions should have removed the protecting groups and reactions reported in the literature using these conditions observe high yielding cleavage.

4.3 Summary

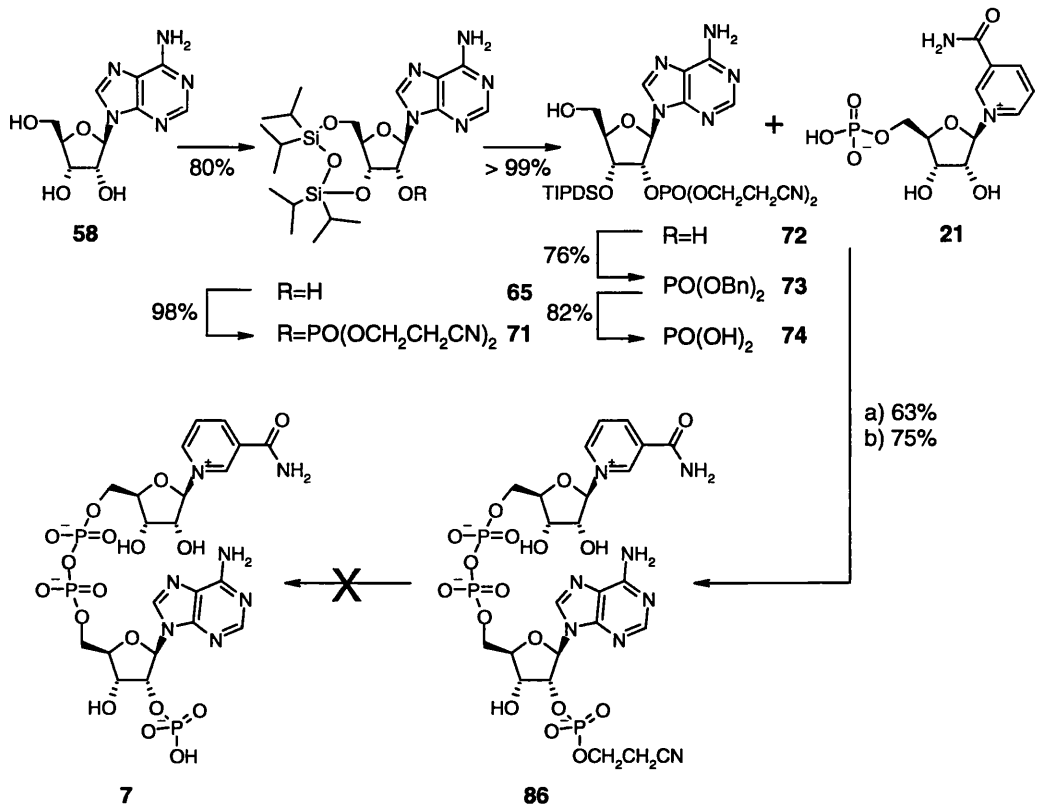

Scheme 43: Overview of the synthetic route adopted in this synthesis

This synthesis provided a high yielding route to the selectively phosphorylated adenosine (Scheme 43) and retains the flexibility to enable rapid analogue synthesis. Pyrophosphate bond formation was successfully optimised and two purification methods were developed, which ultimately provided high yields of pure pyrophosphate. Removal of the final protecting group to afford NADP **7** has proven elusive, but the chemistry developed for the removal of TIPDS group and knowledge gained from the TMS installation will prove invaluable in the development of a secondary route involving different protecting groups at the 2′-phosphate.

Chapter Five

Synthesis of NADP and NAADP

5.1 Introduction

In chapter four it was shown that protection of the 3′-and 5′-hydroxyls allowed installation of a phosphate group at the 2′-hydroxyl without spurious phosphorylation on the purinyl amine. Deprotection and subsequent phosphorylation of the 5′-hydroxyl led to the adenosine diphosphate intermediate **74**. Pyrophosphate chemistry was extensively explored and the resultant CDI coupling proved very reliable affording high yields. Purification was aided by the serendipitous discovery of the cleavage of one phosphate protecting group, enabling isolation and characterisation. Subsequent deprotection however remained elusive and to this end restarting the synthesis with alternative 2′-phosphate protecting groups that could be cleaved under neutral conditions would be required for a route to synthetic NADP **7** and NAADP **3**.

5.2 Selective 2′, 5′ phosphorylation of adenosine

It was anticipated that benzyl phosphoramidite **52**, previously installed at the 5′-alcohol, could be added to the 2′-hydroxyl, ultimately enabling facile cleavage by hydrogenation in the latter stages of the synthesis. It was also expected to be stable to mild basic and acidic conditions and therefore, remain intact throughout the synthesis.

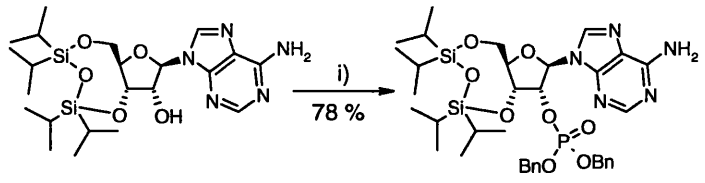

65 **93**

Scheme 44: *Reagents and conditions*: i) a) *Bis*(benzyl)diisopropylaminophosphine **52**, imidazolium triflate **51**, CH_2Cl_2, 18 h; b) *m*CPBA, -78 °C, 30 mins.

The 3′-and 5′-positions were protected as previously described (see chapter four).[46,47] Activation of the phosphitylating reagent required *in-situ* reaction between *bis*benzylphosphoramidate **52** with imidazolium triflate **51** to afford the phosphite at the 2′-hydroxyl.[50] Subsequent oxidation with *m*CPBA afforded the desired phosphate **93** in 78 % yield after silica flash chromatography (Scheme 44). Regio-selective ring opening of the less hindered 5′-silyl-ether was accomplished using mild acidic conditions (TFA–H_2O–THF (1:1:4; *v/v/v*)) leading to the alcohol **94** in 76 % yield (Scheme 45).[52]

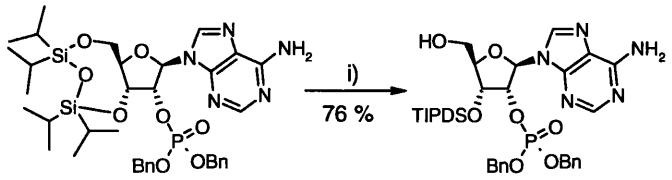

Scheme 45: *Reagents and conditions*: i) TFA–H_2O–THF (1:1:4, *v/v/v*), 0 °C, 4 h.

A range of phosphate protecting groups were explored to generate the 5′-phosphate without degradation of the rest of the molecule.

Treatment of 5′-alcohol **94** with *bis*(2-cyanoethyl)phosphoramidite **69** afforded diphosphate **95**. It was hoped that strong basic conditions could be utilised to afford the free phosphate **96**, however ten equivalents of LiOH destroyed the molecule after one hour with no recognisable peaks remaining in the ^{1}H NMR spectrum (Scheme 46). Removal of the protecting groups was abandoned due to the problems associated with the release of the free phosphate. Only after this work was complete were conditions developed to remove both protecting groups effectively. A second problem was the possibility of base-catalysed cleavage of a benzyl group, which may have been reactive during pyrophosphate bond formation.

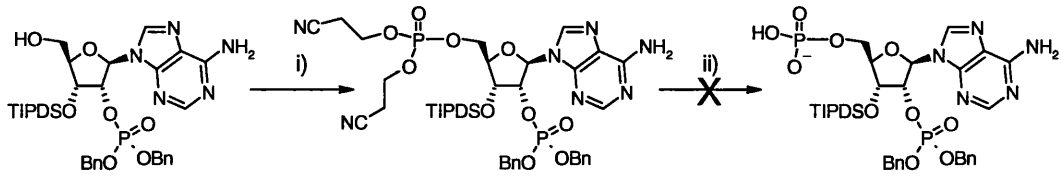

Scheme 46: *Reagents and conditions*: i) a) *bis*(2-cyanoethoxy)diisopropyl-aminophosphine **69**, imidazolium triflate **51**, CH_2Cl_2, 5 h; b) *m*CPBA, -78 °C, 40 mins; ii) 10 equivalents LiOH, 1 h.

Exploring further possible protecting groups suggested that the allyl phosphate could be cleaved using mild, neutral conditions such as, $Pd(PPh_3)_4$, or $Rh(PPh_3)_3Cl$,[68] that should be compatible with the rest of the adenosine functionality. Phosphoramidate chemistry with *bis*allyldiisopropyl-aminophosphine suggested that the reaction had proceeded as expected as observed by the new peak at 0.0 ppm in the ^{31}P NMR spectrum. However, analysis by ^{1}H NMR spectroscopy revealed that the integration for the newly installed allylic C*H*=CH_2 proton was four, rather than two as expected

suggesting that a second protected phosphate had been installed (Scheme 47). This was further confirmed by mass spectrometry data, which showed a peak at 1108 consistent with either the formation of compound **97** or **98**. Based on literature precedent[51] we expected that phosphitylation would only proceed at the purinyl NH_2 if the more reactive phosphotetrazolide was used instead of the imidazolide.[50] To date we have not been able to confirm whether the extra phosphate was bound to the purinyl NH_2 **97** or the silanol hydroxyl **98**. However, an experiment carried out by Christelle Moreau using the protected purinyl amine still observed secondary phosphitylation, suggesting formation of the silanol phosphate related to structure **98**. How an allyl-protected phosphoramidate is sufficiently reactive to attack either the deactivated amine or silanol hydroxyl remains unclear, especially when other phosphitylating reagents, such as *bis*(2-cyanoethyl)-phosphoramidate **69**, only reacted with the riboside hydroxyls.

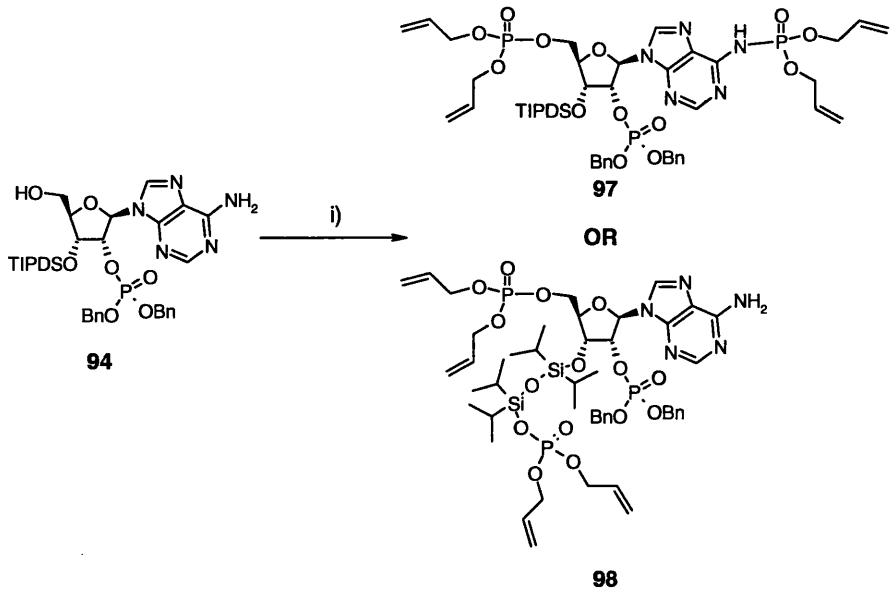

Scheme 47: *Reagents and conditions*: i) a) *bis*(allyl_-diisopropylaminophosphine, imidazolium triflate, CH_2Cl_2, 4 h; b) *m*CPBA, -78 °C, 40 mins.

A diverse range of phosphitylating reagents were screened within the group including the *para*methoxybenzyl, *tertiary*butyl and 2-(methylsulphonyl)ethyl protected phosphoramidites. Unfortunately these were unsuccessful due to difficulties in installing the phosphate using either the *para*methoxybenzyl or *tertiary*butyl phosphoramidites (**102** and **101**); however installation of the sulphonyl

phosphoramidite was possible, affording **99**, but deprotection with 0.1 M NaOH destroyed the molecule (Scheme 48). It was suspected that the failure of the first two routes was due to steric hindrance around the primary hydroxyl. Interestingly though, no secondary phosphitylation was observed on either the purinyl amine or silanol hydroxyl even though large excesses were used to try and drive the reaction to completion.

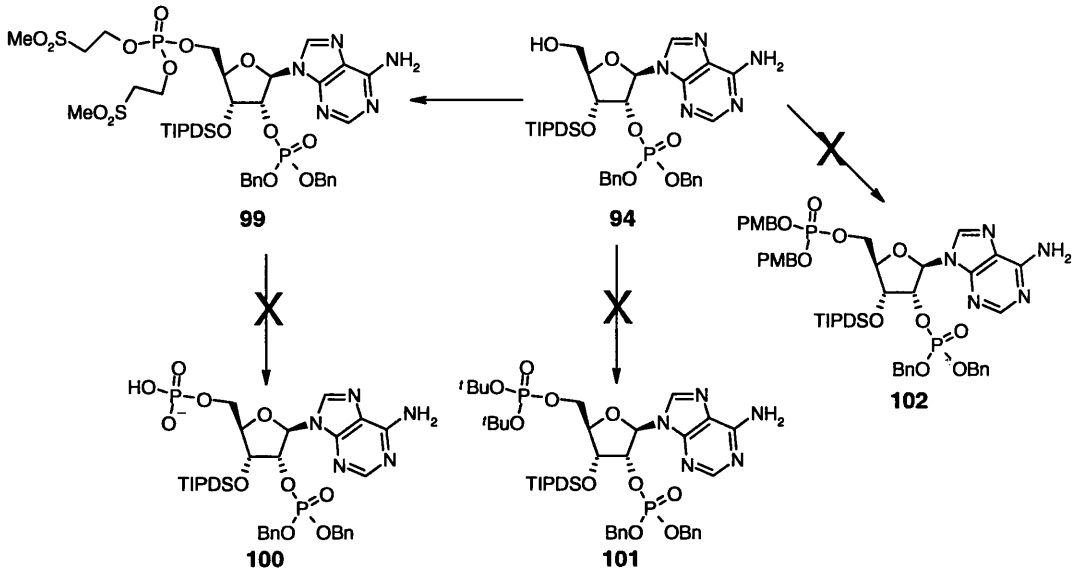

Scheme 48: Overview of work exploring 5′ phosphitylation.

The phosphoramidite chemistry was therefore abandoned and further methods of phosphate installation explored. Formation of *H*-phosphonates is a highly efficient reaction at primary, secondary and aromatic hydroxyls.[69] The resulting *H*-phosphonate is poorly reactive and required activation prior to modification. Work by Christelle Moreau formed the triimidazoylphosphine by the *in-situ* reaction between PCl_3 and imidazole. This species is a mild, yet highly reactive intermediate that upon treatment with hydroxyl efficiently formed the desired 5′-*H*-phosphonate.[69] After quenching with 1 M aq. TEAB and silica flash chromatography the *H*-phosphonate **103** was isolated in 70 % yield (Scheme 49). The identity of this product **103** was confirmed by characteristic signals of the *H*-phosphonate[69] in the ^{31}P and ^{1}H NMR spectra (δ_P 6.8 ppm; δ_H 6.72, $^{1}J_{P,H}$ 630 Hz). The highly reactive P^{III} triimidazoylphosphine is also relatively small and may be able to overcome the steric hindrance difficulties encountered with the phosphoramidite chemistry. Quenching of

the reaction with triethylammonium carbonate led to the formation of an organic soluble salt that could be readily purified using silica flash chromatography.

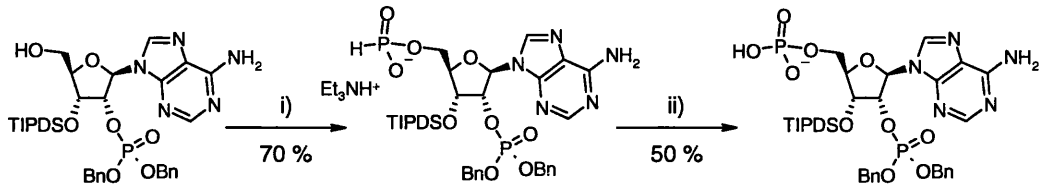

94 **103** **104**

Scheme 49: *Reagents and conditions*: i) a) Imidazole, PCl_3, Et_3N, THF, 0 °C, 15 mins; b) **94**, THF, 15 mins; c) 1 M aq. TEAB, 15 mins, ii) a) BSA, $CDCl_3$, 1 h; b) CSO, 15 mins; c) CH_3OH:$CHCl_3$:D_2O, 2 h.

Oxidation of the *H*-phosphonate is often difficult, but we chose to explore a recently described protocol. Treatment of the *H*-phosphonate with the silylating reagent *bis*(trimethylsilyl)acetamide (BSA) led to a highly reactive trivalent silyl phosphite **105**, which can be oxidised to the silyl phosphate.[70] It was reported that initial treatment with *m*CPBA failed to afford oxidised product, due to excess TMS silylating the peroxide. Oxidising agents were thus sought that did not possess acidic hydrogens.[70] (1*S*)-(+)-(10-camphorsulphonyl) oxaziridine (CSO) **106** performs the oxidation in good yield with no observed side reactions. Consequently, reaction of *H*-phosphonate **103** with *bis*(trimethylsilyl)acetamide proceeded to completion in one hour (**105**). Subsequent oxidation using CSO afforded the *bis*(TMS) phosphate ester **107** in 15 minutes. The two TMS groups were then hydrolysed (with CH_3OH:$CHCl_3$:D_2O over two hours) to afford the free phosphate **104** in 50 % yield after flash chromatography (Scheme 49 and Scheme 50). This process can be conveniently monitored by ^{31}P NMR spectroscopy (Figure 13) that demonstrates satisfyingly clean conversion between each reaction intermediate.

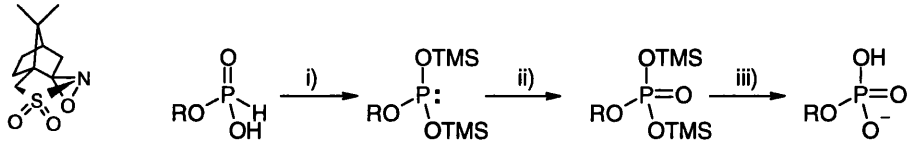

CSO 6 ppm 116ppm -17ppm 1.5 ppm

106 **103** **105** **107** **104**

Scheme 50: *H*-phosphonate oxidation to the phosphate with approximate NMR values and the structure of CSO *Reagents and conditions*: i) BSA, $CDCl_3$, 1 h; ii) CSO, 15 mins; iii) CH_3OH:$CHCl_3$:D_2O, 2 h.

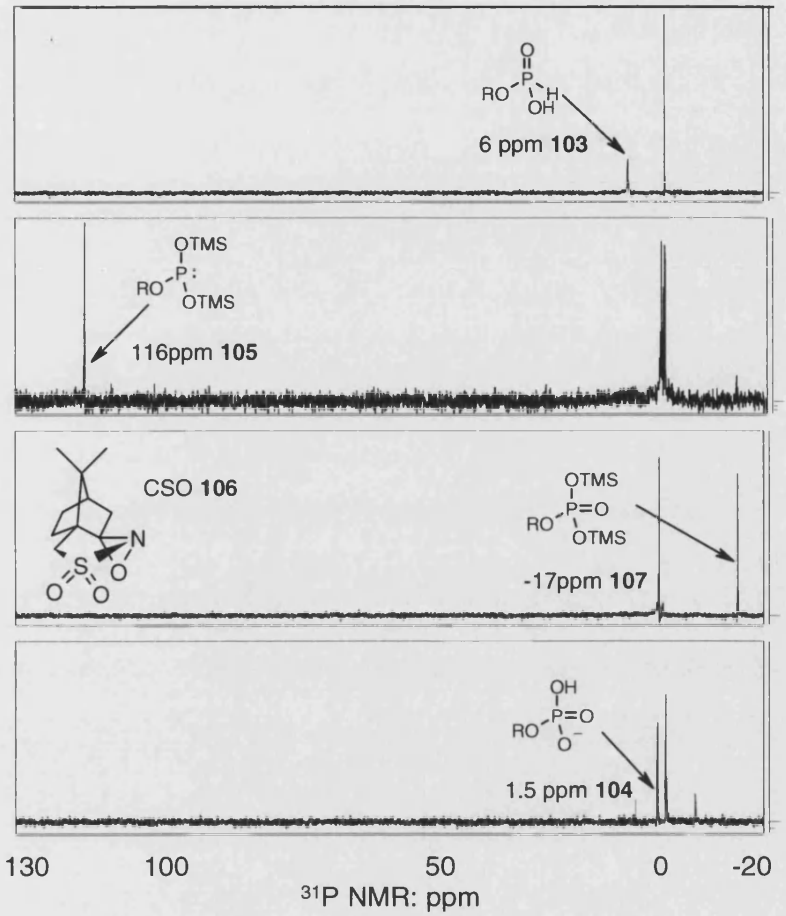

^{1}H-phosphonate **103** peak at δ 5.5 ppm.

Formation of the *bis*-(TMS) phosphonate **105**.

Oxidation to the phosphate ester **107**.

TMS cleavage to afford the phosphate **104**.

Figure 13: A ^{31}P NMR comparison showing the chemical shift associated with the oxidation from *H*-phosphonate **103** to phosphate **104** of the 5′-alcohol. The stationary peak at δ -0.9 ppm is that of the 2′-benzyl phosphate.

It is interesting to note that the *H*-phosphonate is strongly UV active, however upon oxidation to the phosphate the chromophore is apparently quenched. This may be due to a change in conformation causing the aromatic rings on the protected phosphate to interact with the purine ring. This does however make visualisation of the subsequent reactions difficult as HPLC analysis requires a chromophore for detection.

5.3 Pyrophosphate bond formation

With the free phosphate generated, work could be carried out to synthesise the pyrophosphate with subsequent exploration of the deprotection strategy. Pyrophosphate synthesis was performed using the protocol established during previous studies. [58,59] A solution of β-NMN **21** in DMF was activated with carbonyl diimidazole (CDI) and monitored by ^{31}P NMR spectroscopy for generation of the

phosphoimidazolide. CH_3OH was added to quench any remaining CDI, before the addition of the protected adenosine **104**. The coupling was monitored by ^{31}P NMR spectroscopy, which showed the disappearance of starting adenosine **104** after 24 hours and the appearance of the characteristic pyrophosphate multiplet at δ –10 ppm (Scheme 51).

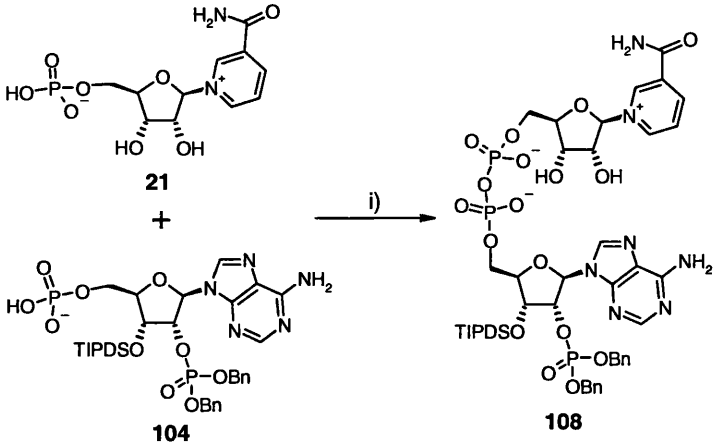

Scheme 51: *Reagents and conditions*: i) a) Carbonyl diimidazole, Et_3N, DMF, 3 h then CH_3OH; b) **104**, DMF, 24 h.

At this stage, HPLC analysis and purification of **108** proved difficult, as the product was still only slightly UV active. Both benzyl groups remained intact throughout the pyrophosphate formation resulting in an amphiphilic product that was difficult to purify by all chromatographic methods. Methods were therefore sought to cleave at least one benzyl group, generating a negative charge that could aid purification by ion exchange chromatography and hopefully enhance the UV activity of the molecule to enable detection.

5.4 Selective protecting group removal

A variety of hydrogenation conditions were explored using the crude pyrophosphate **108** to only release the 2′-phosphate with the aim of aiding purification. 10 % Pd/C with hydrogen and 10 % Pd/C with cyclohexadiene, failed to release the benzyl protected phosphate with only starting material recovered. Catalyst poisoning by the excess imidazole present from the coupling reaction may hinder this debenzylation. Attempts using 20 % $Pd(OH)_2/C$ with cyclohexene at 80 °C resulted in the destruction of the material, presumably a result of the high temperature. Methods were therefore

sought to enable the cleavage of at least one benzyl group to allow purification on ion exchange.

A review of the literature showed that it was possible to achieve monobenzyl deprotection using either TBAF[52] or aqueous TFA,[71] which would be expected to proceed with concomitant desilylation (Scheme 52). The crude pyrophosphate product was treated with a 1:1 (*v/v*) mixture of TFA and H_2O for one hour resulting in simultaneous monobenzyl deprotection and TIPDS cleavage. Monitoring by ion exchange HPLC showed a new peak at 11 minutes, with a retention time similar to peaks observed for the monocyanoethyl pyrophosphate **86**. Notably the monobenzyl NADP **109** was strongly UV absorbing. Observation of the complete shift of the 2′-phosphate peak in the ^{31}P NMR spectrum allowed monitoring of when the reaction was complete (δ_P -1.0 ppm to -0.1 ppm). Complete TIPDS cleavage occurred, thus allowing isolation of the desired mono-protected benzyl NADP **109** using AG-MP1 ion exchange resin, albeit, in a disappointing yield (<5% from starting adenosine **104**).

Further crude pyrophosphate mixture **108** was treated with 1 N TBAF in THF at 0 °C for two hours. AcOH was used to buffer the reaction to protect the labile pyridinium from base hydrolysis (Scheme 52). Again both the TIPDS and a single benzyl group were removed and the mono-benzyl protected NADP **109** was produced in 14 % yield from adenosine 5′ phosphate **104** (Figure 14). Later experiments by Christelle Moreau marginally improved the overall yield to 23 %. Since the fully protected product **108** could not be isolated, we could not conclude whether the pyrophosphate bond formation was high yielding, although we speculate that the main problem is the benzyl deprotection, based on results described in the previous chapter.

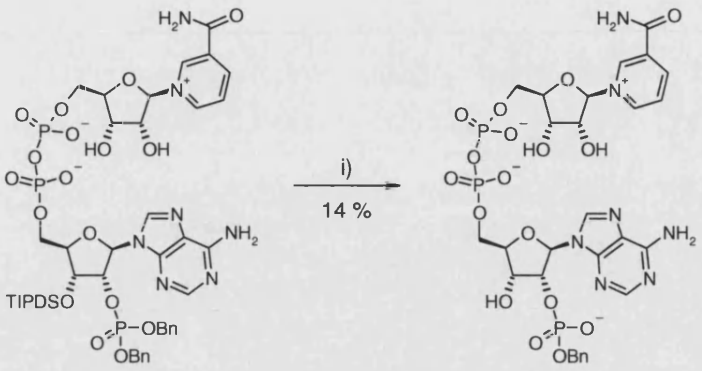

108 109

Scheme 52: *Reagents and conditions*: i) TFA:H_2O (1:1; *v/v*) 1 h, or 1 N TBAF, AcOH, THF, 0 °C, 2 h.

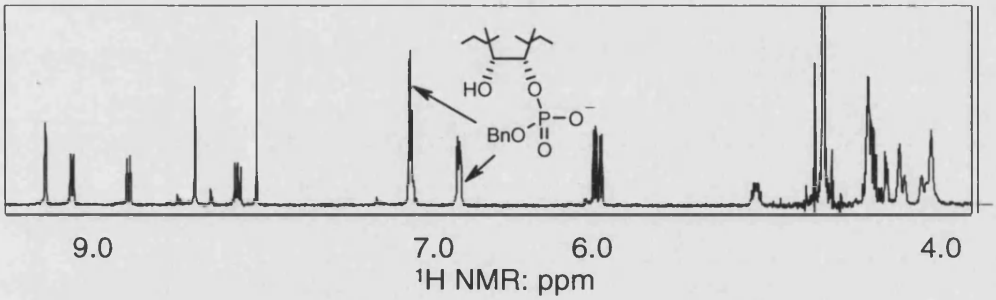

Figure 14: ^{1}H NMR spectrum showing the presence of the benzyl protection.

To check the debenzylation step, fully protected adenosine diphosphate **104** was treated with buffered TBAF, until TLC analysis (with staining) showed that all starting material had been consumed after two hours (Scheme 53). Analysis by ion exchange HPLC showed the desired peak at 14 minutes as well as many impurities. The desired *bis*phosphate **110** was obtained in only a 4 % yield. This is consistent with the destruction observed when the protected NADP **108** analogue was subject to the same conditions and justifies the idea that the poor yield can be attributed to this deprotection step. Further work would be required to explore any other methods for singular benzyl deprotection after pyrophosphate formation that may ultimately aid purification in the same way as for the monocyanoethyl protected NADP **85**.

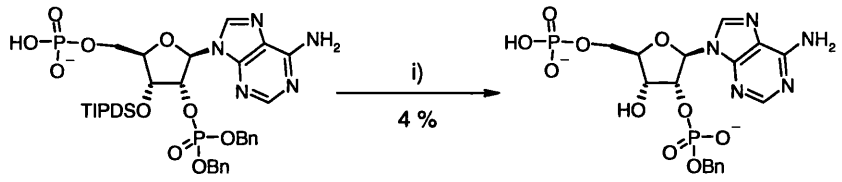

Scheme 53: *Reagents and conditions*: i) 1 M TBAF, AcOH, THF, 0 °C, 2 h.

It appears that to date, at least the best route to monobenzyl protected NADP **109** is using TBAF even though this has been shown to be destructive to the molecule with yields of around 20 %, however this could relate to two 50 % reactions if the pyrophosphate synthesis is not as efficient. It is important to note that the cyanoethyl protected compound afforded a 47 % yield (approximately two times 70 %) over the same two steps with visualisation and isolation available throughout the reactions.

5.5 Synthesis of NADP and NAADP

Isolation of pure monobenzyl NADP **109** did enable hydrogenation conditions to be explored to cleave the final benzyl group. 10 % Pd/C with hydrogen was dismissed as it was found to cleave the pyridinium base. An identical result was obtained when the same conditions were applied to commercial NADP. Transfer hydrogenation using 10 % Pd/C with cyclohexadiene in degassed solvents showed a downfield movement of the 2′-phosphate to δ 0.38 in the ^{31}P NMR spectrum after two hours, indicating the formation of NADP **7**. The mixture was passed through a membrane filter to remove the catalyst and the product eluted on a column of AG-MP1 resin to yield NADP **7** in an unoptimised 31 % (Scheme 54 and Figure 15).

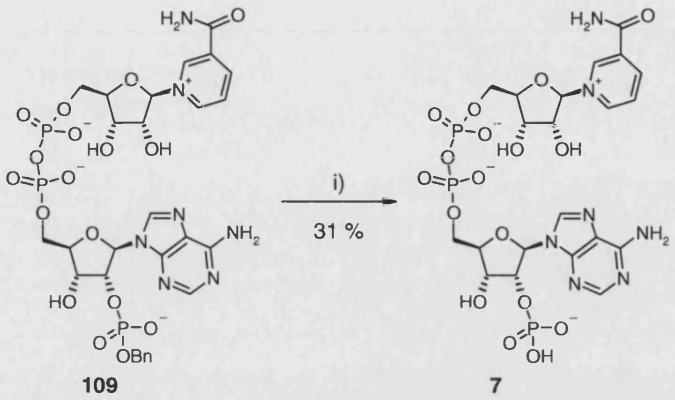

Scheme 54: *Reagents and conditions*: i) 10 % Pd/C, cyclohexadiene, degassed CH_3OH:H_2O (1:3; *v/v*), 2 h.

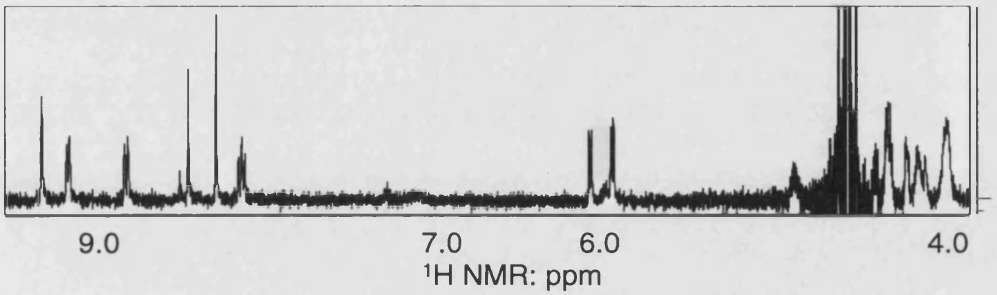

Figure 15: ^{1}H NMR spectrum of NADP showing the total absence of benzyl protons.

Synthetic NADP **7** and nicotinic acid **22** were dissolved in 100 mM AcOH-NaOH buffered to pH 4 to which was added *Aplysia* ADP ribosyl cyclase [EC 3.2.2.5], used to catalyse the base-exchange reaction. The enzyme was used directly from crude extracts from the ovotestis of *Aplysia californica*[72] as it was observed within the group that the quality of the commercially available enzyme varies greatly from batch to batch. The reaction was monitored by ion exchange HPLC for the characteristic increase in retention time, from 10 to 16 minutes (**7** to **3**; Figure 17), caused by the introduction of the acid functionality (Scheme 55). It can also be observed on the HPLC trace the formation of the side product of the reaction with is the hydrolysis of the pyridinium ring to form ADP-ribose (R_T 19 mins). Purification of the reaction by AG-MP1 ion exchange chromatography and isolation of the desired peak at 16 minutes afforded NAADP **3** in 60 % yield (Figure 16 and Figure 17).

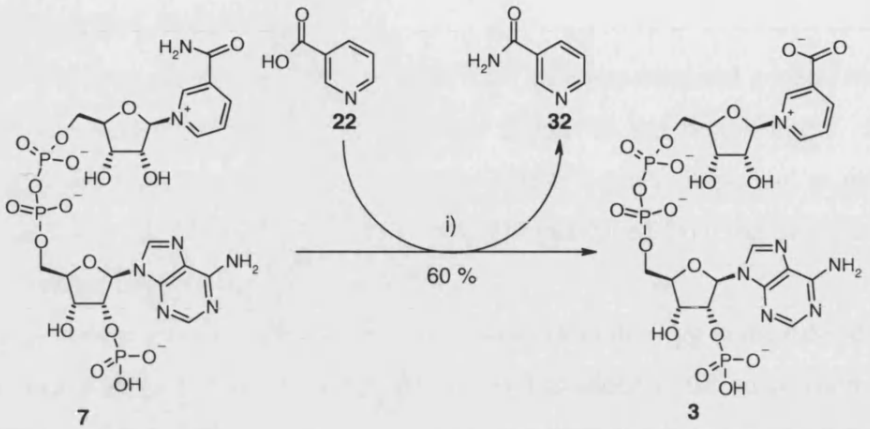

Scheme 55: *Reagents and conditions*: i) *Aplysia* ADP ribosyl cyclase, nicotinic acid, 100 mM AcOH-NaOH (pH 4).

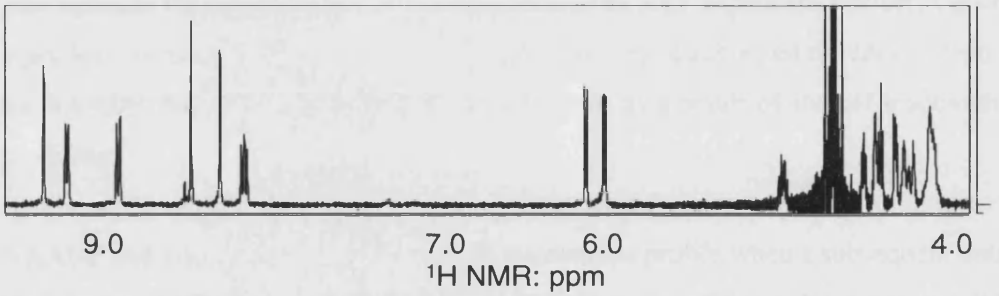

Figure 16: ^{1}H NMR spectrum of NAADP **3**.

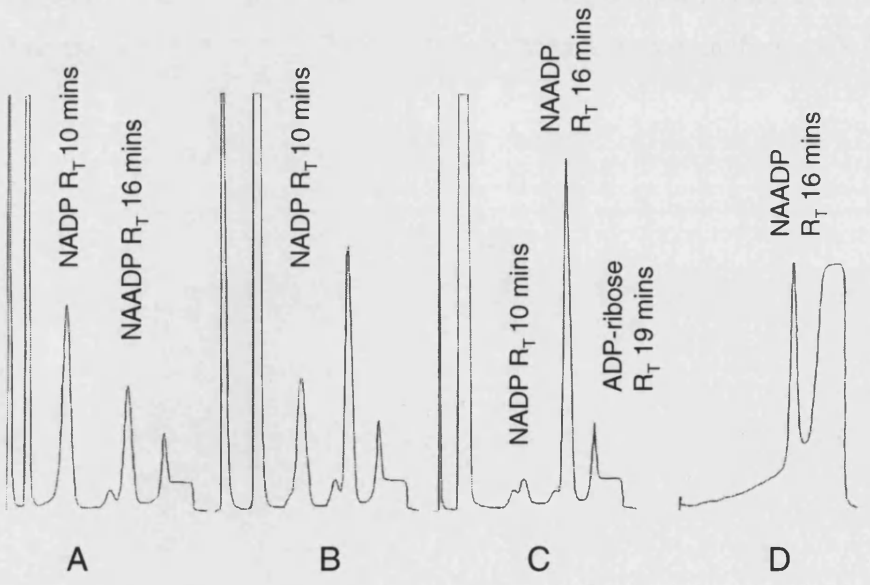

Figure 17: HPLC trace (method A – see experimental general methods) of the enzymatic base-exchange reaction from NADP **7** to NAADP **3**. Part A – Reaction after 1 h. B – Reaction after 3 h. C – reaction after 6 h Also shows the appearance of ADP-ribose as a side product. D – Purified NAADP.

5.6 Biological testing

NAADP **3** was quantified using the Brigg's test[65] (see experimental general method) before being evaluated for inducing calcium release in sea urchin eggs. As the NAADP **3** had been produced from synthetic NADP **7** it was important to establish that its activity was identical to authentic NAADP (produced from the base-exchange reaction carried out on commercial NADP).

Biological results are obtained from homogenised sea urchin egg cells, diluted to 5% and incubated at 17°C. A fluorescent dye, Fluo-3 is added to the suspension before the addition of NAADP. As calcium is released from the homogenate it binds to Fluo-3, causing it to fluoresce, which is detected and recorded. The organelles in the homogenates then pump down the free calcium in an ATP dependant manner, causing a gradual decrease in fluorescence. The cells can then be subjected to repeat injection by NAADP, but this time no calcium is observed as a result of its self-inactivation properties.

Synthetic NAADP **3** produces an identical calcium release profile to authentic NAADP and also produces the same self-inactivation profile when a subsequent batch is re-injected (Figure 18). It is also possible to competitively bind non-labelled, *synthetic* NAADP **3** in preference to [^{32}P] NAADP in exactly the same concentration as non-labelled *authentic* NAADP during binding experiments (Figure 19). This shows that the synthetic NAADP **3** is binding in the same way as authentic NAADP.

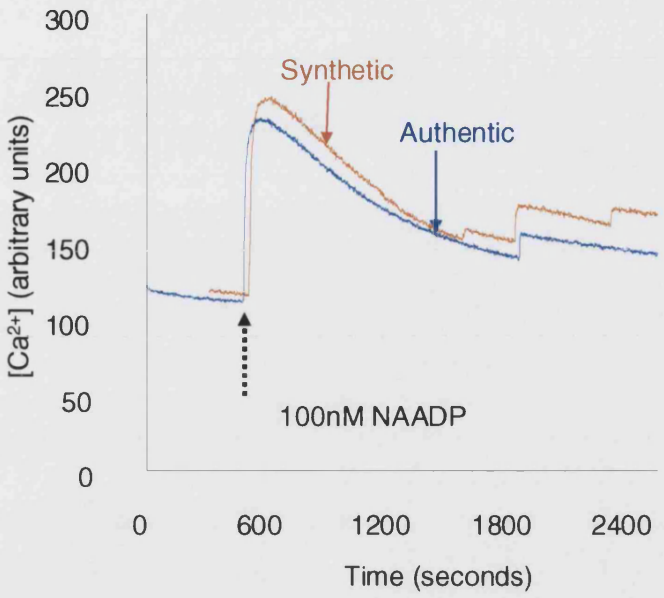

Figure 18: Representation of the calcium release profile observed when synthetic NAADP is compared to authentic NAADP.

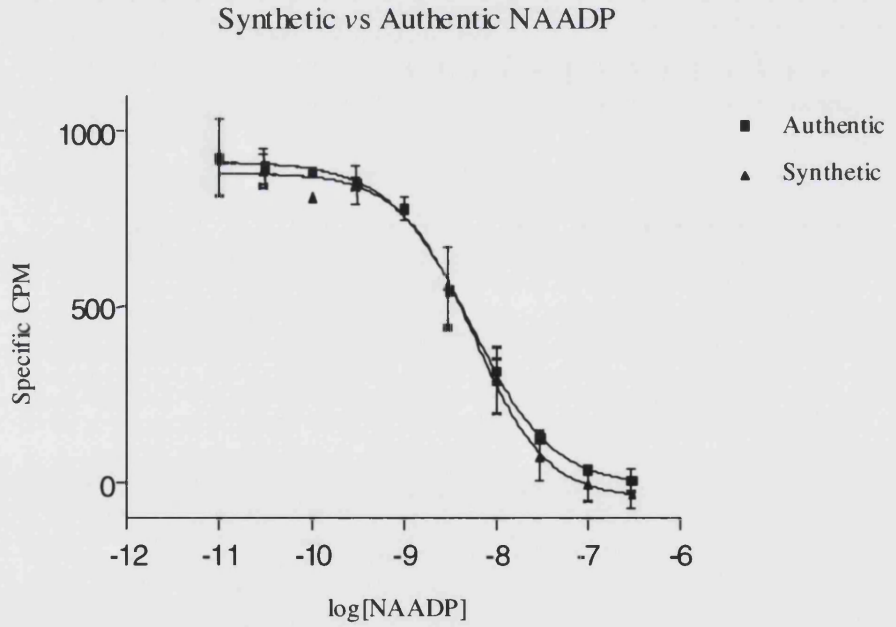

Figure 19: Representation of the competitive binding of 0.2 nM [^{32}P] NAADP with either synthetic or authentic NAADP.

5.6 Summary

Installing a phosphate on the 2′-hydroxyl with protecting groups that are labile to hydrogenation allowed the first total chemical synthesis of NADP **7** to be accomplished. Care was required to isolate the important monobenzyl intermediate **109** ensuring the least amount of material was degraded. Conversion to NAADP **3** afforded the first chemical synthesis to date of this novel calcium releasing second messenger. The biological analysis obtained has proven the identity of the material.

5.7 Future work

Further work will need to be undertaken to synthesise the nicotinic acid ribonucleotide to enable the total chemical synthesis of NAADP **3**, but the overall route is a significant and essential step towards the development of analogues, such as C-glycosides that are inaccessible by any other means. This will allow the interrogation of this important biological pathway to further understand the importance of NAADP at a molecular level.

With a synthetic route in place, work can be undertaken to prepare analogues based on the core structure of NAADP. Initially, this will centre on the replacement of the pyridinium ring with a non-hydrolysable *C-C* bond to the ribose backbone to further understand whether the positive charge, or the labile bond are important in the mechanism of action.

Chapter Six

Synthesis of an NAADP analogue

6.1 Synthesis of a non-hydrolysable β-NaMN analogue

6.1.1 Introduction

With a synthetic route to NA(A)DP **7(3)** developed[73], exploration of analogues was pursued.

Previous reports have shown that replacement of the pyridinium ring with a 4-amide substituted thiazole, have inhibited some NAD dependent enzymes through its increased stability to hydrolysis.[34] Tiazofurin[74] **111** (2-(β-D-ribofuranosyl) thiazole-4-caroxamide) is a non-hydrolysable *C*-nucleoside analogue, which has known biological activity against both human lymphoid and lung tumour cells by being phosphorylated and linked to AMP *via* NMNAT [E.C. 2.7.7.1] to afford thiazole-4-carboxamide adenine dinucleotide (TAD) **112** *in-vivo*.[34,75] As TAD **112**, it mimics the structure of NAD **6** (Figure 20) and inhibits inosine monophosphate dehydrogenase (IMPDH) [EC 1.1.1.205] causing the suppression of *de-novo* biosynthesis of guanidine nucleotides.[34,75] Subsequent decrease in guanidine monophosphate (GMP) and 2′-deoxyGMP not only hinders RNA and DNA synthesis, but also compromises the ability of G-proteins to function as transducers of intracellular signals. Tiazofurin **111** has been shown to be active in reducing the numbers of leukaemic cells in acute myelogenous leukaemia, however, it has been found to be too toxic for clinical application. Recent discovery of two different isoforms of IMPDH,[76] which the type two is up-regulated in human leukaemia has promoted further interest in tiazofurin **111**.

We were interested in producing a carboxylic acid analogue of tiazofurin **113**, which when joined with an appropriately functionalised adenosine would lead to TAADP, **114** that would retain the non-hydrolysable *C-C* bond to the ribose backbone and also its aromaticity. It is anticipated that the negative charge would be held in a spatially similar position when linked to 2′,5′-ADP **87**. This could produce a novel NAADP analogue that may possess activity and enable further investigation of the mechanism of action of NAADP **3** at a molecular level (Figure 20).

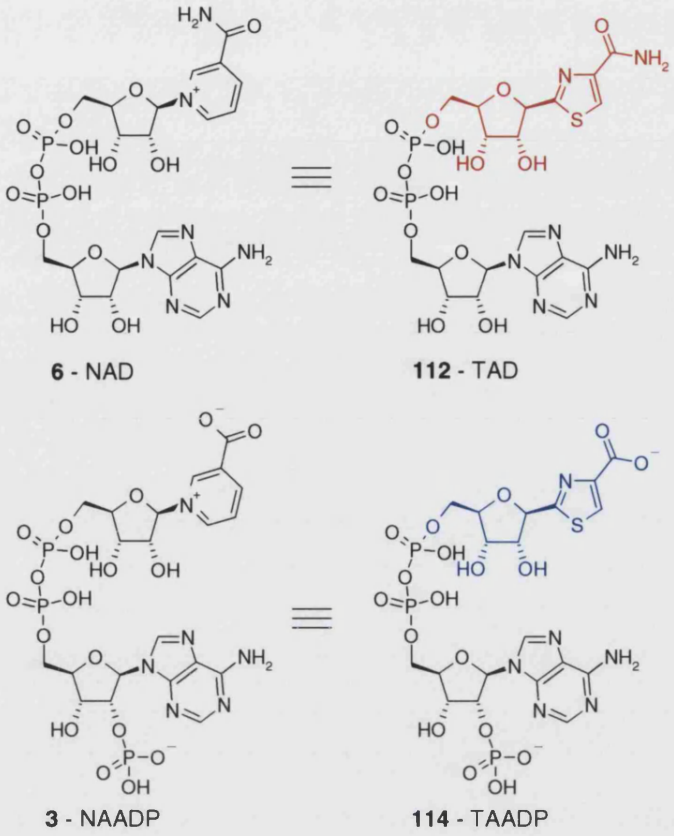

Figure 20: Schematic to show how tiazofurin (red) and its acid counterpart (blue) reflect the structure of the intended pyridinium.

Early syntheses towards tiazofurin **111** used H_2S to generate a thioamide *en route* to the thiazole ring,[77] but H_2S is too toxic and difficult to work with on a large scale. A later synthesis described the formation of the thiazoline ring **115** from the β-cyano ribose **116** using cysteine ethyl ester. Despite testing a wide range of reactions the authors could not oxidise the thiazoline ring instead observing formation of the 1,4-substituted furan **117** (Scheme 56).[75] To alleviate this problem, extra protecting group manipulations were introduced into the synthesis. The 2′-and 3′-benzoate esters were replaced with an isopropylidene group **118**, thus eliminating the unnecessary ribose oxidation. This then allowed successful production of the thiazole **119** *via* the thiazoline **120**, followed by subsequent two-stage deprotection to afford tiazofurin **111** (Scheme 56).

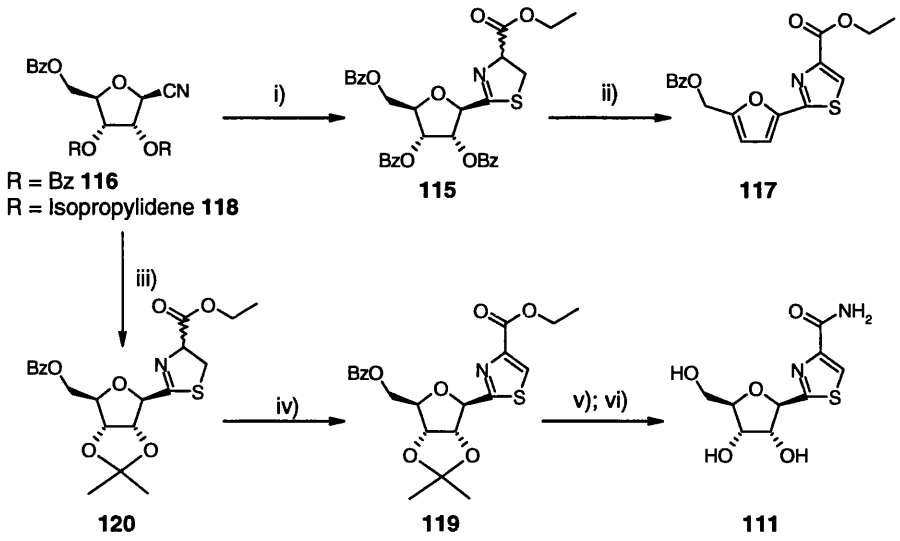

Scheme 56: *Reagents and conditions*: i) Cysteine ethyl ester, Et_3N, CH_3OH, 3 h; ii) MnO_2, benzene or *N*-bromosuccinimide, DBU; iii) cysteine methyl ester, Et_3N, CH_2Cl_2, 24 h; iv) MnO_2, benzene, reflux, 2 h; v) 90% TFA, 1 h; vi) methanolic ammonia, 12 h.

6.1.2 Synthesis of Tiazofurin and analogues

We believed that it was possible to perform the oxidation to the thiazole **121** without concomitant elimination of the two benzoate esters. Commercially available tetra-ester protected ribose **122** was treated with trimethylsilyl cyanide (TMSCN) and 1 M $SnCl_4$ in CH_2Cl_2, leading to the nitrile **116**, in high yield as an orange foam (Scheme 57).[78] The β-stereochemistry was introduced at this stage *via* neighbouring group participation and was confirmed by analysis of the anomeric proton coupling constant of 4.4 Hz in the ^1H NMR spectrum. Near quantitative conversion to the nitrile **116** allowed the product to be used without chromatography of the crude material. Subsequent reaction with cysteine methyl ester led to the ring closure and the thiazoline **123**, again with high conversion.[75] Formation of the thiazoline ring was confirmed by the downfield shift in ^1H NMR spectrum of the methylene and methine protons originally from the starting amino acid. Splitting of the signals was observed due to the epimerisation of the C-4 on the thiazoline ring. Resolution was not required however, as oxidation to the thiazole **121** would remove the stereogenic centre.

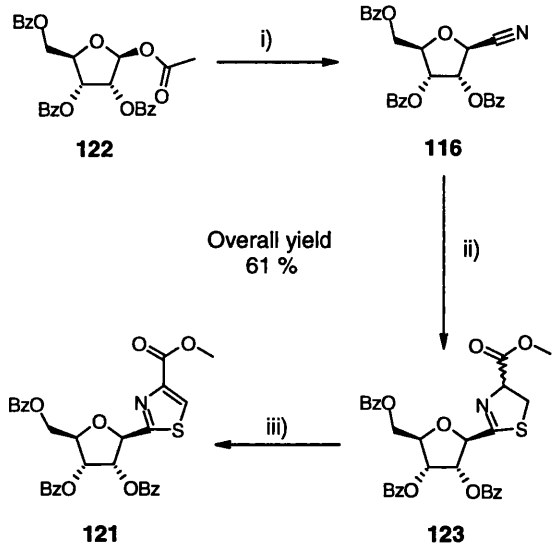

Scheme 57: *Reagents and conditions*: i) TMSCN, 1 M $SnCl_4$, CH_2Cl_2, 2 mins; ii) cysteine methyl ester, Et_3N, CH_2Cl_2, 3 h; iii) $BrCCl_3$, DBU, CH_2Cl_2, 12 h, 0 °C.

The thiazoline **123** was reacted with either I_2–DBU or DDQ–toluene to perform the oxidation to thiazole **121**, but these were found unsuccessful due side reactions complicating isolation.[75] Milder $BrCCl_3$–DBU[79] treatment with the thiazoline **123**, led to smooth dehydrogenation affording the thiazole **121** with no observed 2′,3′-benzoate elimination (Scheme 57). ^1H NMR spectroscopy confirmed the oxidation by the presence of a single aromatic proton (δ 8.15), and the absence of thiazoline methylene and methine protons. The oxidation also removed the chiral centre and simplification of the spectrum was observed. Over the three steps (**122** to **121**) the isolated yield was 61 % (85 % per reaction), which was only subject to flash chromatography at this final stage, providing a high yielding, synthetic route.

Catalytic $CH_3O^-Na^+$ in CH_3OH was utilised to afford the benzoate deprotection with retention of ester functionality to afford the methyl ester **124** as a white gum in 80 % yield. The tribenzoate precursor **121** was also treated with either methanolic ammonia, or 1 M NaOH to afford either tiazofurin **111** in 86 % yield, or the carboxylic acid analogue **113** in 86 % yield (Scheme 58).

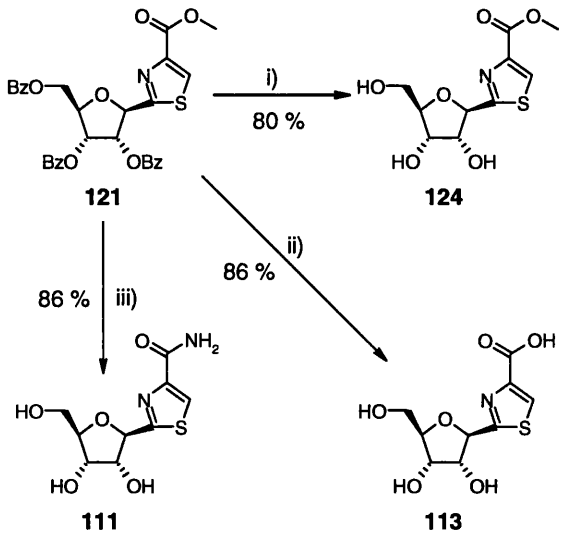

Scheme 58: *Reagents and conditions*: i) $CH_3O^-Na^+$, CH_3OH, 12 h; ii) 1 M NaOH, dioxane, 12 h; iii) methanolic ammonia, 36 h.

This route provided an improved synthesis of tiazofurin **111** and its analogues (**124**, **113**) without the need for toxic H_2S and unnecessary protecting group manipulation. This route confirmed that the selective oxidation of a thiazoline in the presence of sensitive functionality, such as esters is possible with $BrCCl_3$ and DBU. To reach the end products required two chromatographic purifications for the methyl ester **124** or in the case of the carboxylic acid **113** and amide **111** only one due to their hydrophilic nature, making this a very fast and efficient route.[80] Both amide **111** and the ester **124** could be used once phosphorylated, in the formation of a pyrophosphate bond to a suitably modified adenosine analogue that once deprotected would afford either a NADP **7** or NAADP **3** analogue respectively.

6.1.3 Phosphorylation of the primary hydroxyl

Phosphorylation was performed on the methyl ester **124** as it was suspected that the free carboxylic acid **113** might undergo side reactions during pyrophosphate formation. It was reasoned that the carboxylic acid could be unveiled by late stage treatment with alkali, such as 1 M NaOH, but that adequate protection on the 3′-adenosine hydroxyl may be necessary to avoid base catalysed 2′-phosphate cyclisation **125** and/or migration to the 3′-position **126** (Scheme 59).

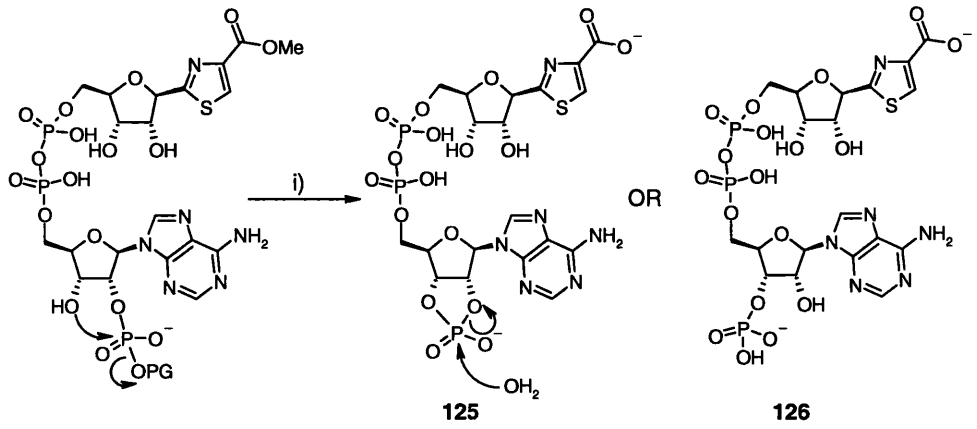

Scheme 59: *Reagents and conditions*: i) 1 M NaOH.

Treatment of the ester **124** with triethylphosphate and $POCl_3$ resulted in the formation of a new peak by ion exchange HPLC analysis (R_T 14 minutes). As the product was negatively charged, purification by quaternary ammonium AG-MP1 ion exchange resin was possible. Isolation from the excess triethylphosphate afforded the phosphate **127** as a hygroscopic yellow gum in 72 % yield after lyophilisation (Scheme 60). This material could then undergo pyrophosphate bond formation. Before that occurred, conditions were sought to provide ester hydrolysis that could be utilised later in the synthesis. Treatment with aqueous alkali (pH 10) produced an increase in retention time as observed by ion exchange HPLC, from 14 to 17 minutes indicating the formation of a second negative charge. Upon isolation using AG-MP1 resin, it was found that the ester **127** had indeed undergone hydrolysis to the acid **128**. This was confirmed by the disappearance of the methyl peak in both the ^1H and ^{13}C NMR spectra. This test reaction confirmed that late stage deprotection may be possible, thus allowing the phosphorylated methyl ester to be carried forward into the pyrophosphate synthesis.

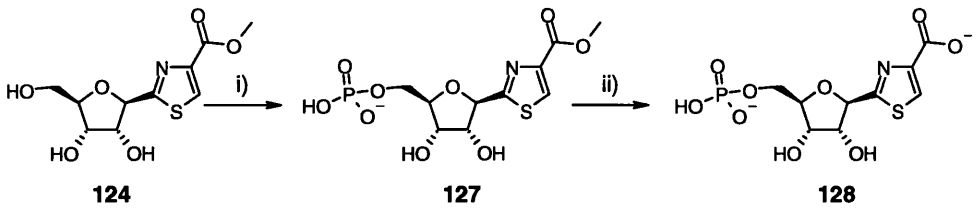

Scheme 60: *Reagents and conditions*: i) Triethylphosphate, $POCl_3$, 0 °C, 90 mins; ii) H_2O (pH 10 with 1 M NaOH), 18 h.

6.2 Synthesis of the NAADP analogue

6.2.1 Pyrophosphate bond formation

The phosphorylated methyl ester **127** was subjected to pyrophosphate coupling using carbonyl diimidazole (CDI) through the formation of the activated phospho-imidazolide *via* the mixed anhydride. ^{31}P NMR spectroscopy was used to monitor the reaction for the formation of the imidazolide peak at δ ~9.5 ppm, which occurred, as expected after three hours; however, the formation of a second peak at δ ~20 ppm was also observed, which remains difficult to explain. After excess CDI was deactivated with CH_3OH 2′-benzyl-phosphate adenosine **104** was introduced, and the reaction monitored for the appearance of the characteristic pyrophosphate multiplet at δ ~10 ppm and the disappearance of the adenosine free phosphate peak at δ 1.2 ppm (Scheme 61).

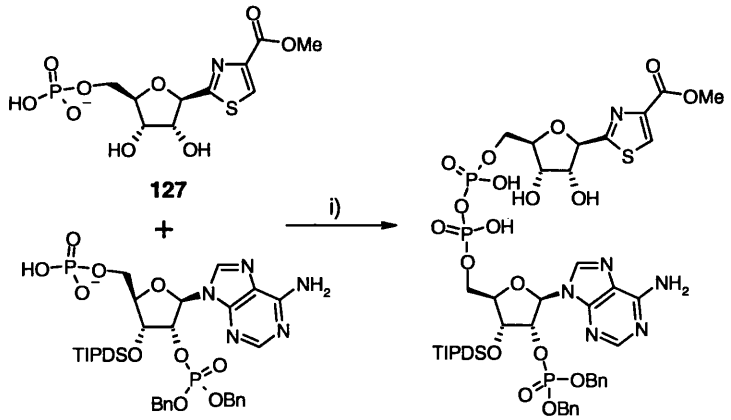

Scheme 61: *Reagents and conditions*: i) a) CDI, Et_3N, DMF, 3 h; b) CH_3OH, 10 mins; c) **104**, DMF, 24 h.

After 24 hours the reaction appeared to be complete, as observed by ^{31}P NMR spectroscopy and initial purification was carried out on silica flash chromatography to try and isolate the pyrophosphate **129**. The product was poorly UV absorbing, presumably due to the quenching of the adenosine chromophore such that TLC only showed the appearance of a new product after staining with PMA (R_F 0.5). Isolation of the material was difficult as the product **129** and starting material **104** have similar R_F's. This did, however, remove excess imidazole from the reaction, allowing hydrogenation to be explored as for the synthetic pathway to NADP **7**. Crude

material **129**, was subject to 10 % Pd/C-catalysed hydrogen transfer conditions to unveil the 2′-phosphate **130** (Scheme 62) that would enable purification by ion exchange chromatography. Analysis by HPLC provided no detectable evidence that debenzylation had occurred, however ^{31}P NMR spectroscopy showed complete conversion to the phosphate (^{31}P δ 1.5 ppm). The material was applied to a Q-Sepharose column, but attempts to elute the product with 1 M aq. TEAB failed to provide product. Without the positive charge normally associated with NA(A)DP **7(3)** the affinity to the quaternary ammonium resin could be greater, and increasing the concentration of buffer to 2 M, did result in compound elution. This material was still impure, however and more importantly, the yield was very low.

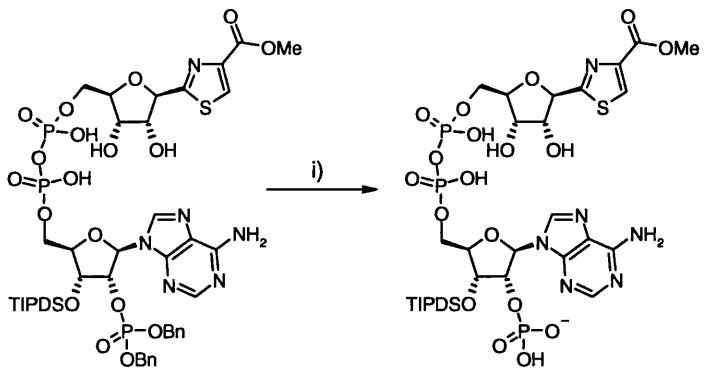

129 **130**

Scheme 62: *Reagents and conditions*: i) 10 % Pd/C, cyclohexadiene, CH_3OH/H_2O (3:1; *v/v*), overnight.

In light of the purification difficulties it was decided that the cyanoethyl protected adenosine **74** would be utilised as it had already provided higher yields along with being easier to handle as a result of the labile 2′ phosphate ester. It was speculated that due to the increased stability of the *C*-glycoside linkage, strongly basic conditions could be used to perform the removal of the second phosphate-protecting group. Also, absence of benzyl groups would preserve the chromophore, thus enabling easier detection.

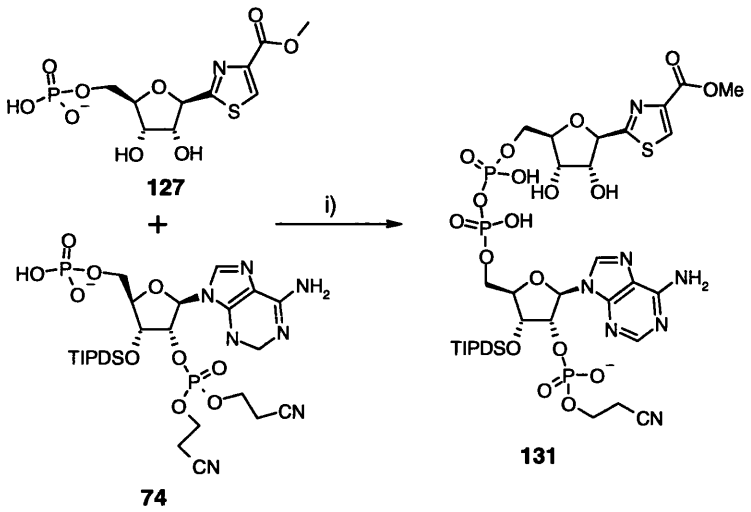

Scheme 63: *Reagents and conditions*: i) a) Carbonyl diimidazole, Et_3N, DMF, 3 h; b) CH_3OH, 10 mins; c) **74**, DMF, 24 h.

The methyl ester **127** was activated following the established protocol and after three hours the cyanoethyl protected adenosine phosphate **74** was added and the reaction stirred overnight. Monitoring of the reaction by ^{31}P NMR spectroscopy showed a complex signal around δ -10 ppm, in conjunction with the consumption of the 5′-adenosine phosphate peak **74**. Analysis by ion exchange HPLC showed the formation of a new peak at 18 minutes enabling the reaction to be purified on Q-Sepharose ion exchange resin and product eluted using 2 M aq. TEAB. HPLC analysis showed the product remained impure however, with a second peak at 14 minutes, that corresponded to starting material **74**. Even though the ion exchange HPLC retention times are different for starting adenosine phosphate **74** and newly formed pyrophosphate **131**, Q-Sepharose resin seemed unable to resolve them. At this stage it was not possible to use AG-MP1 ion exchange resin, as TFA would cause the cleavage of the 3′-TIPDS protection, which is required until basic ester hydrolysis has occurred to ensure that 2′-phosphate migration does not occur (Scheme 59). It was therefore decided to use the product crude in the subsequent phosphate deprotection

6.2.2 Protecting group cleavage

It was speculated that the base labile cyanoethyl group would undergo β-elimination using a strong base, such as aqueous NaOH. As no other base sensitive groups are contained in the molecule and the 2′-phosphate can not migrate, NaOH would afford the concomitant phosphate deprotection and thiazole-methyl ester cleavage to afford

the 3′-protected TAADP **132**. After treatment of crude **131** with aqueous NaOH (pH 10) overnight the ^{31}P NMR spectrum showed the downfield movement of the phosphate peak from δ -2.0 ppm to δ 4.2 ppm suggesting that cyanoethyl deprotection had proceeded as expected (Scheme 64). HPLC analysis showed a new peak at 20 minutes, a result of the carboxylic acid negative charge, but again purification on Q-Sepharose resin afforded a mixture of products, so the product was used crude in the subsequent TIPDS cleavage.

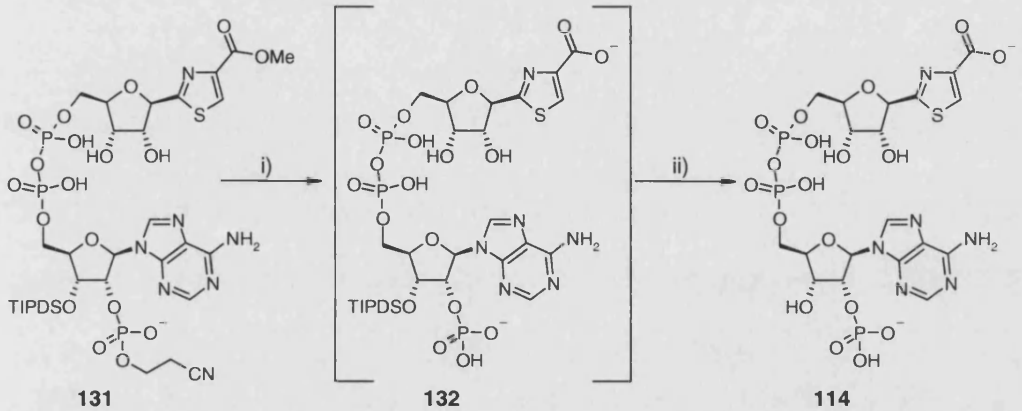

131 **132** **114**

Scheme 64: *Reagents and conditions*: i) H_2O (adjusted to pH 10 with 1 M NaOH), overnight; ii), HF / pyridine (7/3), pyridine, 20 mins.

Finally, with the basic reactions accomplished the 3′-TIPDS[67] protection could be removed using acidic HF in pyridine for 20 minutes. Purification on AG-MP1 allowed successful separation of the two materials and isolation of TAADP **114** as a white hygroscopic powder. Unfortunately, when analysed this material was found to be contaminated with approximately 10 % of an unknown compound. It is speculated that this maybe a result of degradation producing 2′,5′-ADP **87**, but further analysis will be required to confirm this (Figure 21).

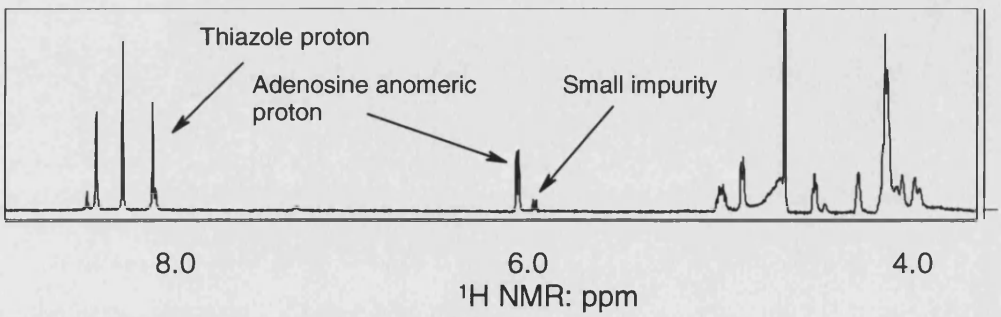

Figure 21: ^1H NMR spectrum of TAADP **114.**

6.3 Biological results

To enable accurate phosphate quantification a Brigg's test[65] (see experimental general methods) was carried out on TAADP **114** before being evaluated for calcium release properties within sea urchin egg homogenates. Preliminary data suggest that crude TAADP **114** does cause calcium release from a pool receptive to either Ins(1,4,5)P_3 **1**, cADPR **2** or NAADP **3** as the data shows a depleted release in response to subsequent activation by TAADP **114** (Figure 23). It has been rationalised that the calcium store depleted by TAADP **114**, is that stimulated by Ins(1,4,5)P_3 **1** as successive exposure leads to a minimal response (Figure 24). Both cADPR **2** and NAADP **3** are unaffected by this store depletion and function as normal. Initial indication therefore is that TAADP **114** is an Ins(1,4,5)P_3R partial agonist. This is a very interesting discovery for two reasons. Firstly it does in fact cause calcium release and secondly it appears to be from a store other than that of NAADP **3**. This was a surprising result, as the SAR data lead us to believe that TAADP **114** could be a potential NAADP receptor agonist, along with a longer duration of action if pyridinium hydrolysis was the mechanism of inactivation. TAADP **114** does share some similarity to the potent Ins(1,4,5)P_3 agonist adenophostin **134** insomuch as the adenosine is phosphorylated at the 2′-position, but this does not account for the thiazole component, but may explain some of the observed activity (Figure 22).

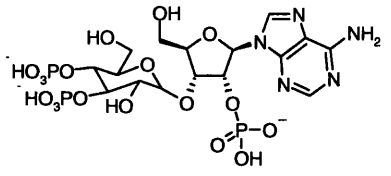

134

Figure 22: Adenophostin

It has also been shown that stores inhibited by thapsigargin are not responsive to calcium release by TAADP **114** and that the release from NAADP stores is independent of TAADP **114** concentration, confirming its action on the Ins(1,4,5)P_3R. At this stage though the material that is being tested does contain a small percentage of impurity as observed in Figure 21 and this does need to be characterised to enable accurate data to be obtained.

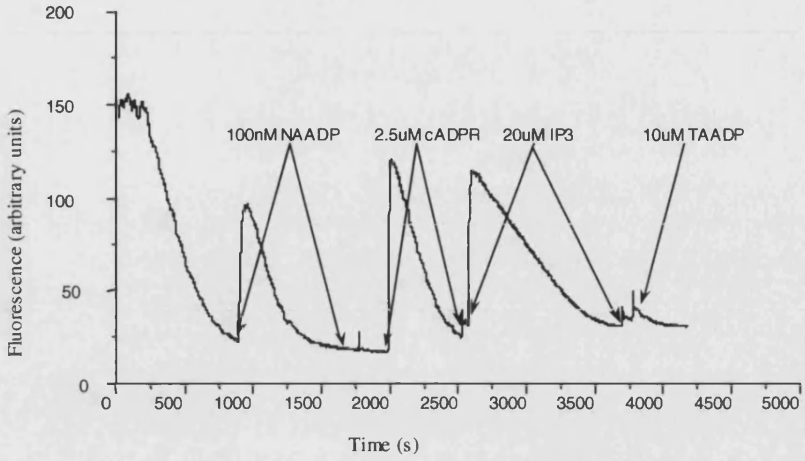

Figure 23: Data representing depletion of all three discrete calcium stores followed by subsequent exposure to TAADP **114** causing no calcium release.

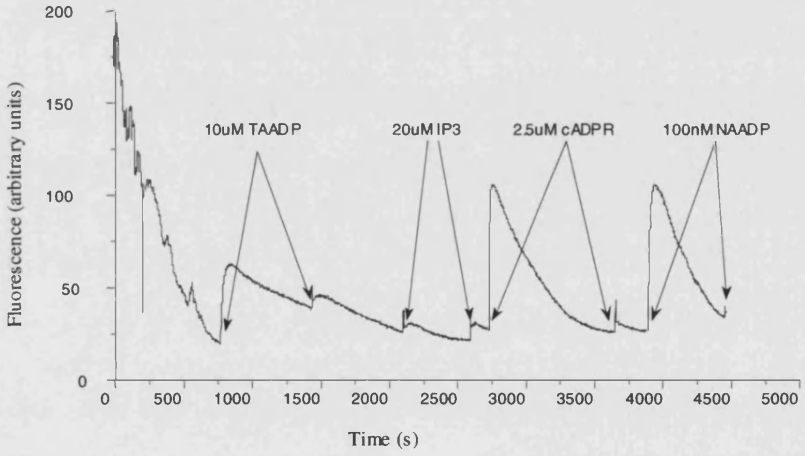

Figure 24: Data representing the depletion of Ins(1,4,5)P_3 **1** sensitive calcium stores after exposure to TAADP **114**. Calcium stores responsive to cADPR **2** and NAADP **3** are unaffected.

6.4 Summary

This synthetic route provided an analogue, which has undergone biological testing. It brings together two very high yielding and efficient synthetic schemes through the formation of a pyrophosphate bond between phosphorylated thiazole riboside **127** and cyanoethyl protected adenosine *bis*phosphate **74**. Unfortunately, even though the pyrophosphate formation appeared high yielding, problems with purification meant that the intermediates could not be accurately characterised. It has been possible though to synthesise an analogue that retains the 2′-phosphate, without formation of the 3′-regio-isomer, whilst retaining the negative charge on the aromatic ring.

Disappointingly, it proved problematic to remove the small percentage of impurity from this sample and to obtain indisputable biological results, requires this to be accomplished.

6.5 Future work

Isolation of the impurity observed in the sample of TAADP **114** is important and as it is currently suspected to be 2′,5′-ADP **87**, this could be synthesised by the hydrolysis of NADP **7**. Work will need to be carried out to try and develop the purification techniques to allow the isolation of the intermediates from the pyrophosphate formation. This will not only allow accurate quantification and characterisation of the compounds, but will also help overall yield optimisation by highlighting the poor reactions. For the purposes of biological evaluation further analogues would need to be produced to provide standards and also SAR information. These would need to include the amide derivative of the carboxylic acid, TADP **135** and also the dephosphorylated product TAAD **136** (Scheme 65).

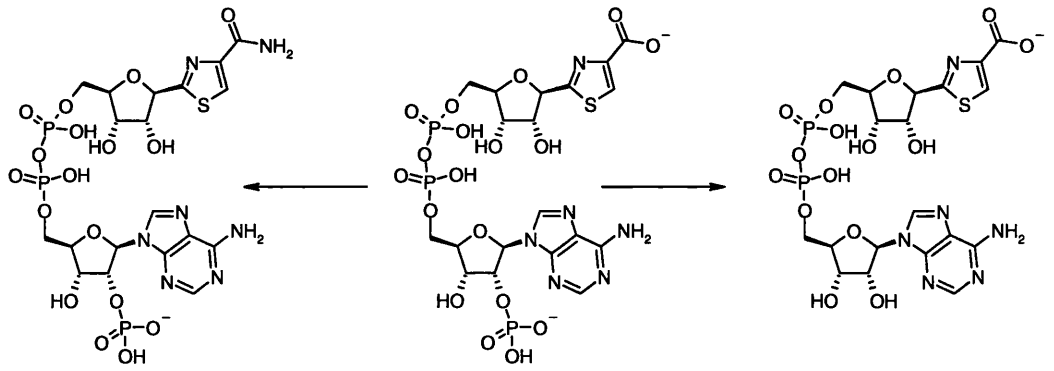

Scheme 65: Proposed analogues required for biological testing. The FGI to the amide, TADP **135** and the dephosphorylation to TAAD **136**.

Chapter Seven

Experimental

Experimentals

7.1 General methods

All compounds were used as received unless otherwise stated. ^{1}H and ^{13}C NMR spectra were recorded on either a Jeol JMX GX-270 MHz, Varian EX-400 MHz or 600 MHz Inova spectrometer using deuterated chloroform, acetone, methanol, dimethylsulfoxide or D_2O. ^{31}P NMR reaction monitoring was accomplished in either a deuterated solvent or *via* an internal capillary filled with either CD_3COCD_3 or CD_3OD. ^{31}P NMR chemical shifts were measured in ppm and relative to external reference 85 % H_3PO_4. The following abbreviations are used to describe the signals in the ^{1}H NMR spectra. s, singlet; br, broad singlet; d, doublet; t, triplet; q, quartet; m, multiplet. For dinucleotides, the top half (*e.g.* nicotinamide ribose) is no prime and the bottom half (*e.g.* adenosine) is prime. To differentiate the base (*e.g.* adenine) is by subscript letters (*e.g.* $_{ad}$). The ribose moiety is without letters.

Thin layer chromatography (TLC) was performed on precoated plates (Merck silica gel 60 F_{254} aluminium sheets) with visualization using UV light and staining with $KMnO_4$, anisaldehyde in EtOH and phosphomolybdic acid in MeOH. Column chromatography was carried out using silica gel (Matrix 60 particle size 35 – 70 microns).

Mass spectrometry data were obtained using a Micromass Autospec machine. IR spectra were obtained using a Perkin Elner spectrum RX IFT-IR using either a KBr disk or thin film and are expressed as cm^{-1}.

Optical rotations were obtained at ambient temperature using an Optical Activity Ltd AA-10 polarimeter in a cell volume of 1 ml or 5 mL and specific rotation are expressed as $^{\circ}$ ml g^{-1} dm^{-1}.

Melting points were determined using a Reichert-Jung Therm Galen Kofler block and are uncorrected.

CH_3CN was distilled from CaH_2 and stored over 4 Å molecular sieves. Et_3N was distilled from Et_3N and stored over KOH. Pyridine was distilled from KOH and stored over KOH. Trifluoroacetic anhydride was freshly distilled from P_2O_5 and used immediately.

Ion exchange analysis was carried out on a Hewlet Packard 1050 HPLC using an AG MP-1 column (3 x 150 mm) with UV detection set at 254 nm. Small particles were removed from the AG MP-1 by suspending in a large volume of Milli-Q (MQ) water

(100 mL / 10g) then discarding any material left in suspension. The AG MP-1 was washed with 1 M NaOH (20 mL / g) then with MQ water until pH < 9. This was then washed with 150 mM aq. trifluoroacetic acid (TFA) (20 mL / g). To pack the column, two columns were joined together with a sleeve, securing them vertically, fitting an end cap with a frit to the bottom, then adding the slurry and allowing it to settle by gravity. An end cap with a frit was fitted to the column and it was then attached to the HPLC machine and 150 mM aq. TFA was pumped through at 5 mL / min for 15 minutes to pack the column. The sleeve was then removed and the bottom column fitted with an end cap with a frit. The compounds were then eluted from the column using a gradient of water – 150 mM aq. TFA to elute the compounds.

Method A: 1minute – 1% aq. TFA, 2 minutes - 2% aq. TFA, 5 minutes - 4% aq. TFA, 9 minutes – 8% aq. TFA, 13 minutes – 16% aq. TFA, 17 minutes - 32% aq. TFA, 18 minutes – 100% aq. TFA, 21.10 minutes - 0% aq. TFA, 25 minutes – 0% aq. TFA.

Reverse phase ion exchange chromatography was carried out on a Phenomenex Aqua column, 5 microns, C18; 125A 150 x 4.60 mm.

Method B: 100 % H_2O for 10 mins, linear gradient to H_2O:CH_3CN 1:1 over 20 mins, linear gradient to 100 % H_2O over 1 min, 100 % H_2O for 5 mins.

Product isolation using ion exchange was carried out on a Pharmacia LKB-gradifac. The conductivity of solutions loaded onto the resins was adjusted to less than 400 μS. AG-MP1 resin was eluted using a linear gradient of water – 150 mM aq. TFA eluting at 2 mL / min and Q-Sepharose fast flow resin eluted using a linear gradient of either 1 or 2 M aq. TEAB at 5 mL / min. Both methods collected 10 mL fractions per test tube. Peak determination was carried out using UV absorption at 260 nm.

Synthetic phosphates were assayed by adaptations of the Brigg's test[65] as follows. For a quantitative test a standard curve was generated to calculate the quantity of the synthetic compound. Care was taken to use clean test tubes free from detergent. Using a series of tubes (in triplicate) increasing quantities of 10 mM KH_2PO_4 (10 nmol phosphate in 10 μL) were added.

Tube 1	0 µL phosphate	200 µL MQ water.
Tube 2	10 µL phosphate	190 µL MQ water.
Tube 3	20 µL phosphate	180 µL MQ water.
Tube 4	30 µL phosphate	170 µL MQ water.
Tube 5	40 µL phosphate	160 µL MQ water.
Tube 6	50 µL phosphate	150 µL MQ water.
Tube 7	60 µL phosphate	140 µL MQ water.
Tube 8	30 µL of compound	170 µL MQ water.
Tube 9	40 µL of compound	160 µL MQ water.
Tube 10	50 µL of compound	150 µL MQ water.

Tubes were placed in the oven at 180 °C for 15-30 minutes to evaporate to dryness.

Once dry 4 drops of conc. H_2SO_4 was added to each tube and replaced in the oven for 90 minutes at 180 °C.

The following solutions were then freshly prepared.

Solution 1 – ammonium molybdate (5 g) in MQ water (40 mL) and conc. H_2SO_4 (16 mL) while cooling.

Solution 2 – hydroquinone (200 mg) in MQ water (40 mL) and conc. H_2SO_4 (2 drops).

Solution 3 – sodium sulphite (8 g) in MQ water (40 mL).

Tubes were the removed and cooled to room temperature.

To each tube was added:
- 250 µL of MQ water
- 500 µL of solution 1
- 250 µL of solution 2
- 250 µL of solution 3

The resulting mixtures were heated until boiled for 10 seconds.

Each solution was diluted with MQ water to 10 mL in a volumetric flask.

Each sample was analysed using a UV spectrophotometer at 340 nm.

Quantification of the compound is then calculated using the standard curve.

Extraction of ADP-ribosyl cyclase enzyme from ovotestis.
Buffer: 250 mM sucrose, 20 mM HEPES pH 8, 1 mM EDTA, 1 mM phenylmethyl-sulfonylfluoride (PMSF) and 1 μg/mL leupeptin.

2.8 g of ovotestis were homogenisedin buffer (5:1 buffer volume to wet weight of tissue) followed by a two-step centrifugation procedure. The first step was a low speed centrifugation (13000 rpm at 4 °C for 20 minutes). The pellets were then discarded and the supernatant was subjected to a high-speed centrifugation (37000 rpm at 4°C for 2 hours). The supernatant was collected and the enzyme activity was assayed by completing the sunthesis of NAADP.

Enyme assay
5 mM NADP (4 mg) and 100 mM nicorinic acid (12 mg) in a 100 mM solution of AcOH / NaOH (pH 4, 1 mL) were incubated with 5 μL of crude enzyme at room temperature. After 5 hours, HPLC analysis (method A) showed complete comsumption of NADP and formation of NAADP (R_T = 16 minutes).

7.2 Synthesis of pyridinium ribonucleotides

1-Nicotinamide-β-D-ribose[36]

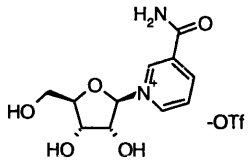

39

Nicotinamide (86 mg, 0.70 mmol) and trimethylsilyl trifluoromethanesulphonate (TMSOTf) (1.0 mL, 5.2 mmol) were added to a solution of tetra-1,2,3,5-*O*-acetyl-β-D-ribose (200 mg, 0.63 mmol) in CH_3CN (5 mL) and stirred at room temperature under a nitrogen atmosphere for one hour after which time TLC (CH_3OH:CH_2Cl_2 1:9; R_F 0.1) showed complete conversion to a new peak. The reaction was then treated with CH_3OH (2.5 mL) and stirred for a further thirty minutes. The reaction was then evaporated to dryness, suspended in H_2O (20 mL) and extracted three times with butan-1-ol (3 x 20 mL). The organic layer was extracted with H_2O (3 x 10 mL) and the combined aqueous layers washed five times with CH_2Cl_2 (5 x 10 mL). The aqueous layer was collected and evaporated to dryness. The residue was subjected to flash chromatography (CH_2Cl_2 to CH_2Cl_2:CH_3OH; 8:2) to afford the desired product **39** as a pale orange syrup (232 mg, 91 %).

R_F 0.35 (butan-1-ol:AcOH:H_2O, 5:2:3); ^{1}H NMR δ_H (270 MHz; D_2O) 9.60 (1H, s, H-2_{nic}), 9.27 (1H, d, *J* 6.2, H-6_{nic}), 8.98 (1H, d, *J* 7.9, H-4_{nic}), 8.27 (1H, m, H-5_{nic}), 6.24 (1H, d, *J* 4.2, H-1′), 4.52-4.47 (2H, m, H-2′, H-3′), 4.35 (1H, m, H-4′), 4.05 (1H, dd, *J* 13.1, 2.7, H-$5'_a$) and 3.89 (1H, dd, *J* 13.1, 3.3, H-$5'_b$); ^{13}C NMR δ_C (100 MHz; D_2O) 164.5 (C=O), 144.8, 141.6, 139.4 (CH), 133.1 (C), 127.8, 99.3, 87.1, 76.8, 69.3 (CH) and 59.9 (CH_2); *m/z* [FAB$^+$] 255.1 (M^+, 98 %) [found 255.0982 $C_{11}H_{15}N_2O_5$ requires 255.0981].

1-Methylnicotinate-β-D-ribose

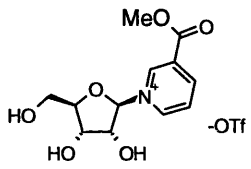

40

Methyl nicotinate (96 mg, 0.70 mmol) and TMSOTf (1.0 mL, 5.2 mmol) were added to a solution of tetra-1,2,3,5-*O*-acetate-β-D-ribose (200 mg, 0.63 mmol) in CH_3CN (5 mL) and stirred at room temperature under a nitrogen atmosphere for one hour after which time TLC (CH_3OH:CH_2Cl_2 1:9) showed complete conversion to a new peak (R_F 0.15). The reaction was then treated with CH_3OH (2.5 mL) and allowed to stir for a further thirty minutes. The reaction was evaporated to dryness, suspended in H_2O (20 mL) and extracted with butan-1-ol (3 x 20 mL). The organic layer was back extracted three times with H_2O (3 x 10 mL) and the combined aqueous layers were washed five times with CH_2Cl_2 (5 x 10 mL). The aqueous layer was collected and evaporated to dryness. The residue was subjected to flash chromatography (CH_2Cl_2 to CH_2Cl_2:CH_3OH; 8:2) to produce the desired product **40** as an orange syrup (215 mg, 81 %).

R_F 0.38 (butan-1-ol:AcOH:H_2O, 5:2:3); ^{1}H NMR δ_H (270 MHz; CD_3OD) 9.81 (1H, s, H-2_{nic}), 9.40 (1H, d, *J* 6.3, H-6_{nic}), 9.85 (1H, d, *J* 7.9, H-4_{nic}), 8.27 (1H, dd, *J* 7.9, 6.3, H-5_{nic}), 6.18 (1H, d, *J* 4.4, H-1′), 4.44-4.38 (2H, m, H-2′, H-3′), 4.30 (1H, m, H-4′), 4.03 (3H, s, OCH_3), 3.98 (1H, m, H-5′$_a$) and 3.84 (1H, dd, *J* 12.4, 2.5, H-5′$_b$); ^{13}C NMR δ_C (100 MHz; CD_3OD) 162.1 (C=O), 146.9, 143.5, 142.0 (CH), 131.1 (C), 128.3, 101.2, 89.0, 78.4, 70.7 (CH), 60.7 (CH_2) and 53.2 (CH_3); *m/z* [FAB$^+$] 270.2 (M^+, 100 %) [found 270.0981 $C_{11}H_{15}NO_6$ requires 270.0978].

Benzyl nicotinate

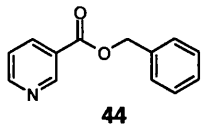

44

Benzyl alcohol (0.76 mL, 7.39 mmol), DCC (1.7 g, 8.13 mmol) and DMAP (90 mg, 0.81 mmol) were added to a solution of nicotinic acid (1.0 g, 8.13 mmol) in CH_2Cl_2 (36 mL) under a nitrogen atmosphere. The solution was stirred at room temperature overnight after which the resulting precipitate was removed by filtration and washed with CH_2Cl_2. The organic phase was extracted with aq. saturated $NaHCO_3$ (3 x 50 mL) and brine (3 x 50 mL), dried (Na_2SO_4), filtered and evaporated to dryness under vacuum. The resulting oil was subject to flash chromatography on silica gel using a gradient of CH_2Cl_2 to CH_2Cl_2:CH_3OH (100 to 98:2) as eluent. The required fractions were collected and evaporated to dryness to afford the ester **44** as a clear colourless oil (1.0 g, 67 %).

^{1}H NMR δ_H (400 MHz; $CDCl_3$) 9.21 (1H, s, H-2_{nic}), 8.69 (1H, d, *J* 4.7, H-6_{nic}), 8.24 (1H, d, *J* 7.8, H-4_{nic}), 7.42-7.39 (2H, m, H-Ar), 7.37-7.28 (4H, m, H-5_{nic}, H-Ar) and 5.35 (2H, s, CH_2); ^{13}C NMR δ_C (100 MHz; $CDCl_3$) 165.1 (C=O), 153.6, 151.1, 151.0, 137.3 (CH), 135.7 (C), 128.9, 128.7, 128.5 (CH), 126.2 (C) and 67.4 (CH_2). 2 carbon signals equivalent; *m/z* [FAB$^+$] 214.2 (M^+, 100 %) [found 214.0865 $C_{13}H_{12}NO_2^+$ requires 214.0868].

1-Benzylnicotinate-β-D-ribose

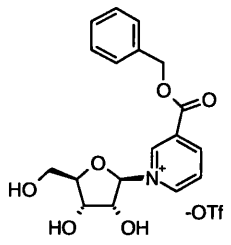

45

Benzyl nicotinate **44** (147 mg, 0.69 mmol) and TMSOTf (1 mL, 5.2 mmol) were added to a solution of tetra-1,2,3,5-*O*-acetate-β-D-ribose (200 mg, 0.63 mmol) in CH_3CN (5 mL). This was stirred at room temperature under a nitrogen atmosphere

for two hours after which time TLC (CH_2Cl_2:CH_3OH 9:1) showed complete conversion to a new peak (R_F 0.5). The reaction mixture was then treated with CH_3OH (2.5 mL) and allowed to stir for a further hour. The reaction was evaporated to dryness and the resulting oil subject to flash chromatography on silica gel using a gradient of CH_2Cl_2 to CH_2Cl_2:CH_3OH (10 to 8:2). The required fractions were collected and evaporated to dryness to afford the benzyl nicotinate ribose **45** as a pale brown oil (254 mg, 82 %).

ν_{max} (NaCl disk)/cm 3401 (OH), 1651 (COOBn); ^{1}H NMR δ_H (400 MHz; CD_3OD) 9.70 (1H, s, H-2_{nic}), 9.32 (1H, d, *J* 6.3, H-6_{nic}), 9.00 (1H, d, *J* 8.1, H-4_{nic}), 8.19 (1H, dd, *J* 8.1, 6.3, H-5_{nic}), 7.45-7.43 (2H, m, H-Ar), 7.34-7.25 (3H, m, H-Ar), 6.17 (1H, d, *J* 4.7, H-1′), 5.42 (2H, s, CH_2Ar), 4.44 (1H, t, *J* 4.7, H-2′), 4.38 (1H, dd, *J* 5.8, 2.5, H-4′), 4.31 (1H, m, H-3′), 3.95 (1H, dd, *J* 12.5, 2.5, H-5′$_a$) and 3.83 (1H, dd, *J* 12.5, 2.5, H-5′$_b$); ^{13}C NMR δ_C (67.5 MHz; CD_3OD) 162.2 (C=O), 147.63, 147.61, 144.1, 142.7 (CH), 135.7, 131.5 (C), 129.2, 129.1, 129.0, 101.7, 89.6, 78.8, 71.2 (CH), 69.0, 61.2 (CH_2). 2 carbon signals equivalent; *m/z* [FAB$^+$] 346.1 (M^+, 100%).

1-Nicotinic acid-β-D-ribose

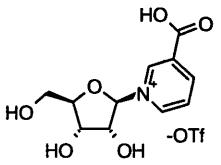

41

Repeat of method for 1-Benzylnicotinate-β-D-ribose but after silica flash chromatography the product was then fractionated between EtOAc (20 mL) and water (20 mL). The organic layer was extracted with water (3 x 5 mL) and the aqueous layer extracted with EtOAc (3 x 20 mL). The combined aqueous layers were evaporated to dryness to generate the acid **41** as a pale yellow oil (220 mg, 87 %).

ν_{max} (NaCl disk)/cm 3422 (OH), 1919 (COOH); ^{1}H NMR δ_H (400 MHz; D_2O) 9.38 (1H, s, H-2_{nic}), 8.90 (1H, d, *J* 6.3, H-6_{nic}), 8.74 (1H, d, *J* 9.2, H-4_{nic}), 7.92 (1H, m, H-5_{nic}), 5.89 (1H, d, *J* 3.9, H-1′), 4.15 (1H, m, H-2′), 4.13 (1H, m, H-4′), 4.01 (1H, t, *J* 4.9, H-3′), 3.73 (1H, m, H-5′$_a$) and 3.55 (1H, dd, *J* 12.9, 3.5, H-5′$_b$); ^{13}C NMR δ_C (67.5 MHz; D_2O) 162.3 (C=O), 147.3, 143.6, 142.3, 128.6 (CH), 122.8 (C), 101.3,

89.6, 78.6, 71.2 (CH) and 61.0 (CH_2); *m/z* [FAB$^+$] 256.1 (M^+, 100%) [found 256.0819 $C_{11}H_{14}NO_6^+$ requires 256.0821].

β-Nicotinamide mononucleotide (β-NMN)[37]

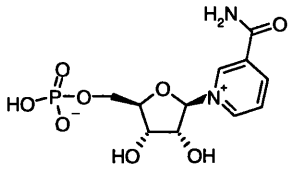

21

Nicotinamide ribose triflate **39** (350mg, 0.87 mmol) was treated with activated charcoal and freeze dried from H_2O. This was suspended in a solution of trimethylphosphate (4.5 mL) and water (12 μL, 0.67 mmol) at 0°C. $POCl_3$ (528 μL, 5.6 mmol) was added and the reaction stirred at 0°C for four hours after which time a second portion of $POCl_3$ (200 μL, 2.1 mmol) was added. After a further hour a solution of CH_3CN:ether (1:3) as added causing the formation of a white precipitate. The supernatant was removed, the precipitate dissolved in water (5 mL) and applied to a Dowex 1 X 2 formamide (1 cm x 5 cm), which was eluted with water (50 mL). The volume was reduced under vacuum to 5 mL and the solution applied to a second column of Dowex 50 WX8-100 H^+ (1 cm x 5 cm) washed with water (50 mL). The solution was evaporated to dryness and lyophilised from D_2O to afford β-NMN **21** as a white solid (42 mg, 14 %).

^{1}H NMR δ_H (400 MHz; D_2O) 9.23 (1H, s, H-2_{nic}), 9.04 (1H, d, *J* 6.3, H-6_{nic}), 8.75 (1H, d, *J* 7.8, H-4_{nic}), 8.07 (1H, dd, *J* 7.8, 6.3, H-5_{nic}), 6.00 (1H, d, *J* 5.4, H-1′), 4.43 (1H, m, H-2′), 4.33 (1H, m, H-3′), 4.22 (1H, m, H-4′), 4.14 (1H, ddd, *J* 12.1, 4.3, 2.3, H-$5'_a$), 3.97 (1H, ddd, *J* 12.1, 5.0, 2.3, H-5_b); ^{13}C NMR δ_C (100 MHz, D_2O) 165.7 (C=O), 145.8, 142.3, 139.8 (CH), 133.8 (C), 128.4, 99.8, 87.2, 77.6, 70.8 (CH) and 64.3 (CH_2); ^{31}P NMR δ_P (109 MHz; D_2O) 0.96; *m/z* [FAB$^+$] 334.2 (M^+, 80%)

5-*O*-Triphenylmethyl-β-D-ribose[40]

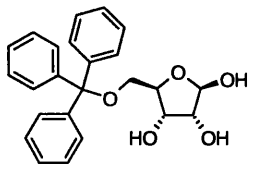

47

Triphenylchloromethane (5.4 g, 19.5 mmol) was added to a solution of β-D-ribose **43** (3.0 g, 20.0 mmol) in pyridine (10 mL) and stirred at 45°C for sixty minutes. The solution was evaporated to dryness under vacuum, re-suspended in CH_2Cl_2 (20 mL) and extracted with H_2O (3 x 10 mL). The organic layer was dried ($MgSO_4$), filtered and evaporated to dryness. The residue was dissolved in CH_2Cl_2 (6 mL), added dropwise to a solution of hexane (20 mL) and CH_2Cl_2 (2 mL) and stirred at room temperature for one hour. The resulting precipitate was filtered, washed with hexane and H_2O and dried at 50°C under vacuum to afford the 5′-protected ribose **47** as a white solid (5.1 g, 67 %).

mp 124-128°C (from hexane) (lit.[40] 125°C); ^{1}H NMR δ_H (400 MHz; $CDCl_3$) 7.49-7.44 (6H, m, H-Ar), 7.32-7.22 (9H, m, H-Ar), 5.42 (1H, d, *J* 4.0, H-1), 4.81 (1H, br s, OH-1), 4.27 (1H, dd, *J* 7.0, 3.8, H-4), 4.23 (1H, m, H-3), 4.07 (1H, m, H-2), 3.98 (1H, br s, OH-3), 3.58 (1H, br s, OH-2), 3.32 (1H, dd, *J* 10.1, 3.8, H-5_a) and 3.13 (1H, dd, *J* 10.1, 3.8, H-5_b); ^{13}C NMR δ_C (100 MHz; $CDCl_3$) 143.7 (C), 128.7, 127.9, 127.2, 96.8 (CH), 86.9 (C), 83.2, 72.0, 71.9 (CH) and 64.1 (CH_2). 2 C and 14 CH equivalent.

1,2,3-Tri-*O*-acetyl-5-triphenylmethyl-β-D-ribose[40]

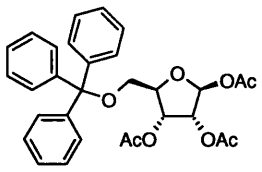

48

Acetic anhydride (4.1 mL, 43.4 mmol) and Et_3N (6.9 mL, 50 mmol) were added to a solution of 5-trityl-β-D-ribose **47** (4.9 g, 12.5 mmol) in toluene (12.5 mL) and stirred at room temperature overnight. Iced water (15 mL) was added and the reaction stirred for a further ten minutes, separated and the aqueous layer extracted with toluene (3 x 10 mL). The combined organic layers were collected, washed with water (2 x 10 mL), dried ($MgSO_4$), filtered and evaporated to dryness. The oil was subject to flash chromatography on silica gel using a gradient of hexane to hexane-EtOAc (7:3) as the eluent to afford the triacetate protected ribose **48** as a white foam (4.43 g, 69 %).
^{1}H NMR δ_H (270 MHz; $CDCl_3$) 7.46-7.43 (6H, m, H-Ar), 7.31-7.22 (9H, m, H-Ar), 6.20 (1H, d, *J* 1.0, H-1), 5.49 (1H, dd, *J* 7.0, 4.8, H-3), 5.43 (1H, dd, *J* 4.8, 1.0, H-2), 4.07 (1H, ddd, *J* 7.0, 4.1, 3.5, H-4), 3.35 (1H, dd, *J* 10.4, 3.5, H-5_a), 3.14 (1H, dd, *J* 10.4, 4.1, H-5_b), 2.03 (3H, s, CH_3), 2.00 (3H, s, CH_3) and 1.98 (3H, s, CH_3); ^{13}C NMR δ_C (100 MHz; $CDCl_3$) 169.7, 169.5, 169.4 (C=O), 143.7 (C), 128.7, 127.9, 127.1, 98.4 (CH), 86.8 (C), 80.9, 74.4, 70.9 (CH), 63.2 (CH_2), 21.1, 20.6 and 20.5 (CH_3). 2 C and 14 CH equivalent.

1,2,3-Tri-*O*-acetyl-β-D-ribose[40]

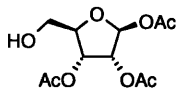

49

A solution of 1,2,3-tri-*O*-acetyl-5-trityl-β-D-ribose **48** (1.9 g, 3.67 mmol) in CH_2Cl_2 (48 mL), H_2O (1 mL) and TFA (1 mL) was stirred at room temperature for three hours. The reaction was extracted with H_2O (3 x 15 mL), dried ($MgSO_4$) filtered and evaporated to dryness. The residue was subject to flash chromatography on silica gel eluting with a gradient of hexane to hexane-EtOAc (7:3) then EtOAc-CH_3OH (9:1) to afford the alcohol **49** as a white foam (768 mg, 76 %).

^{1}H NMR δ_H (270 MHz; $CDCl_3$) 6.00 (1H, d, *J* 0.9, H-1), 5.26 (1H, dd, *J* 6.9, 4.9, H-3), 5.21 (1H, dd, *J* 4.9, 0.9, H-2), 4.12 (1H, ddd, *J* 6.9, 4.0, 3.4, H-4), 3.69 (1H, dd, *J* 12.4, 3.4, H-5_a), 3.51 (1H, dd, *J* 12.4, 4.0, H-5_b), 2.00 (3H, s, CH_3), 1.97 (3H, s, CH_3) and 1.94 (3H, s, CH_3); ^{13}C NMR δ_C (100 MHz; $CDCl_3$) 169.0, 168.5, 168.2 (C=O), 97.2, 81.3, 73.5, 68.8 (CH), 60.8 (CH_2), 20.1 (CH_3) and 19.5 (2 x CH_3).

N,N-diisopropylaminodichlorophosphine[48]

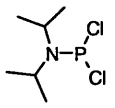

68

N,N-diisopropylamine (141.0 mL, 1.0 mol) in dry ether (150 mL) was added dropwise to a stirred solution of phosphorus trichloride (44.0 mL, 0.5 mol) in dry ether (100 mL) at -78°C. The solution was diluted with dry ether (100 mL), vigorously stirred overnight at room temperature and the precipitated amine salt filtered, washed with ether (500 mL) and discarded. The organic phase was evaporated to dryness to afford a crude oil that was distilled (50-52°C; 0.5 mmHg, lit.[48] 62-63 °C; 7 mmHg) to afford the phosphine **68** as a clear colourless oil (72.0 g, 71 %).

^{1}H NMR δ_H (400 MHz; $CDCl_3$) 3.93 (2H, m, 2 x CH) and 1.20 (12H, d, *J* 7.0, 4 x CH_3); ^{31}P NMR δ_P (162 MHz; $CDCl_3$) 169.5.

Bis(benzyloxy)diisopropylaminophosphine[53]

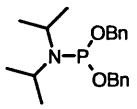

52

Benzyl alcohol (3.1 mL, 29.4 mmol) in dry CH_2Cl_2 (25 mL) was added dropwise to a stirred solution of *N,N*-diisopropylaminodichlorophosphine **68** (3.0 g, 14.7 mmol) in dry CH_2Cl_2 (25 mL) and dry triethylamine (4.4 mL, 31.6 mmol) at –78°C. This was stirred for two hours at room temperature, then poured into aq. saturated $NaHCO_3$ (100 mL) and extracted with three portions of CH_2Cl_2 (3 x 50 mL). The combined organic layers were dried (Na_2SO_4), filtered, evaporated to dryness. The crude mixture was subject to flash chromatography on silica gel conditioned using

ether:hexane:Et_3N (74:25:1) (400 mL). The column was eluted using ether:hexane:Et_3N 74:25:1 to obtain the phosphine **52** as a clear oil (3.9 g, 79 %).
R_F 0.45 (ether:hexane 3:1); ^1H NMR δ_H (400 MHz; $CDCl_3$) 7.42-7.30 (10H, m, H-Ar), 4.86-4.74 (4H, m, 2 x CH_2Ar), 3.82-3.71 (2H, m, 2 x CH), 1.29-1.25 (12H, dd, *J* 6.7, 2.2, 4 x CH_3); ^{31}P NMR δ_P (162 MHz; $CDCl_3$) 148.5.

Imidazolium triflate[50]

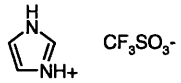

51

To a stirred solution of imidazole (0.77g, 11.3 mmol) in CH_2Cl_2 (15 mL) at 0°C was added triflic acid (1.0 mL, 11.3 mmol). The reaction was warmed to room temperature and stirred for twenty minutes after which time ether (20 mL) was added. The white precipitate **51** was filtered dried under vacuum (2.2 g, 90%) and stored under nitrogen and used within twenty-four hours.
mp 197-198°C (from ether) (lit.[50] 197-198°C)

5-(Dibenzylphosphoryl)-1,2,3-tri-*O*-acetyl-β-D-ribose

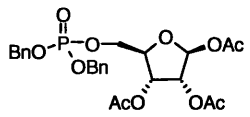

53

Bis(benzyloxy)diisopropylaminophosphine **52** (339 mg, 1.00 mmol) and imidazolium triflate **51** (436 mg, 2.00 mmol) were added to a solution of 1,2,3-tri-*O*-acetyl-β-D-ribose **49** (130 mg, 0.47 mmol) in CH_2Cl_2 (10 mL) and stirred for three hours. TLC analysis showed quantitative conversion to the phosphite intermediate (hexane:EtOAc 7:3 R_F 0.3). The reaction was cooled to –78°C, *m*CPBA (517 mg, 3.00 mmol) was added and the oxidation was monitored by ^{31}P NMR (139 ppm to –0.69 ppm) and TLC (hexane:EtOAc 1:1 R_F 0.2). The reaction was quenched with 10% $Na_2S_2O_3$ (50 mL) and warmed to room temperature. The mixture was washed three times with aq. saturated $NaHCO_3$ (3 x 20 mL), brine (3 x 20 mL), dried ($MgSO_4$), filtered and evaporated to dryness. The product was then subject to flash chromatography on

silica gel using a gradient of hexane to hexane:EtOAc (1:1) as eluent to produce the protected phosphate **53** as a glassy solid (164 mg, 85 %).

^{1}H NMR δ_H (400 MHz; $CDCl_3$) 7.36-7.34 (10H, m, H-Ar), 6.15 (1H, s, H-1), 5.39 (1H, dd, *J* 7.2, 4.9, H-3), 5.34 (1H, d, *J* 4.9, H-2), 5.06 (2H, t, J_{PH} 2.5, CH_2Ar), 5.04 (2H, t, J_{PH} 2.5, CH_2Ar), 4.33 (1H, m, H-4), 4.18 (1H, ddd, J_{HH} 11.3, 6.2, J_{PH} 2.5, H-5_a), 4.09 (1H, ddd, J_{HH} 11.3, 6.3, J_{PH} 2.5, H-5_b), 2.12 (3H, s, CH_3), 2.04 (3H, s, CH_3) and 1.99 (3H, s, CH_3); ^{13}C NMR δ_C (100 MHz; $CDCl_3$) 169.6, 169.4, 169.2 (C=O), 135.7, 135.6 (C), 128.6, 128.0 (10 x CH), 98.0, 79.8, 74.1, 70.1 (CH), 69.5, 69.4, 66.3 (CH_2), 20.6, 20.5 and 20.4 (CH_3); ^{31}P NMR δ_P (109 MHz; $CDCl_3$) –0.52.

1,2,3-Tri-*O*-acetyl-β-D-ribose-5-phosphate

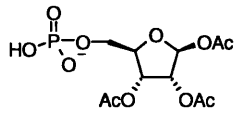

50

To a stirred solution of 5-*bis*(benzylphosphate)-1,2,3-tri-*O*-acetylribose **53** (75 mg, 0.15 mmol) in CH_3OH (5 mL) and H_2O (0.25 mL) was added 20% $Pd(OH)_2/C$ (50 mg) and cyclohexene (2 mL, 20 mmol). This was heated to 80°C for three hours after which time the catalyst was removed using a membrane filter and the product evaporated to dryness under vacuum to afford the free phosphate **50** as a white foam (27 mg, 50 %).

^{31}P NMR δ_P (109 MHz; CD_3OH) 0.69; *m/z* [FAB$^-$] 355.0 (M^+, 100%). ^{1}H and ^{13}C NMR proved inconclusive.

7.3 Synthesis of protected adenosine diphosphate

Bis(2-cyanoethoxy)diisopropylaminophosphine[49]

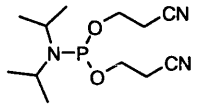

69

Hydroxypropionitrile (4.4 mL, 64.5 mmol) in dry CH_2Cl_2 (50 mL) was added dropwise to a stirred solution of *N,N*-diisopropylaminodichlorophosphine **68** (6.5 g, 32.3 mmol) in dry CH_2Cl_2 (50 mL) and dry triethylamine (9.6 mL, 69.4 mmol) at –78°C. This was stirred for two hours at room temperature, poured into aq. saturated $NaHCO_3$ (200 mL) and extracted with three times with CH_2Cl_2 (3 x 100 mL). The combined organic extracts were dried (Na_2SO_4), filtered, evaporated to dryness. The resulting oil was subject to flash chromatography on silica gel conditioned using ether:hexane:Et_3N (74:25:1) (400 mL) then ether:hexane 3:1 (400 mL) before loading. The column was eluted using ether:hexane 3:1 to obtain the phosphine **69** as a clear oil (6.5 g, 74%).

R_F 0.61 (ether:hexane 3:1); ^1H NMR δ_H (400 MHz; $CDCl_3$) 3.92–3.77 (4H, m, 2 x CH_2CN), 3.68–3.44 (2H, m, 2 x CH), 2.65 (4H, t, *J* 6.2, 2 x CH_2O), 1.18 (12H, d, *J* 7.0, 4 x CH_3); ^{31}P NMR δ_P (162 MHz; $CDCl_3$) 149.6.

3′,5′-*O*-(1,1,3,3-Tetraisopropyldisiloxane-1,3-diyl)adenosine[45,46]

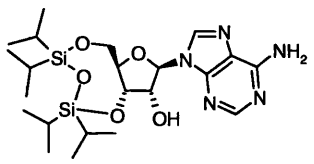

65

1,3-Dichloro-1,1,3,3-tetraisopropyldisiloxane (1.20 mL, 3.75 mmol) was added to a solution of adenosine **58** (1.0 g, 3.75 mmol) in pyridine (40 mL) and stirred for three hours at room temperature. The solvent was removed under vacuum and the product dissolved in CH_2Cl_2 (20 mL) washed with aq. saturated $NaHCO_3$ (3 x 20 mL), dried (Na_2SO_4), filtered and evaporated to dryness. The compound was then subject to

flash chromatography on silica gel using CH_2Cl_2-CH_3OH as eluent to afford the cyclic protected adenosine **65** as a white solid (1.5 g, 80 %).

R_F 0.34 (CH_2Cl_2:CH_3OH 95:5); mp 95-96 °C (from CH_2Cl_2) (lit.[46] 97-99 °C); $[\alpha]^{25}_D$ – 33 (*c* 1 in $CHCl_3$); ^1H NMR δ_H (400 MHz; $CDCl_3$) 8.29 (1H, s, H-2_{ad}), 8.03 (1H, s, H-8_{ad}), 6.01 (1H, d, *J* 0.8, H-1′), 4.99 (1H, dd, *J* 8.2, 5.4, H-3′), 4.56 (1H, dd, *J* 5.4, 0.8, H-2′), 4.19-4.13 (2H, m, H-4, H-$5'_a$), 4.04 (1H, m, H-$5'_b$) and 1.12-1.04 (28H, m, 4 x C*H*(CH_3)$_2$); ^{13}C NMR δ_C (100 MHz; $CDCl_3$) 155.6 (C), 152.8 (CH), 149.1 (C), 139.5 (CH), 120.4 (C), 90.1, 82.3, 75.4, 70.7 (CH), 61.8 (CH_2), 17.9, 17.82, 17.80, 17.76, 17.54, 17.46, 17.43, 17.36 (CH_3), 13.8, 13.5, 13.2 and 13.0 (CH); *m/z* [FAB$^+$] 510.2, $(M+H)^+$, 74% [found 510.2571 $C_{22}H_{40}N_5O_5Si_2^+$ requires 510.2568].

2′-(Di(2-cyanoethoxyphosphoryl))-3′,5′-*O*-(1,1,3,3-tetraisopropyldisiloxane-1,3-diyl) adenosine

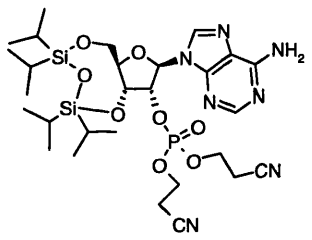

71

Bis(2-cyanoethoxy)diisopropylaminophosphine **69** (455 mg, 1.68 mmol) and imidazolium triflate **51** (976 mg, 4.48 mmol) were added to a solution of 3′, 5′ protected adenosine **65** (522 mg, 1.03 mmol) in CH_2Cl_2 (30 mL) and stirred under a nitrogen atmosphere. After three hours TLC analysis showed quantitative conversion to the phosphite intermediate ($CHCl_3$:acetone 2:8; R_F 0.45 $P^{(III)}$). The reaction was cooled to –78°C, *m*CPBA (293 mg, 1.7 mmol) added and the oxidation was monitored by ^{31}P NMR (139.6 ppm to –1.3 ppm), then quenched with 10% $Na_2S_2O_3$ (50 mL) and warmed to room temperature. The mixture was washed with aq. saturated $NaHCO_3$ (3 x 20 mL) and brine (3 x 20 mL), dried (Na_2SO_4), filtered and evaporated to dryness. The product was then subject to flash chromatography on silica gel using chloroform-acetone as eluent to afford the protected phosphate adenosine **71** as a white solid (699 mg, 98 %).

R_F 0.34 $P^{(V)}$ ($CHCl_3$:acetone 2:8); mp 168-170 °C (from $CHCl_3$); $[\alpha]^{25}_D$ –24 (*c* 1 in $CHCl_3$); ^1H NMR δ_H (400 MHz; $CDCl_3$) 8.24 (1H, s, H-2_{ad}), 8.12 (1H, s, H-8_{ad}), 6.18 (1H, s, H-1′), 5.30 (1H, m, H-2′), 4.92 (1H, m, H-3′), 4.50-4.35 (4H, m, 2 x CH_2CH_2O) 4.26 (1H, dd, *J* 13.4, 2.4, H-5′$_a$), 4.15 (1H, m, H-4′), 4.03 (1H, dd, *J* 13.4, 2.4, H-5′$_b$), 2.90 (2H, t, *J* 6.2, CH_2CN), 2.81 (2H, t, *J* 6.2, CH_2CN) and 1.20-1.02 (28H, m, 4 x $CH(CH_3)_2$); ^{13}C NMR δ_C (100 MHz; $CDCl_3$) 155.3 (C), 152.8 (CH), 148.9 (C), 138.8 (CH), 120.2, 116.3, 116.0 (C), 88.2, 81.2, 80.7, 68.0 (CH), 62.7, 62.6, 59.4, 19.7, 19.6 (CH_2), 17.4, 17.2 (3 x CH_3), 16.97, 16.88, 16.85, 16.81 (CH_3),13.4, 12.9, 12.8, 12.5 (CH); ^{31}P NMR δ_P (162 MHz; $CDCl_3$) –1.30; *m/z* [FAB^+] 696.2 $(M+H)^+$, 100% [found 696.2760 $C_{28}H_{47}N_7O_8PSi_2$ requires 696.2762].

2′-(Di(2-cyanoethoxyphosphoryl))-3′-*O*-(3-hydroxy-1,1,3,3-tetraisopropyldisiloxane-1-yl) adenosine

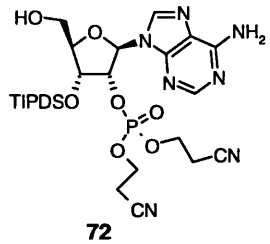

72

A solution of 2′ phosphate adenosine **71** (689 mg, 0.99 mmol) in TFA–H_2O–THF (1:1:4; *v/v/v*) (60 mL) was stirred at 0°C for three hours. The reaction was neutralised with aq. saturated $NaHCO_3$ (60 mL) and the organic phase washed with H_2O (3 x 20 mL) and brine (3 x 20 mL), dried (Na_2SO_4), filtered and evaporated to dryness to yield the selectively deprotected hydroxyl **72** as a white solid (705 mg, 100 %).

R_F 0.19 ($CHCl_3$:acetone 2:8); mp 142-144 °C (from THF); $[\alpha]^{25}_D$ –52 (*c* 1 in $CHCl_3$); ^1H NMR δ_H (400 MHz; $CDCl_3$) 8.43 (1H, s, H-2_{ad}), 8.22 (1H, s, H-8_{ad}), 6.31 (1H, d, *J* 6.2, H-1′), 5.59 (1H, m, H-2′), 4.89 (1H, m, H-3′), 4.34 (1H, d, *J* 2.0, H-4′), 4.26-4.06 (4H, m, 2 x CH_2O), 3.92 (1H, dd, *J* 12.5, 2.0, H-5′$_a$), 3.40 (1H, dd, *J* 12.5, 2.0, H-5′$_b$), 2.78 (2H, dd, *J* 10.1, 5.4, CH_2CN), 2.73 (2H, dd, *J* 10.1, 5.4, CH_2CN) and 1.15-1.01 (28H, m, 4 x $CH(CH_3)_2$); ^{13}C NMR δ_C (100 MHz; $CDCl_3$) 160.2 (C), 156.5 (CH), 152.8 (C), 144.7 (CH), 123.7 (C), 121.0 (2 x C), 91.5, 91.3, 82.7, 75.6 (CH), 67.6 , 67.6, 65.4, 23.1, 23.0 (CH_2), 21.0 (3 x CH_3), 20.93 (2 x CH_3), 20.91, 20.84, 20.80

(CH_3), 17.8 (2 x CH), 17.52, 17.50 (CH); ^{31}P NMR δ_P (162 MHz; $CDCl_3$) –1.80; *m/z* [FAB$^+$] 714.4 $(M+H)^+$, 82% [found 714.2856 $C_{28}H_{49}N_7O_9PSi_2$ requires 714.2868].

5′-(Dibenzylphosphoryl)-2′-(di(2-cyanoethoxyphosphoryl))-3′-*O*-(3-hydroxy-1,1,3,3-tetraisopropyldisiloxane-1-yl) adenosine

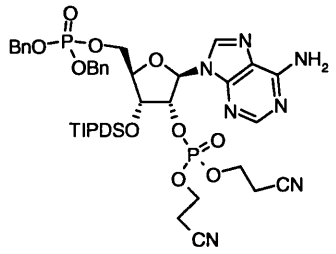

73

Bis(benzyl)diisopropylaminophosphine **52** (1.07 g, 3.15 mmol) and imidazolium triflate **51** (1.83 g, 8.40 mmol) were added to a solution of 5′ alcohol **72** (1.50 g, 2.10 mmol) in CH_2Cl_2 (50 mL) and stirred overnight after which time TLC showed complete conversion to phosphite intermediate ($CHCl_3$:acetone 2:8; R_F 0.3 $P^{(III)}$). The reaction was cooled to –78°C, *m*CPBA (1.35 g, 6.0 mmol) added and the oxidation monitored by ^{31}P NMR (140.4 ppm to –2.0 ppm), then quenched with 10% $Na_2S_2O_3$ (100 mL) and warmed to room temperature. The mixture was washed with aq. saturated $NaHCO_3$ (3 x 20 mL) and brine (3 x 20 mL), dried (Na_2SO_4), filtered and evaporated to dryness. The product was then subject to flash chromatography on silica gel using chloroform-acetone as eluent to afford the diphosphate **73** as a white solid (1.55 g, 76 %).

R_F 0.23 $P^{(V)}$ ($CHCl_3$:acetone 2:8); mp 157–159 °C (from $CHCl_3$); ^{1}H NMR δ_H (400 MHz; $CDCl_3$) 8.16 (1H, s, H-2), 8.08 (1H, s, H-8), 7.28-7.14 (10H, m, H-Ar), 6.19 (1H, d, *J* 3.7, H-1′), 5.41(1H, m, H-2′), 4.96-4.88 (5H, m, 2 x (OCH_2Ph), H-3′), 4.38-3.97 (7H, m, 2 x (CH_2CH_2O), H-4′, 5′$_a$, H-5′$_b$), 2.64-2.55 (4H, m, 2 x CH_2CN) and 1.01-0.72 (28H, m, 4 x $CH(CH_3)_2$); ^{13}C NMR δ_C (100 MHz; $CDCl_3$) 155.9 (C), 153.1 (CH), 149.4 (C), 139.4 (CH), 135.6 (C), 135.5 (C), 128.88, 128.87, 128.81, 128.79, 128.20, 128.17 (CH), 120.0, 116.7, 116.4 (C), 87.0, 82.9, 79.1 (CH), 70.1, 70.0 (CH_2), 70.0 (CH), 68.2, 66.4, 66.3, 20.0, 19.9 (CH_2), 17.81, 17.75, 17.70, 17.68, 17.61 (CH_3), 14.0, 13.9, 13.8 and 13.7 (CH), 4 aromatic CH and 3 silanol CH_3 occluded; ^{31}P NMR

δ_P (162 MHz; $CDCl_3$) –2.00 and -0.42; *m/z* [FAB^+] 974.9 (M^+,H^+, 56%) [found 974.3447 $C_{42}H_{62}N_7O_{12}P_2Si_2$ requires 974.3470].

2′-(Di(2-cyanoethoxyphosphoryl))-3′-*O*-(3-hydroxy-1,1,3,3-tetraisopropyldisiloxane-1-yl) adenosine-5′-phosphate

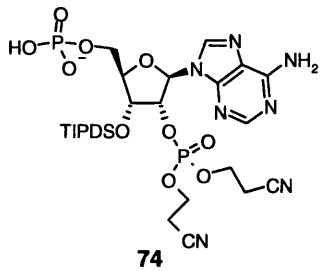

74

To a stirred mixture of 2′, 5′ phosphorylated adenosine **73** (300 mg, 0.304 mmol) in CH_3OH (10 mL) and water (0.5 mL) was added 20% $Pd(OH)_2/C$ (100 mg) and cyclohexene (3.5 mL). The reaction was heated to 80°C for three hours and monitored by ^{31}P NMR (-0.42 ppm to 1.03 ppm) for completion. After cooling the reaction mixture was passed through a membrane filter and the catalyst washed copiously with a methanol / water mixture (1:1). Concentration of the filtrate afforded the deprotected phosphate **74** as a white solid (200 mg, 82 %).

mp 139–141 °C (from methanol); $[\alpha]^{25}_D$ –14° (*c* 0.36 in Methanol); ^1H NMR δ_H (270 MHz; CD_3OD) 8.65 (1H, s, H-2_{ad}), 8.25 (1H, s, H-8_{ad}), 6.32 (1H, d, *J* 5.9, H-1′), 5.33 (1H, m, H-2′), 4.82 (1H, m, H-3′), 4.41 (1H, m, H-4′), 4.16-4.07 (6H, m, 2 x CH_2O, H-5′$_a$, H-5′$_b$), 2.76-2.67 (4H, m, 2 x CH_2CN)) and 1.05-0.75 (28H, m, 4 x $CH(CH_3)_2$); ^{13}C NMR δ_C (100 MHz; $CDCl_3$) 150.8, 147.7 (C), 146.4 (CH), 141.2 (CH), 118.8 117.4, 117.1 (C), 88.1, 81.9, 80.5, 71.5 (CH), 67.3, 63.9, 62.1, 19.1, 19.0 (CH_2), 16.9, 16.84, 16.75 (CH_3), 16.62 (2 x CH_3), 16.55, 16.51, 16.3 (CH_3), 13.9, 13.7, 13.4, 13.2 (CH); ^{31}P NMR δ_P (109 MHz; $CDCl_3$) –2.40 and 1.03; *m/z* [FAB^+] 794.3 $(M+H)^+$, 100% [found 794.2548 $C_{28}H_{50}N_7O_{12}P_2Si_2$ requires 794.2531].

7.4 Synthesis of the pyrophosphate bond

Adenosine-5′-monophosphate morpholidate[61]

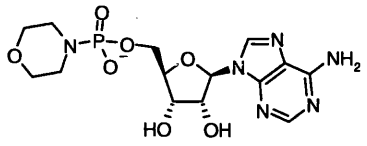

75

Powdered triphenylphosphine (131 mg, 0.5 mmol), 2,2′-dipyridyldisulphide (110 mg, 0.5 mmol) and morpholine (87 μL, 1.0 mmol) were added to a stirred solution of adenosine 5′-monophosphate **58** (free acid) (69 mg, 0.2 mmol) in DMSO (1.0 mL). The reaction was stirred at room temperature and monitored using ion exchange HPLC. After three hours another portion triphenylphosphine (68 mg, 0.25 mmol) and 2,2′-dipyridyldisulphide (55 mg, 0.25 mmol) were added and stirred for a further hour. The reaction was quenched using 0.1 M NaI in acetone (10 mL) and the white precipitate filtered, washed with acetone until any yellow discolouration had been removed. The product was dried under vacuum over phosphorous pentoxide to afford the morpholidate **75** as a white solid (83 mg, 100 %).

^{1}H NMR δ_H (400 MHz; D_2O) 8.21 (1H, s, H-2_{ad}), 8.00 (1H, s, H-8_{ad}), 5.88 (1H, d, *J* 5.1, H-1′), 4.58 (1H, m, H-2′), 4.30 (1H, t, *J* 4.6, H-3′), 4.13 (1H, br s, H-4′), 3.89-3.82 (2H, m, H-5′$_a$, H-5′$_b$), 3.32 (4H, t, *J* 4.7, 2 x CH_2N) and 2.69 (4H, t, *J* 4.7, 2 x CH_2CH_2O); ^{31}P NMR δ_P (162 MHz; D_2O) 8.77. Identical to commercially available compound.

Nicotinamide adenine dinucleotide[37]

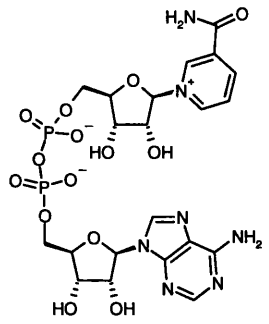

6

β-NMN **21** (25 mg, 0.075 mmol) and $MgSO_4 \cdot 7H_2O$ (34 mg, 0.136 mmol) were added to a solution of AMP morpholidate **75** (28 mg, 0.068 mmol) in 0.2 M $MnCl_2$* in formamide (563 μL, 0.1125 mmol) under a nitrogen atmosphere. The solution was stirred at room temperature for eighteen hours after which time RP ion pair HPLC analysis showed completion of the reaction. The mixture was applied to a column of Q-Sepharose and eluted with a gradient of water–1 M TEAB (eluting at 5-8%). The required fractions were analysed by reverse phase HPLC, collected, treated with chelex resin, filtered, concentrated under vacuum and lyophilised from D_2O to afford NAD **6** as a white hygroscopic powder (12 mg, 27 %).

* $MnCl_2$ dissolved in formamide and left over 4 Å molecular sieves for three days.[37]

R_T 7.5 minutes (RP-HPLC 94 % aq. 0.1 M KH_2PO_4, 6 mM tetrabutylammonium bromide and 6% CH_3OH; Isocratic for 30 mins); ^1H NMR δ_H (270 MHz; D_2O) 9.29 (1H, s, H-2_{nic}), 9.11 (1H, d, *J* 6.1, H-6_{nic}), 8.78 (1H, d, *J* 8.2, H-4_{nic}), 8.37, (1H, s, H-$2'_{ad}$), 8.15 (1H, m, H-5_{nic}), 8.05 (1H, s, H-$8'_{ad}$), 6.04 (1H, d, *J* 5.2, H-1′), 5.98 (1H, d, *J* 5.8, H-1), 4.72 (1H, t, *J* 5.8, H-2) and 4.51-4.21 (9H, m, H-3, H-4, H-5, H-2′, H-3′, H-4′, H-5′); ^{13}C NMR δ_C (100MHz; D_2O) 165.1, 155.1 (C), 152.5 (CH), 148.7 (C), 145.7, 142.3, 139.8, 139.6 (CH), 133.5 (C), 128.5 (CH), 118.2 (C), 99.9, 86.9, 86.5, 83.7, 77.5, 73.9, 70.6, 70.3 (CH), 65.3 and 64.8 (CH_2); ^{31}P NMR δ_P (162 MHz; D_2O) –11.5; *m/z* [FAB$^-$] 663.3 (M^-, 35%). Identical to commercial sample.

Nicotinamide adenine dinucleotide 2′(2-cyanoethoxy) phosphate

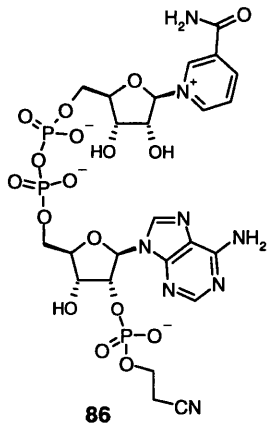

86

Carbonyl diimidazole (48 mg, 0.3 mmol) and Et_3N (14 μL, 0.1 mmol) were added to a solution of β-NMN **21** (33 mg, 0.1 mmol) in DMF (300 μL). This was stirred at room temperature under a nitrogen atmosphere for three hours and monitored by ^{31}P NMR (–9.5 ppm). Once complete a few drops of methanol were added and the solution stirred for a further five minutes. The solution was evaporated to dryness, co-evaporated with DMF (3 x 100 μL) to afford a yellow oil, to which was added a solution of 5′ phosphate adenosine **74** (63 mg, 0.08 mmol) in DMF (300 μL) and the resulting mixture stirred at room temperature overnight. The reaction was then quenched with 25 mM NH_4OAc (6 mL) and extracted with CH_2Cl_2 (3 x 5 mL). The aqueous phase was evaporated to dryness and re-suspended in a solution of 10 % aq. TFA (10 mL) and EtOAc (0.5 mL). This was stirred for three hours and monitored by reverse phase TLC for the disappearance of starting material. The reaction was evaporated to dryness, re-suspended in H_2O, loaded onto an ion exchange gradifac column (AG-MP1) and eluted using a linear gradient of 150 mM aq. TFA. Fractions analysed by ion exchange HPLC (method A) and the appropriate fractions were concentrated and lyophilised from D_2O to afford the pyrophosphate **86** as a white hygroscopic powder (6 mg, 10 %).

R_T 11 minutes (AG-MP1 water:150 mM aq. TFA); ^1H NMR δ_H (600 MHz; D_2O) 9.27 (1H, s, H-2_{nic}), 9.11 (1H, d, *J* 6.3, H-6_{nic}), 8.79 (1H, d, *J* 8.0, H-4_{nic}), 8.44, (1H, s, H-$2'_{ad}$), 8.29 (1H, s, H-$8'_{ad}$), 8.14 (1H, m, H-5_{nic}), 6.15 (1H, s, H-1′), 6.01 (1H, s, H-1), 5.00 (1H, m, H-2′), 4.53 (1H, m, H-3′), 4.44-4.41 (2H, m, H-2, H-3), 4.34 (1H, m, H-4), 4.27-4.10 (5H, m, H-4′, 5′, 5), 3.81 (2H, m, CH_2CH_2O), 2.58 (2H, m, CH_2CN); ^{13}C

NMR δ_C (100MHz; D_2O) 166.6, 150.3, 148.4 (C), 146.1, 145.1, 142.9, 142.7, 139.9 (CH), 134.0 (C), 128.8 (CH), 119.6, 118.0 (C), 100.1, 94.5, 87.4, 83.9, 77.8, 77.4, 71.1, 69.8 (CH), 65.2, 65.1, 60.8 and 19.7 (CH_2); ^{31}P NMR δ_P (109 MHz; D_2O) –0.30 and –11.03; *m/z* [FAB$^+$] 795.1 (M^+, 60 %) [found 795.0953 $C_{24}H_{30}N_8O_{17}P_3^+$ requires 795.0942].

Nicotinamide adenine 3′-*O*-(3-hydroxy -1,1,3,3-tetraisopropyldisiloxane-1-yl) dinucleotide 2′-(2-cyanoethoxy) phosphate

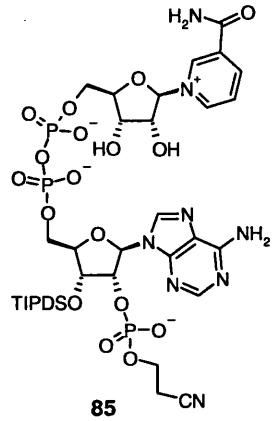

85

Carbonyl diimidazole (107 mg, 0.60 mmol) and Et_3N (34 µL, 0.24 mmol) were added to a solution of β-NMN **21** (75 mg, 0.22 mmol) in DMF (750 µL). This was stirred at room temperature under a nitrogen atmosphere for three hours and monitored by ^{31}P NMR (–9.5 ppm). Once complete a few drops of methanol were added and the solution stirred for a further five minutes. The solution was then evaporated to dryness and co-evaporated with DMF (3 x 100 µL). A solution of 5′ phosphate adenosine **74** (140 mg, 0.17 mmol) in DMF (700 µL) was added to the residue and the reaction stirred at room temperature overnight. The reaction was evaporated to dryness under reduced pressure, suspended in H_2O (5 mL), extracted with CH_2Cl_2 (3 x 5 mL) and loaded onto Q sepharose fast flow resin. The compound was eluted using a linear gradient of 1 M aq. TEAB. Fractions were analysed by ion exchange HPLC (method A) and the appropriate fractions evaporated to dryness. The white powder was then re-suspended in CH_3OH, repeatedly co-evaporated with CH_3OH to

remove excess Et_3N and lyophilised from D_2O to afford the pyrophosphate triethylammonium salt **85** as a white hygroscopic powder (129 mg, 63 %).

R_T 11 minutes (AG-MP1 water:150 mM aq. TFA); ^1H NMR δ_H (400 MHz; CD_3OD) 9.32 (1H, s, H-2_{nic}), 9.12 (1H, d, *J* 6.6, H-6_{nic}), 8.63 (1H, d, *J* 6.6, H-4_{nic}), 8.27, (1H, s, H-$2'_{ad}$), 7.94 (1H, t, *J* 6.6, H-5_{nic}), 7.86 (1H, s, H-$8'_{ad}$), 6.00 (1H, d, *J* 6.2, H-1′), 5.81 (1H, d, *J* 5.1, H-1), 4.98 (1H, m, H-2′), 4.24 (1H, t, *J* 5.1, H-2), 4.17-3.97 (7H, m, H-3, H-4, H-5, H-4′, H-5′), 3.55 (2H, m, CH_2CH_2O), 2.22 (2H, dd, J_{HH} 10.9, J_{PH} 6.2, CH_2CN) 1.33-0.95 (28H, m, ($CH(CH_3)_2)_4$). H-3′ occluded by HDO peak at 4.60; ^{13}C NMR δ_C (100MHz; CD_3OD) 163.9, 155.5, 152.2 (C), 149.8, 145.6, 142.9, 140.9, 140.5 (CH), 134.3 (C), 128.3 (CH), 118.8, 117.8 (C), 100.7, 88.3, 85.8, 85.6, 78.2, 77.4, 72.9, 71.3 (CH), 66.0, 65.0, 60.5, 19.0 (CH_2), 17.14 (4 x CH_3), 17.09 (2 x CH_3), 17.0 (2 x CH_3), 14.0, 13.9, 13.8 and 13.1 (CH); ^{31}P NMR δ_P (109 MHz; D_2O) –0.82 and –10.95; *m/z* [FAB^+] 1055.2 (M^+, 40 %).

Cyclic-2′,3′-phosphoryl-adenosine-5′-phosphate

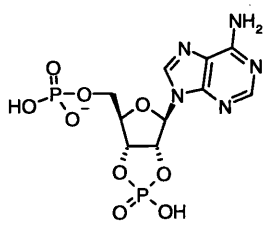

87

To a solution of 5′ phosphate adenosine **74** (50 mg, 0.063 mmol) in THF (1 mL) at 0°C buffered with AcOH (6 μL) was added 1 N TBAF in THF (120 μL). The solution was stirred under a nitrogen atmosphere for three hours, evaporated to dryness, re-suspended in water (10 mL) and extracted with CH_2Cl_2 (3 x 10 mL). The aqueous phase was applied to a Q sepharose fast flow column and eluted with a gradient of water to 1 M aq. TEAB and analysed by ion exchange HPLC. Fractions eluting at 80% TEAB (R_t 14.9 min) were collected and evaporated to dryness under reduced pressure. The white powder was then re-suspended in CH_3OH, repeatedly co-evaporated with CH_3OH to remove excess Et_3N and lyophilised from D_2O to afford the cyclic phosphate **87** as a white hydroscopic powder (8 mg, 32%).

R_T 15 min (AG-MP1 water:150 mM aq. TFA); ^1H NMR δ_H (400 MHz; D_2O) 8.23 (1H, s, H-2), 8.08 (1H, s, H-8), 6.17 (1H, d, *J* 3.9, H-1′), 5.28 (1H, m, H-2′), 5.04 (1H, m, H-3′), 4.45 (1H, m, H-4′) and 4.00-3.97 (2H, m, H-5′); ^{31}P NMR δ_P (109 MHz; D_2O) 20.7 and 1.2; *m/z* [FAB$^+$] 408.1 (M^+, 70 %).

Nicotinamide adenine dinucleotide 2′-(2-cyanoethoxy) phosphate

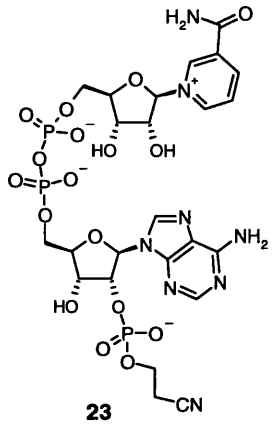

23

To a solution of purified pyrophosphate (TEA salt) **24** (73 mg, 0.063 mmol) in THF (700 µL) at 0°C were added AcOH (4 µL) and 1N TBAF in THF (80 µL). The solution was stirred for three hours, then evaporated to dryness under reduced pressure, re-suspended in water (10 mL) and extracted with CH_2Cl_2 (3 x 10 mL). The aqueous phase was loaded onto a column of AG-MP1 resin, eluted using a gradient of water:150 mM aq. TFA and analysed by ion exchange HPLC. The desired fractions were then evaporated to dryness and lyophilised from D_2O to afford desilylated pyrophosphate **23** as a white hydroscopic powder (37mg, 75 %).

R_T 11 minutes (AG-MP1 water:150 mM aq. TFA); ^1H NMR δ_H (400 MHz; D_2O) 9.24 (1H, s, H-2_{nic}), 9.08 (1H, d, *J* 6.6, H-6_{nic}), 8.76 (1H, d, *J* 7.8, H-4_{nic}), 8.41, (1H, s, H-$2'_{ad}$), 8.27 (1H, s, H-$8'_{ad}$), 8.10 (1H, dd, *J* 7.8, 6.6, H-5_{nic}), 6.13 (1H, d, *J* 5.0, H-1′), 5.98 (1H, d, *J* 5.4, H-1), 4.96 (1H, m, H-2′), 4.50 (1H, m, H-3′), 4.41-4.38 (2H, m, H-2, 3), 4.30 (1H, m, H-4′), 4.24-4.04 (5H, m, H-4, H-5′, H-5), 3.81-3.73 (2H, m, CH_2CH_2O), 2.56-2.53 (2H, m, CH_2CN); ^{31}P NMR δ_P (109 MHz; D_2O) –0.25 and –10.70. *m/z* [FAB$^+$] 795.1 (M^+, 60 %) [found 795.0953 $C_{24}H_{30}N_8O_{17}P_3^+$ requires 795.0942].

Adenosine-2′,5′-*bis*phosphate

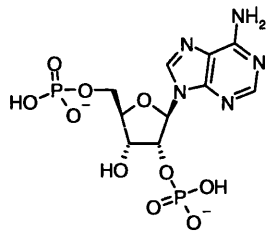

87

Method One

N,O-Bis(trimethylsilyl)acetamide (232 μL, 0.94 mmol) and DBU (23 μL, 0.15 mmol) were added to a solution of 5′ phosphate adenosine **74** (20 mg, 0.025 mmol) in pyridine (2.5 mL). It was stirred under a nitrogen atmosphere for ninety minutes, after which time the solvent was removed under reduced pressure, re-suspended in water (5 mL) and extracted with ether (3 x 10 mL). The aqueous phase was evaporated to dryness, co-evaporated with toluene and suspended in THF (500 μL). 1 N TBAF in THF (50 μL) was added and the solution stirred for two hours at 0°C under a nitrogen atmosphere. This was evaporated to dryness under reduced pressure, re-suspended in water (5 mL), extracted with CH_2Cl_2 (3 x 10 mL) and loaded onto a column of AG-MP1 resin. Fractions were analysed by ion exchange HPLC (method A) and the desired fractions were evaporated to dryness and lyophilised from D_2O to afford 2′,5′-ADP **87** as a white hydroscopic powder (4 mg, 36 %).

Method Two

N,O-Bis(trimethylsilyl)acetamide (185 μL, 0.75 mmol) and DBU (18 μL, 0.12 mmol) were added to a solution of purified pyrophosphate **85** (20 mg, 0.017 mmol) in pyridine (2.0 mL). It was stirred under a nitrogen atmosphere for ninety minutes, after which time the solvent was removed under reduced pressure, re-suspended in water (5 mL) and extracted with ether (3 x 10 mL). The aqueous phase was evaporated to dryness and co-evaporated with toluene and suspended in THF (500 μL). 1 N TBAF in THF (50 μL) was added and the reaction stirred for two hours at 0°C under a nitrogen atmosphere. This was evaporated to dryness under reduced pressure, re-suspended in water (5 mL), extracted with CH_2Cl_2 (3 x 10 mL) and loaded onto a column of AG-MP1 resin. Fractions were analysed by ion exchange

HPLC and the desired fractions were evaporated to dryness to afford 2′,5′-ADP **87** as a clear glassy solid (3 mg, 42 %).

R_T 14 minutes (AG-MP1 water:150 mM aq. TFA); ^{1}H NMR δ_H (400 MHz; D_2O) 8.45 (1H, s, H-2), 8.26 (1H, s, H-8), 6.16 (1H, d, *J* 5.8, H-1′), 4.97 (1H, m, H-2′), 4.47 (1H, m, H-3′), 4.27 (1H, m, H-4′) and 4.00-3.99 (2H, m, H-5′); ^{31}P NMR δ_P (109 MHz; D_2O) 1.1 and 0.6.

7.5 Modified synthesis of 2′, 5′ adenosine diphosphate

2′-(Dibenzyloxyphosphoryl)-3′,5′-*O*-(3-hydroxy-1,1,3,3-tetraisopropyldisiloxane-1,3-diyl) adenosine

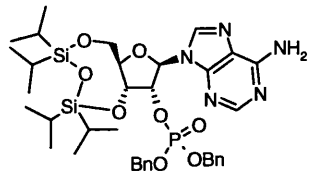

93

Bis(benzyloxy)diisopropylaminophosphine **52** (499 mg, 1.47 mmol) and imidazolium triflate **51** (856 mg, 3.98 mmol) were added to a solution of 3′,5′ protected adenosine **65** (500 mg, 0.98 mmol) in CH_2Cl_2 (30 mL) under a nitrogen atmosphere and stirred overnight. TLC analysis showed quantitative conversion to the phosphite intermediate ($CHCl_3$:acetone 1:1 R_F 0.6). The reaction was cooled to –78°C, *m*CPBA (508 mg, 2.95 mmol) was added and the oxidation monitored by ^{31}P NMR (149 ppm to –0.77 ppm) and TLC ($CHCl_3$:acetone 2:8 R_F 0.6). The reaction was quenched with 10% $Na_2S_2O_3$ (50 mL) and warmed to room temperature. The mixture was washed with $NaHCO_3$ (3 x 20 mL), brine (3 x 20 mL), dried (Na_2SO_4), filtered and evaporated to dryness. The product was then subject to flash chromatography on silica gel using CH_2Cl_2 to CH_2Cl_2:CH_3OH (95:5) as the eluent to afford the protected phosphate **93** as a white solid (591 mg, 78 %).

R_F 0.4 (CH_2Cl_2:CH_3OH 95:5); mp 160-162 °C (from CH_2Cl_2); ^{1}H NMR δ_H (600 MHz; $CDCl_3$) 8.20 (1H, s, H-2_{ad}), 7.82 (1H, s, H-8_{ad}), 7.33-7.30 (10H, m, H-Ar), 6.00 (1H, s, H-1′), 5.73 (2H, s, NH_2), 5.33 (1H, dd, J_{HH} 8.2, J_{PH} 4.9, H-2′), 5.17-5.07 (5H, m, 2 x OCH_2Ph, H-3′), 4.16 (1H, dd, *J* 13.2, 2.0, H-5′$_a$), 4.06 (1H, dt, *J* 2.6, 2.0, H-4′), 4.00 (1H, dd, *J* 13.2, 2.6, H-5′$_b$) and 1.10-1.00 (28H, m, 4 x $CH(CH_3)_2$); ^{13}C NMR δ_C

(150 MHz; $CDCl_3$) 155.6 (C), 153.2 (CH), 149.3 (C), 139.6 (CH), 135.9, 135.7 (C), 128.77, 128.76, 128.73, 128.71, 128.13, 128.08 (CH), 120.4 (C), 88.8, 81.5, 79.8 (CH), 69.9, 69.8 (CH_2), 68.8 (CH), 60.1 (CH_2), 17.6, 17.49, 17.48, 17.46, 17.2, 17.0 (CH_3), 13.5, 13.2, 13.0 and 12.8 (CH), 4 aromatic CH and 2 silanol CH_3 occluded; ^{31}P NMR δ_P (162 MHz; $CDCl_3$) –0.77 *m/z* [FAB$^+$] 770.3 (M^+, 100%) [found 770.3156 $C_{36}H_{53}N_5O_8PSi_2^+$ requires 770.3170].

2′-(Dibenzyloxyphosphoryl)-3′-*O*-(3-hydroxy-1,1,3,3-tetraisopropyldisiloxane-1-yl) adenosine

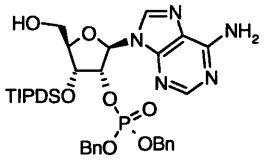

94

Benzyl protected phosphate adenosine **93** (591 mg, 0.77 mmol) at 0 °C was dissolved in TFA–H_2O–THF (1:1:4; *v/v/v*, 60 mL, 0 °C) and stirred for four hours at 0 °C after which TLC analysis (CH_2Cl_2:CH_3OH, 9:1; R_F 0.55) showed the reaction had gone to completion. It was neutralised with aq. saturated $NaHCO_3$ and the organic layer extracted with H_2O (3 x 20 mL) and brine (3 x 20 mL). The organic phase was collected, dried (Na_2SO_4), filtered and evaporated to dryness to afford the deprotected hydroxyl **94** as a white solid (456 mg, 76 %).

mp >210°C (decomposed); ^1H NMR δ_H (400 MHz; CD_3OD) 8.48 (1H, s, H-2_{ad}), 8.17 (1H, s, H-8_{ad}), 7.32-7.30 (6H, m, Ar-H), 7.19-7.13 (4H, Ar-H), 6.32 (1H, d, *J* 6.6, H-1′), 5.57 (1H, m, H-2′), 4.95-4.81 (5H, m, 2 x OCH_2Ph, H-3′), 4.35 (1H, m, H-4′), 3.89 (1H, dd, *J* 12.5, 2.7, H-5′$_a$), 3.85 (1H, dd, *J* 12.5, 2.5, H-5′$_b$) and 1.16-1.10 (28H, m, 4 x C*H*(CH_3)$_2$); ^{13}C NMR δ_C (100 MHz; CD_3OD) 153.2, 148.8 (C), 148.1 (CH), 141.9 (CH), 135.3 (2 x C), 128.6, 128.5, 127.79 127.75, 127.71, 127.69 (CH), 119.5 (C), 87.9, 87.0, 78.6, 72.3 (CH), 70.1, 70.0, 61.5 (CH_2), 17.0 (8 x CH_3), 13.9 (2 x CH) and 13.6 (2 x CH); ^{31}P NMR δ_P (109 MHz; CD_3OD) –1.16. *m/z* [FAB$^+$] 788.4 (M^+, 100%) [found 788.3276 $C_{36}H_{55}N_5O_9PSi_2^+$ requires 788.3276].

2′-(Dibenzyloxyphosphoryl)-3′-*O*-(3-hydroxy-1,1,3,3-tetraisopropyldisiloxane-1-yl)-5′-*H*-phosphonate-adenosine

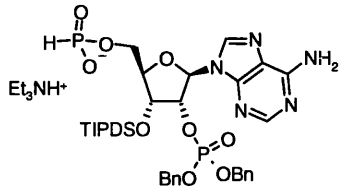

103

A solution of imidazole (69 mg, 1.01 mmol), PCl_3 (142 μL, 1.62 mmol) and Et_3N (300 μL, 2.16 mmol) in THF (8 mL) was stirred at 0°C for fifteen minutes after which time the 5′ alcohol **94** (425 mg, 0.54 mmol) in THF (12 mL) was added in one portion. The reaction was warmed to room temperature and stirred for fifteen minutes, quenched using 1 M aq. triethylammonium bicarbonate (TEAB) (20 mL) and stirred for a further fifteen minutes before the addition of CH_2Cl_2 (20 mL). The organic phase was washed with equal portions of 1 M aq. TEAB (1 x 20 mL), ice water (3 x 20 mL) and 1 M aq. TEAB (3 x 40 mL). The combined aqueous layers were extracted with CH_2Cl_2 (5 x 20 mL). The combined organic layers were dried ($MgSO_4$), filtered and evaporated to dryness. The oil was then subject to flash chromatography on silica gel eluting with a gradient of EtOAc to EtOAc:CH_3OH:H_2O (10:2:1). The desired fractions were collected and evaporated to dryness to afford the *H*-phosphonate salt **103** as a white foam (358 mg, 70 %).

^1H NMR δ_H (270 MHz; $CDCl_3$) 8.69 (1H, s, H-2_{ad}), 8.08 (1H, s, H-8_{ad}), 7.18-7.04 (10H, m, H-Ar), 6.72 (1H, d, J_{PH} 630, P-H), 6.33 (1H, d, *J* 5.7, H-1′), 5.45 (1H, m, H-2′), 4.83-4.74 (4H, m, CH_2Ar), 4.73-4.62 (2H, m, H-3′, H-4′), 3.96 (2H, m, H-5′) and 1.04-0.89 (28H, m, 4 x ($CH(CH_3)_2$)). ^{13}C NMR δ_C (100 MHz; $CDCl_3$) 155.4, 150.0 (C), 149.8 (CH), 140.0 (CH), 135.1, 135.0 (C), 128.6, 127.7 (CH), 118.8 (C), 85.1, 79.1, 71.5 (CH) (one carbon under $CHCl_3$ peak), 69.9, 69.8, 29.9 (CH_2), 17.53 (4 x CH_3), 17.47 (3 x CH_3), 17.39 (CH_3), 13.8 (CH), 13.7 (2 x CH) and 13.5 (CH). 8 aromatic CH occluded; ^{31}P NMR δ_P (109 MHz; $CDCl_3$) 6.78 and –0.90; *m/z* [FAB$^-$] 849.9 (M^-, 100 %) [found 850.2856 $C_{36}H_{54}N_5O_{11}P_2Si_2^-$ requires 850.2834].

2′-(Dibenzyloxyphosphoryl)-3′-*O*-(3-hydroxy-1,1,3,3-tetraisopropyldisiloxane-1-yl)-5′-phosphate-adenosine

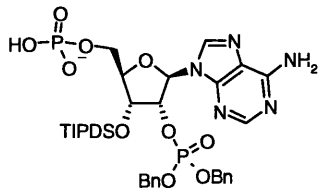

104

N,O-Bis(trimethylsilyl)acetamide (500 μL, 2.0 mmol) was added to a solution of *H*-phosphonate **29** (160 mg, 0.17 mmol) in $CDCl_3$ (2 mL) and allowed to react for one hour after which time ^{31}P NMR showed the presence of a new peak at δ 116 ppm. (1*S*)-(+)-10-(Camphorsulphonyl)oxaziridine **106** (135 mg, 0.59) was added and the oxidation monitored by ^{31}P NMR (–17 ppm). After fifteen minutes the solution was evaporated to dryness and the white precipitate re-suspended in a 1:1 mixture of CH_3OH:$CHCl_3$ (1 mL) with two drops of D_2O. The reaction was stirred for two hours and monitored by ^{31}P NMR for the phosphate peak (1.5 ppm). It was then evaporated to dryness and subject to flash chromatography on silica gel eluting with a gradient of EtOAc to EtOAc:CH_3OH:H_2O (8:2:1). The desired fractions were collected and evaporated to dryness to afford the phosphate **104** as a white foam (73 mg, 50 %).

^1H NMR δ_H (270 MHz; CH_3OD) 8.70 (1H, s, H-2_{ad}), 8.14 (1H, s, H-8_{ad}), 7.31-7.04 (10H, m, H-Ar), 6.43 (1H, d, *J* 7.4, H-1′), 5.43 (1H, m, H-2′), 4.94-4.90 (4H, m, CH_2Ar), 4.83-4.64 (2H, m, H-3′, H-4′), 4.13 (2H, m, H-5′) and 1.09-0.88 (28H, m, 4 x ($CH(CH_3)_2$)); ^{13}C NMR δ_C (67.5 MHz; $CDCl_3$) 157.0 (C), 153.6 (CH), 151.2 (C), 141.2 (CH), 136.4, 136.3 (C), 129.7 (4 x CH), 129.6 (4 x CH), 128.9 (2 x CH), 119.9 (C), 87.6, 86.1, 80.2, 74.3 (CH), 71.1, 71.0, 65.9 (CH_2), 18.1, 18.0 (CH_3), 17.92 (2 x CH_3), 17.89 (4 x CH_3), 14.8 (2 x CH), 14.5, 14.0 (CH); ^{31}P NMR δ_P (109 MHz; $CDCl_3$) 1.2 and –0.90. *m/z* [FAB$^-$] 869.7 (M^-, 65 %).

7.6 Synthesis of NADP and NAADP

Nicotinamide adenine dinucleotide 2′-(*bis*benzyloxy) phosphate

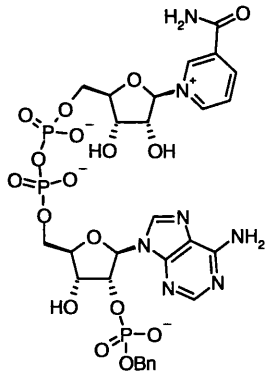

109

Carbonyl diimidazole (43 mg, 0.26 mmol) and Et_3N (14 μL, 0.096 mmol) were added to a solution of β-NMN **21** (30 mg, 0.088 mmol) in DMF (300 μL) and stirred at room temperature under a nitrogen atmosphere for three hours monitoring by ^{31}P NMR (–9.5 ppm). A few drops of methanol were then added and the solution was stirred for a further five minutes. It was then evaporated to dryness and co-evaporated with DMF (3 x 100 μL). A solution of *bis*phosphate adenosine **104** (69 mg, 0.08 mmol) in DMF (500 μL) was added and the resulting mixture was stirred at room temperature for twenty-four hours. The reaction material was evaporated to dryness under reduced pressure, suspended in H_2O (5 mL), extracted with CH_2Cl_2 (3 x 5 mL) and the aqueous phase evaporated to dryness before being used crude in the following reaction.

Crude silylated pyrophosphate **108** (70mg) was suspended in THF (2.5 mL) and treated with a solution of 1 N TBAF in THF (300 μL) buffered with AcOH (15 μL). This reaction was stirred at 0°C for three hours after which complete conversion to a new peak was observed by ion exchange HPLC (R_T 11 minutes). The reaction was evaporated to dryness, re-suspended in water (10 mL), extracted three times with EtOAc (3 x 10 mL) and loaded onto a column of AG-MP1. The compound was then eluted using a gradient of water:150 mM aq. TFA and the fractions were analysed by ion exchange HPLC (method A). The desired fractions were combined and

lyophilised from D_2O to afford monobenzyl NADP **109** as a white hygroscopic powder (11 mg, 14 % from starting adenosine **104**).

R_T 11 minutes (AG-MP1 water:150 mM aq. TFA); ^1H NMR δ_H (400 MHz; D_2O) 9.26 (1H, s, H-2_{nic}), 9.10 (1H, d, *J* 6.3, H-6_{nic}), 8.76 (1H, d, *J* 8.2, H-4_{nic}), 8.37 (1H, s, H-$2'_{ad}$), 8.12 (1H, dd, *J* 8.2, 6.3, H-5_{nic}), 8.01 (1H, s, H-$8'_{ad}$), 7.12-7.09 (3H, m, H-Ar), 6.83-6.81 (2H, m, H-Ar), 6.03 (1H, d, *J* 6.6, H-1), 5.99 (1H, d, *J* 5.4, H-1′), 5.11-5.05 (1H, m, H-2′), 4.73 (2H, s, CH_2Ar), 4.46-4.43 (2H, m, H-4′ and H-2), 4.31 (1H, m, H-3) and 4.23-4.05 (5H, m, H-4, H-5, H-5′). H-3′ under HDO peak; ^{13}C NMR δ_C (100 MHz; D_2O) 164.5, 149.3 148.7 (C), 146.2, 144.5, 142.9, 142.7, 140.0 (CH), 136.8, 134.0 (C), 128.84, 128.77, 128.44, 128.41, 127.9, 125.9 (CH), 118.3 (C), 100.1, 87.3, 86.4, 84.5, 77.7, 77.1, 74.0 (CH), 70.9 (CH_2), 70.5 (CH), 66.7, and 65.6 (CH_2); ^{31}P NMR δ_P (109 MHz; D_2O) -0.04 and –11.6.

Nicotinamide adenine dinucleotide phosphate (NADP)

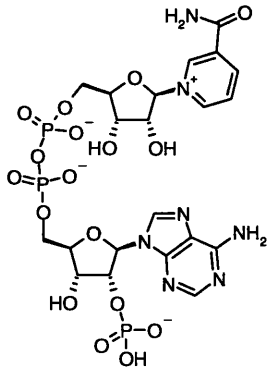

7

Monobenzyl NADP **109** (11mg, 0.013 mmol) was suspended in a degassed mixture of H_2O:CH_3OH (3:1) (2 mL). Cyclohexadiene (100 μL, 1.04 mmol) and 10 % Pd/C (10 mg) were added and the reaction was stirred for two hours at room temperature. The palladium was filtered through a membrane filter, washed with water, applied to a column of AG-MP1 and eluted using a gradient of water:150 mM aq. TFA. Fractions were analysed by ion exchange HPLC and the appropriate fractions (R_T 11 minutes) were combined and lyophilised from D_2O to afford NADP **7**as a white hygroscopic powder (3 mg, 31 %).

R_T 11 minutes (AG-MP1 water:150 mM aq. TFA); ^1H NMR δ_H (400 MHz; D_2O) 9.30 (1H, s, H-2_{nic}), 9.14 (1H, d, *J* 5.4, H-6_{nic}), 8.81 (1H, d, *J* 8.2, H-4_{nic}), 8.46 (1H, s, H-

2′$_{ad}$), 8.31 (1H, s, H-8′$_{ad}$), 8.16 (1H, m, H-5$_{nic}$), 6.16 (1H, d, *J* 5.4, H-1), 6.03 (1H, d, *J* 5.5, H-1′), 4.99 (1H, m, H-2′), 4.52 (1H, m, H-3′), 4.46-4.43 (2H, m, H-4′, H-2), 4.35 (1H, m, H-3), 4.28-4.12 (5H, m, H-4, H-5, H-5′); ^{13}C NMR δ_C (100 MHz; D_2O) 165.4, 151.9 148.5 (C), 147.9, 145.9, 142.5, 141.6, 139.8 (CH), 133.7 (C), 128.6 (CH), 118.2 (C), 99.9, 87.1, 86.4, 83.7, 77.5, 76.7, 70.7, 69.9 (CH), 65.3, and 64.9 (CH_2); ^{31}P NMR δ_P (109 MHz; D_2O) 0.38 and –10.6.

Nicotinic acid adenine dinucleotide phosphate (NAADP)

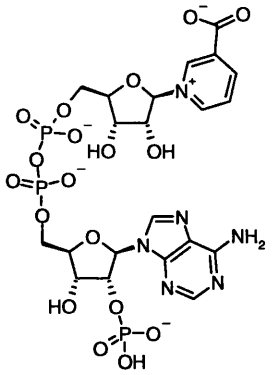

3

To a solution of NADP **7** (5.0 mg, 0.007 mmol) in a 100 mM AcOH-NaOH buffer (pH 4, 1.25 mL) was added nicotinic acid (15 mg, 0.12 mmol) and crude ADP ribosyl cyclase enzyme (7 μL). It was stirred at room temperature for six hours and monitored by ion exchange HPLC. Once complete the reaction was applied to an ion exchange column of AG-MP1 and purified using a water-150 mM aq. TFA gradient. The desired fractions were combined, evaporated to dryness, co-evaporated from D_2O and lyophilised from D_2O to afford NAADP **3** as a white hygroscopic powder (3 mg, 60 %).

R_T 16 minutes (AG-MP1 water:150 mM aq. TFA); ^{1}H NMR δ_H (400 MHz; D_2O) 9.32 (1H, s, H-2$_{nic}$), 9.18 (1H, d, *J* 5.9, H-6$_{nic}$), 8.87 (1H, d, *J* 8.1, H-4$_{nic}$), 8.45 (1H, s, H-2′$_{ad}$), 8.28 (1H, s, H-8′$_{ad}$), 8.13 (1H, m, H-5$_{nic}$), 6.14 (1H, d, *J* 5.5, H-1), 6.03 (1H, d, *J* 5.1, H-1′), 4.98 (1H, m, H-2′), 4.51 (1H, m, H-3′), 4.44 (2H, br s, H-4′) 4.41 (1H, m, H-2), 4.32 (1H, m, H-3), 4.27-4.10 (5H, m, H-4, H-5, H-5′); ^{13}C NMR δ_C (105 MHz; D_2O) 165.5 (COOH), 149.8 (C_A4) 148.3 (C_A6), 147.0 (CH_A2), 144.6 (CH_N6), 142.8 (CH_N4), 141.8 (CH_A8, CH_N2), 133.8 (C_N3), 128.6 (CH_N5), 118.4 (C_A5), 99.8 (CH_N1′), 86.8 (CH_A4′), 83.9 (CH_A1′), 77.4 (CH_N2′), 76.8 (CH_A2′), 73.9 (CH_N4′), 70.5

(CH_N3'), 69.9 (CH_A3'), 65.2, and 64.8 (CH_2); ^{31}P NMR δ_P (109 MHz; D_2O) 1.47 and –9.67; *m/z* [FAB$^+$] 744.8 (M^+, 50 %) [found 745.0658 $C_{21}H_{28}N_6O_{18}P_3^+$ requires 745.0673].

7.7 Synthesis of an NAADP analogue

1-Cyano-2,3,5-tri-*O*-benzoyl-β-D-ribose[78]

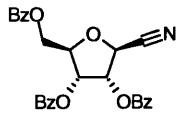

116

To a stirred solution of 1-*O*-acetyl-2,3,5-tri-*O*-benzoyl-β-D-ribofuranose **122** (5.0 g, 9.9 mmol) in CH_2Cl_2 under a nitrogen atmosphere (13 mL) was added TMSCN (2.7 mL, 20.3 mmol). The reaction mixture was treated with one portion of tin (IV) chloride (1M in CH_2Cl_2) (11.9 mL, 10.2 mmol). The darkening solution was stirred for two minutes then poured into aq. saturated $NaHCO_3$ (100 mL) and stirred for five minutes. CH_2Cl_2 (125 mL) was added and the emulsion filtered through a celite pad. The CH_2Cl_2 layer was separated and the aqueous layer further extracted with CH_2Cl_2 (3 x 20 mL). The combined organics were dried (Na_2SO_4), filtered and evaporated to dryness to afford the nitrile **116** as a light orange syrup. A portion was removed and subject to flash chromatography on silica gel using a gradient of hexane-EtOAc as eluent. The required fractions were collected and evaporated to dryness to afford the nitrile **116** as a white foam.

R_F 0.41 (hexane:EtOAc 8:2); mp 59-60 °C (from hexane) (lit.[78] 58 °C); ν_{max} (KBr)/cm^{-1} 2956 (Ar-H), 1728 (C=O) and 1268 (C-O); ^1H NMR δ_H (400 MHz; $CDCl_3$) 8.04-8.07 (2H, m, Ar-H), 7.85-7.91 (4H, m, Ar-H), 7.48-7.55 (3H, m, Ar-H), 7.29-7.42 (6H, m, Ar-H), 5.94 (1H, dd, *J* 5.4, 4.4, H-2), 5.79 (1H, t, *J* 5.4, H-3), 4.92 (1H, d, *J* 4.4, H-1), 4.66 (1H, dd, *J* 10.2, 5.4, H-5_a), 4.65 (1H, m, H-4) and 4.54 (1H, m, H-5_b); ^{13}C NMR δ_C (100 MHz; $CDCl_3$) 166.2, 165.1, 164.9 (C=O), 134.2, 134.0, 133.6, 130.02, 130.00, 129.9 (CH), 129.3 (C), 128.9, 128.8, 128.7 (CH), 128.5, 128.3 (C) 115.9 (C), 81.2, 74.7, 72.1, 69.7 (CH) and 63.5 (CH_2), 6 aromatic CH and 1 aromatic C occluded; *m/z* [FAB$^+$] 472.0 (M^+, 30 %) [found 472.1394 $C_{27}H_{22}NO_7$ requires 472.1396].

Methyl-2-(2′,3′,5′-tri-*O*-benzoyl-β-D-ribofuranosyl) thiazoline-4-carboxylate

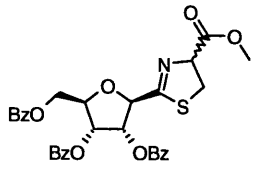

123

Cysteine methyl ester (2.5 g, 14.8 mmol) and Et_3N (2.1 mL, 14.8 mmol) were added to a solution of the crude nitrile **116** (5.0 g, 10.6 mmol) in CH_3OH (200 mL) and stirred under nitrogen at room temperature. After three hours the solution was evaporated to dryness, dissolved in CH_2Cl_2 (20 mL), washed twice with equal volumes of water (2 x 20 mL), 5% aq. $NaHCO_3$ (2 x 20 mL) and brine (2 x 20 mL). The organic layers were combined, dried (Na_2SO_4), filtered and evaporated to dryness under reduced pressure to afford the thiazoline **123** as an equal mixture of diastereoisomers. A portion was removed and subject to flash chromatography on silica gel using a gradient of hexane-EtOAc as eluent. The required fractions were collected and evaporated to dryness to afford the nitrile as a white foam.

R_F 0.36 (hexane:EtOAc 7:3); mp 60-63 °C (from hexane); ^1H NMR δ_H (400 MHz; $CDCl_3$) 8.13-8.10 (4H, m, H-Ar), 8.00-7.90 (8H, m, H-Ar, H-Ar*), 7.59-7.52 (6H, m, H-Ar, H-Ar*), 7.46-7.33 (12H, m, H-Ar, H-Ar*), 5.91 (1H, t, *J* 5.1, H-2′), 5.89 (1H, t, *J* 5.1, H-2′*), 5.83 (1H, t, *J* 5.1, H-3′), 5.82 (1H, t, *J* 5.1, H-3′*), 5.23 (1H, m, H-1′), 5.23 (1H, m, H-1′*), 5.18 (1H, t, *J* 9.4, H-4), 5.14 (1H, t, *J* 9.4, H-4*), 4.80 (1H, dd, *J* 10.0, 3.5, H-5′$_a$), 4.77 (1H, dd, *J* 10.0, 3.5, H-5′$_a$*), 4.69 (2H, m, H-4′, H-4′*), 4.61 (1H, dd, *J* 10.0, 4.3, H-5′$_b$), 4.58 (1H, dd, *J* 10.0, 4.3, H-5′$_b$*), 3.79 (3H, s, CH_3), 3.70 (3H, s, CH_3*), 3.59 (1H, dd, *J* 11.5, 9.3, H-5$_a$), 3.57 (1H, dd, *J* 11.5, 9.3, H-5$_a$*), 3.52 (1H, dd, *J* 11.5, 9.3, H-5$_b$) and 3.46 (1H, dd, *J* 11.5, 9.3, H-5$_b$*); ^{13}C NMR δ_C (100 MHz; $CDCl_3$) 174.0, 173.9, 170.8, 170.6, 166.22, 166.18 (C, C*), 165.3 (C and C*), 165.14, 165.09 (C, C*), 133.6 (CH and CH*), 133.5 (CH and CH*), 133.2 (CH and CH*), 129.9, 129.8 (6 x CH, 6 x CH*), 129.63, 129.59, 129.0, 128.9, 128.7 (3 x C, 3 x C*), 128.5 (6 x CH, 6 x CH*), 80.8, 80.6, 78.14, 78.10, 74.9, 74.8, 72.54, 72.47 (CH, CH*), 64.0, 63.9 (CH_2, CH_2*), 60.4 (CH and CH*), 52.83, 52.76 (CH_3, CH_3*), 34.6 and 34.4 (CH_2, CH_2*); *m/z* [FAB$^+$] 590.2 (M^+, 35 %).

Methyl 2-(2′,3′,5′-tri-*O*-benzoyl-β-D-ribofuranosyl)thiazole-4-carboxylate

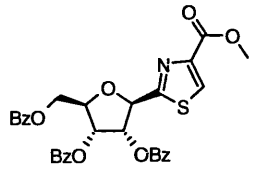

121

To a solution of crude thiazoline **123** (4.7 g, 8.0 mmol) in CH_2Cl_2 (250 mL) was added DBU (16 mmol, 2.4 mL). This was cooled to 0°C and $BrCCl_3$ (0.95 mL, 9 mmol) was added dropwise, stirred overnight and concentrated under vacuum. The solution was washed three times with aq. saturated NH_4Cl (3 x 20 mL) and the aqueous phase extracted twice with EtOAc (2 x 20 mL). The combined organics were dried (Na_2SO_4), filtered and evaporated to dryness under vacuum. The residue was subject to flash chromatography on silica gel using a gradient of hexane-EtOAc (9:1 to 7:3) as eluent. The required fractions were collected and evaporated to dryness to afford the thiazole **121** as a light yellow foam (3.6 g, 61 % over three steps).

R_F 0.48 (hexane:EtOAc, 6:4); mp 61 °C (from hexane); $[\alpha]^{25}_D$ –43 (*c* 1 in $CHCl_3$); ν_{max} (KBr)/cm^{-1} 2962 (Ar-H), 1726 (C=O) and 1269 (C-O); ^1H NMR δ_H (400 MHz; $CDCl_3$) 8.15 (1H, s, H-5), 8.09-8.07 (2H, m, H-Ar), 8.00-7.97 (2H, m, H-Ar), 7.92-7.89 (2H, m, H-Ar), 7.58-7.51 (3H, m, H-Ar), 7.45-7.3 (6H, m, Ar-H), 5.91-5.88 (2H, m, H-2′, H-3′), 5.75 (1H, d, *J* 4.7, H-1′), 4.89 (1H, dd, *J* 12.1, 3.1, H-5′$_a$), 4.78-4.75 (1H, m, H-4′) 4.61 (1H, dd, *J* 12.1, 3.9, H-5′$_b$) and 3.91 (3H, s, CH_3); ^{13}C NMR δ_C (100 MHz; $CDCl_3$) 169.6, 166.2, 165.3, 165.2, 161.6, 147.3 (C), 133.72, 133.68, 133.5, 130.1, 129.92, 129.90 (CH), 129.6, 129.0, 128.9 (C), 128.8, 128.7, 128.6, 80.9, 80.8, 76.8, 72.5 (CH), 64.0 (CH_2) and 52.8 (CH_3), 7 aromatic CH occluded; *m/z* [FAB$^+$] 588.1 (M^+, 56 %) [found 588.1342 $C_{31}H_{26}NO_9S$ requires 588.1328].

Methyl 2-(β-D-ribofuranosyl)thiazole-4-carboxylate

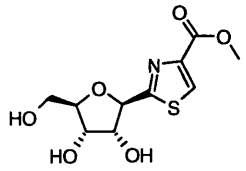

124

$CH_3O^-Na^+$ (92 mg, 0.017 mmol) was added to a solution of thiazole **121** (100 mg, 0.17 mmol) in CH_3OH (3 mL) and stirred overnight at room temperature then quenched with Dowex 50WX 4-100. The mixture was filtered, evaporated to dryness subject to flash chromatography on silica gel using a gradient CH_2Cl_2 to CH_2Cl_2:CH_3OH (100 to 97:3) as eluent to afford the methyl carboxylate **124** as a white solid (37 mg, 80 %).

R_F 0.46 (CH_2Cl_2:CH_3OH, 9:1); mp 119-121 °C (from CH_2Cl_2); $[\alpha]^{25}_D$ –6 (*c* 1 in CH_3OH); ν_{max} (KBr disk)/cm^{-1} 3369 (O-H), 1726 (C=O) and 1237 (C-O); ^1H NMR δ_H (400 MHz; CD_3OD) 8.20 (1H, s, H-5), 4.95 (1H, d, *J* 5.5, H-1′), 4.10 (1H, m, H-4′), 3.98-3.94 (2H, m, H-2′, H-3′), 3.72 (3H, s, CH_3), 3.68 (1H, dd, *J* 12.5, 2.3 H-5′$_a$) and 3.56 (1H, dd, *J* 12.5, 4.6, H-5′$_b$); ^{13}C NMR δ (100 MHz; CD_3OD) 172.2, 163.1, 145.7 (C), 129.8, 84.7, 81.8, 76.8, 71.2 (CH), 61.8 (CH_2) and 53.0 (CH_3); *m/z* [FAB$^+$] 276.1 (M^+, 100 %) [found 276.0538 $C_{10}H_{14}NO_6S$ requires 276.0542].

2-(β-D-Ribofuranosyl)thiazole-4-carboxamide (Tiazofurin)

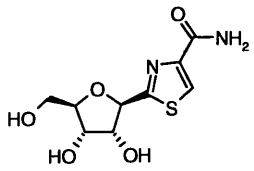

111

To a stirred solution of freshly prepared saturated methanolic ammonia (5 mL) at 0°C was added the methyl carboxylate **121** (40 mg, 0.68 mmol). The reaction was stirred at room temperature overnight in a glass pressure tube, then evaporated to dryness, re-suspended in methanolic ammonia (5 mL), and stirred for a further twenty-four hours. The solvent was evaporated, the residue dissolved in water (10 mL) and washed with EtOAc (5 x 20 mL). The aqueous phase was concentrated under reduced pressure and

lyophilised from D_2O to afford tiazofurin **111** as a yellowish waxy solid (152 mg, 86 %).

mp 145-147 °C (from D_2O) (lit.[75], 143 °C); $[\alpha]^{25}_D$ –7.5 (*c* 1 in H_2O); ν_{max} (film)/cm^{-1} 3390 (O-H) and 1667 (C=O); ^1H NMR δ_H (400 MHz; D_2O) 8.02 (1H, s, H-5), 4.98 (1H, d, *J* 5.1, H-1′), 4.16 (1H, dd, *J* 5.5, 3.9, H-4′), 4.03-3.99 (2H, m, H-2′, H-3′), 3.70 (1H, dd, *J* 12.5, 3.9, H-5′$_a$) and 3.59 (1H, dd, *J* 12.5, 5.5, H-5′$_b$); ^{13}C NMR δ_C (100 MHz; D_2O) 171.5, 165.4, 148.3 (C), 129.2, 84.9, 81.7, 76.7, 71.4 (CH) and 61.9 (CH_2); *m/z* [FAB$^+$] 261.1 (M^+, 100 %) [found 261.0543 $C_9H_{13}N_2O_5S$ requires 261.0545].

2-(β-D-Ribofuranosyl)thiazole-4-carboxylic acid

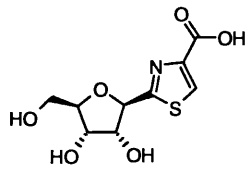

113

To a stirred solution of methyl carboxylate **121** (10 mg, 0.17 mmol) in dioxane (3 mL) was added 1 M NaOH (3 mL) and stirred overnight. The reaction was acidified using Dowex resin (50WX 4-100), filtered, washed with water and extracted three times with EtOAc (3 x 5 mL). The aqueous phase was concentrated under reduced pressure and lyophilised from D_2O to afford the carboxylic acid **113** as a white hygroscopic solid (38 mg, 86 %).

$[\alpha]^{25}_D$ –10 (*c* 1 in H_2O); ν_{max} (film)/cm^{-1} 3390 (O-H) 1713 (C=O); ^1H NMR δ_H (400 MHz; D_2O) 8.02 (1H, s, H-5), 5.01 (1H, d, *J* 5.1, H-1′), 4.18 (1H, m, H-4′), 4.03-4.01 (2H, m, H-2′, H-3′), 3.72 (1H, dd, *J* 12.5, 3.1, H-5′$_a$) and 3.61 (1H, dd, *J* 12.5, 5.1, H-5′$_b$). ^{13}C NMR δ_C (100 MHz; D_2O) 172.1, 163.8, 146.1 (C), 129.9, 84.6, 81.9, 76.8, 71.2 (CH) and 61.9 (CH_2). *m/z* [FAB$^+$] 261.9 (M^+, 100 %) [found 262.0398 $C_9H_{13}NO_6S$ requires 262.0385].

Methyl-2-(5′-phosphoryl-β-D-ribofuranosyl)thiazole-4-carboxylate

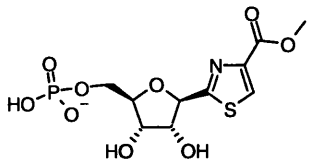

127

$POCl_3$ (20 μL, 0.22 mmol) was added to a stirred solution of methyl carboxylate **124** (50 mg, 0.18 mmol) in triethylphosphate (0.75 mL) under a nitrogen atmosphere at 0°C. The reaction was monitored by using an ion exchange HPLC (method A) and after ninety minutes the reaction was quenched using H_2O (5 mL) and stirred for 5 minutes. The excess triethylphosphate was extracted five times with ethyl acetate (5 x 15 mL) and the aqueous phase loaded onto ion exchange gradifac column (AG-MP1) eluted with a gradient of 150 mM aq. TFA. Fractions were analysed by ion exchange HPLC (method A), desired fractions collected, evaporated to dryness and lyophilised from D_2O to afford the phosphate **127** as a light yellow hygroscopic gum (46 mg, 72 %).

R_T 14 minutes (AG-MP1 water:150 mM aq. TFA); ^1H NMR δ_H (400 MHz; D_2O) 8.13 (1H, s, H-5), 4.88 (1H, d, *J* 5.1, H-1′), 4.06 (1H, t, *J* 5.1, H-4′), 4.01-3.98 (2H, m, H-2′, H-3′), 3.93-3.80 (2H, m, H-5′) and 3.63 (3H, s, CH_3); ^{13}C NMR δ_C (100 MHz; D_2O) 172.4, 163.0, 145.4 (C), 130.0, 83.3, 82.0, 76.8, 71.3 (CH), 65.4 (CH_2) and 53.0 (CH_3); ^{31}P NMR δ_P (162 MHz; D_2O) 0.97.

2-(5′-Phosphoryl-β-D-ribofuranosyl)thiazole-4-carboxylic acid

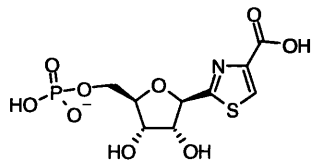

128

$POCl_3$ (70 μL, 0.75 mmol) was added to a stirred solution of methyl carboxylate **124** (180 mg, 0.67 mmol) in triethylphosphate (3.0 mL) under a nitrogen atmosphere at 0°C. The reaction was monitored by using an ion exchange HPLC (method A) and after 1.5 hours the reaction was quenched using H_2O (5 mL) and stirred for 5 minutes. The excess triethylphosphate was extracted five times with ethyl acetate (5 x 15 mL)

and the pH of the aqueous phase adjusted to 10 with 1 M NaOH and stirred overnight then loaded onto ion exchange column (AG-MP1) and eluted using a gradient of TFA. Fractions were analysed by ion exchange HPLC (method A), desired fractions collected, evaporated to dryness and lyophilised from D_2O to afford the phosphate **128** as a light yellow hygroscopic solid (187 mg, 82 %).

R_T 17 minutes (AG-MP1 water:150 mM aq. TFA); ^1H NMR δ_H (400 MHz; D_2O) 8.14 (1H, s, H-5), 4.92 (1H, d, *J* 5.1, H-1′), 4.09 (1H, t, *J* 4.9, H-4′), 4.07-4.01 (2H, m, H-2′, H-3′) and 4.01-3.88 (2H, m, H-5′); ^{13}C NMR δ_C (100 MHz; D_2O) 172.5, 163.7, 145.7 (C), 130.2, 82.9, 81.9, 76.7, 71.0 (CH) and 65.5 (CH_2); ^{31}P NMR δ_P (162 MHz; D_2O) 0.21.

2-Thiazole-4-carboxylate adenine dinucleotide phosphate

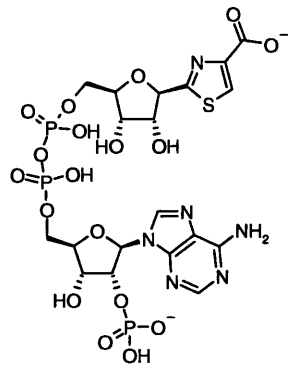

114

Carbonyl diimidazole (88 mg, 0.6 mmol) and Et_3N (31 μL, 0.22 mmol) were added to a solution of methyl carboxylate phosphate **127** (70 mg, 0.2 mmol) in DMF (500 μL) and stirred at room temperature under a nitrogen atmosphere for three hours (^{31}P NMR δ–10ppm). Two drops of CH_3OH were added and the solution stirred for further 10 minutes. The reaction was evaporated to dryness, co-evaporated with DMF (3 x 100 μL), a solution of diphosphate adenosine **74** (151 mg, 0.19 mmol) in DMF (500 μL) added and the reaction stirred overnight. The solution was applied to a column of Q-Sepharose and eluted with a gradient of water- 2 M aq. TEAB. The desired fractions were analysed by ion exchange HPLC, collected and evaporated to dryness. The product was then used crude in the following reaction.

To a crude solution of protected pyrophosphate **131** (60 mg) in CH_3OH (1.5 mL) was added 1 M NaOH (1.5 mL) and stirred overnight. ^{31}P NMR showed a new peak at 4.2 ppm corresponding to a free phosphate. The reaction was neutralised to pH 7, loaded onto a Q-Sepharose column and eluted with a gradient of water- aq. 2 M TEAB. The desired fractions were analysed by HPLC, collected and evaporated to dryness. The product was then used crude in the following reaction.

HF/pyridine (7:3 *v/v*) (25 μL, 0.96 mmol) was added to a solution of crude silyl protected pyrophosphate **132** (23 mg) in pyridine (1 mL) and stirred for 20 minutes then neutralised with aq. saturated $NaHCO_3$. The solution was evaporated to dryness, re-suspended in H_2O, applied to a column of AG-MP1 and eluted using a gradient of water:150 mM aq. TFA. The desired fractions were analysed, collected, evaporated to dryness and lyophilised from D_2O to afford TAADP **114** as a white hygroscopic powder (7 mg, 5 % over three steps from starting adenosine **74**).
R_T 20 minutes (AG-MP1 water:150 mM aq. TFA); ^1H NMR δ_H (400 MHz; D_2O) 8.39 (1H, s, H-$2'_{ad}$), 8.25 (1H, s, H-$8'_{ad}$), 8.09 (1H, s, H-5_{th}), 6.12 (1H, d, *J* 5.5, H-1′), 5.03 (1H, m, H-2′), 4.91 (1H, d, *J* 5.1, H-1), 4.52 (1H, t, *J* 3.9, H-3′), 4.29 (1H, m, H-4′), 4.14 (5H, m, H-2, H-3, H-4, H-5 ′) and 4.00 (2H, m, H-5); ^{13}C NMR δ_C (150 MHz; D_2O) 172.9, 164.1, 150.0 (C), 148.6, (CH) 145.8 (C), 144.9, 143.2 (CH), 130.5, 118.7 (C), 87.2, 84.3, 83.5, 82.0, 77.3, 77.1, 71.5, 70.3 (CH), 66.0 and 65.7 (CH_2); ^{31}P NMR δ_P (109 MHz; D_2O) 0.73 and 10.69; *m/z* [FAB$^-$] 749.0 (M^-, 100 %) [found 749.0062 $C_{19}H_{24}N_6O_{18}P_3S^-$ requires 749.0081].

Reference List

1. Patel, S.; Churchill, G. C.; Galione, A. *Trends Biochem. Sci.* **2001**, *26*, 482-489.

2. Bootman, M. D.; Collins, T. J.; Peppiatt, C. M.; Prothero, L. S.; MacKenzie, L.; De Smet, P.; Travers, M.; Tovey, S. C.; Seo, J. T.; Berridge, M. J.; Ciccolini, F.; Lipp, P. *Sem. Cell Devel. Biol.* **2001**, *12*, 3-10.

3. Berridge, M. J.; Lipp, P.; Bootman, M. D. *Nature Rev. Mol. Cell Biol.* **2000**, *1*, 11-21.

4. Carafoli, E. *Proc. Natl. Acad. Sci. USA* **2002**, *99*, 1115-1122.

5. East, M. Life, death and calcium. Chemistry in Britain , pp 42-44. 2002. 1-3-2002.

6. Clapper, D. L.; Walseth, T. F.; Dargei, P. J.; Lee, H. C. *J. Biol. Chem.* **1987**, *262*, 9561-9568.

7. Galione, A.; Cancela, J. M.; Churchill, G. C.; Genazzani, A. A.; Lad, C.; Thomas, J. M.; Wilson, H.; Terrar, D. in *Methods in cADPR and NAADP research*, p 249-296, 2000.

8. Lee, H. C.; Walseth, T. F.; Bratt, G. T.; Hayes, R. N.; Clapper, D. L. *J. Biol. Chem.* **1989**, *264*, 1608-1615.

9. Lee, H. C.; Aarhus, R.; Graeff, R. M.; Gurnack, M. E.; Walseth, T. F. *Nature* **1994**, *370*, 307-309.

10. Lee, H. C.; Aarhus, R.; Levitt, D. *Nature Struct. Biol.* **1994**, *1*, 143-144.

11. Aarhus, R.; Graeff, R. M.; Dickey, D. M.; Walseth, T. F.; Lee, H. C. *J. Biol. Chem.* **1995**, *270*, 30327-30333.

12. *Cyclic ADP-ribose and NAADP*, ed. H. C. Lee, Kluwer Academic Publishers, Boston, 2002.

13. Lee, H. C. *Annu. Rev. Pharmacol. Toxicol.* **2001**, *41*, 317-345.

14. Guse, A. H. *Curr. Mol. Med.* **2002**, *2*, 259-268.

15. Chini, E. N.; Chini, C. C. S.; Kato, I.; Takasawa, S.; Okamoto, H. *Biochem. J.* **2002**, *362*, 125-130.

16. Lee, H. C.; Aarhus, R. *J. Biol. Chem.* **1995**, *270*, 2152-2157.

17. Chini, E. N.; Beers, K. W.; Dousa, T. P. *J. Biol. Chem.* **1995**, *270*, 3216-3223.

18. Lee, H. C.; Aarhus, R. *J. Biol. Chem.* **1997**, *272*, 20378-20383.

19. Patel, S.; Churchill, G. C.; Galione, A. *Biochem. J.* **2000**, *352*, 725-729.

20. Genazzani, A. A.; Billington, R. A. *Trends. Pharmacol. Sci.* **2002**, *23*, 165-167.

21. Churchill, G. C.; Galione, A. *EMBO J.* **2001**, *20*, 2666-2671.

22. Billington, R. A.; Ho, A.; Genazzani, A. A. *J. Physiol. - (London)* **2002**, *544*, 107-112.

23. Genazzani, A. A.; Galione, A. *Biochem. J.* **1996**, *315*, 721-725.

24. Churchill, G. C.; Okada, Y.; Thomas, J. M.; Genazzani, A. A.; Patel, S.; Galione, A. *Cell* **2002**, *111*, 703-708.

25. Yamasaki, M.; Masgrau, R.; Morgan, A. J.; Churchill, G. C.; Patel, S.; Ashcroft, S. J. H.; Galione, A. *J. Biol. Chem.* **2004**, *279*, 7234-7240.

26. Galione, A.; Patel, S.; Churchill, G. C. *Biol. Cell* **2000**, *92*, 197-204.

27. Berg, I.; Potter, B. V. L.; Mayr, G. W.; Guse, A. H. *J. Cell Biol.* **2000**, *150*, 581-588.

28. Berridge, G.; Cramer, R.; Galione, A.; Patel, S. *Biochem. J.* **2002**, *365*, 295-301.

29. Billington, R. A.; Thuring, J. W.; Conway, S. J.; Packman, L.; Holmes, A. B.; Genazzani, A. A. *Biochem. J.* **2004**, *378*, 275-280.

30. Lee, H. C.; Aarhus, R. *Biochim. Biophy. Acta-General Subjects* **1998**, *1425*, 263-271.

31. Lee, H. C.; Aarhus, R.; Gee, K. R.; Kestner, T. *J. Biol. Chem.* **1997**, *272*, 4172-4178.

32. Aarhus, R.; Dickey, D. M.; Graeff, R. M.; Gee, K. R.; Walseth, T. F.; Lee, H. C. *J. Biol. Chem.* **1996**, *271*, 8513-8516.

33. Berghauser, J.; Jeck, R.; Pfeiffer, M. *Biotechnol. Lett.* **1981**, *3*, 339-344.

34. Zhou, T. J.; Kurnasov, O.; Tomchick, D. R.; Binns, D. D.; Grishin, N. V.; Marquez, V. E.; Osterman, A. L.; Zhang, H. *J. Biol. Chem.* **2002**, *277*, 13148-13154.

35. Walt, D. R.; Findeis, M. A.; Riosmercadillo, V. M.; Auge, J.; Whitesides, G. M. *J. Am. Chem. Soc.* **1984**, *106*, 234-239.

36. Tanimori, S.; Ohta, T.; Kirihata, M. *Bioorg. Med. Chem. Lett.* **2002**, *12*, 1135-1137.

37. Lee, J.; Churchil, H.; Choi, W. B.; Lynch, J. E.; Roberts, F. E.; Volante, R. P.; Reider, P. J. *Chem. Commun.* **1999**, 729-730.

38. Ciuffreda, P.; Casati, S.; Santaniello, E. *Tetrahedron* **2000**, *56*, 3239-3243.

39. Ikemoto, T.; Haze, A.; Hatano, H.; Kitamoto, Y.; Ishida, M.; Nara, K. *Chem. Pharm. Bull.* **1995**, *43*, 210-215.

40. Kristinsson, H.; Nebel, K.; Osullivan, A. C.; Struber, F.; Winkler, T.; Yamaguchi, Y. *Tetrahedron* **1994**, *50*, 6825-6838.

41. Wagner, D.; Verheyden, P. H.; Moffatt, J. G. *J. Org. Chem.* **1974**, *39*, 24-30.

42. David, S.; Malleron, A. *Carbohydr. Res.* **2000**, *329*, 215-218.

43. Ishido, Y.; Nakazaki, N.; Sakairi, N. *J. Chem. Soc., Perkin Trans. 1* **1979**, 2088-2098.

44. Nishino, S.; Takamura, H.; Ishido, Y. *Tetrahedron* **1986**, *42*, 1995-2004.

45. Robins, M. J.; Wilson, J. S.; Hansske, F. *J. Am. Chem. Soc.* **1983**, *105*, 4059-4065.

46. Marriott, J. H.; Mottahedeh, M.; Reese, C. B. *Carbohydr. Res.* **1991**, *216*, 257-269.

47. Huang, W. C.; Orban, J.; Kintanar, A.; Reid, B. R.; Drobny, G. P. *J. Am. Chem. Soc.* **1990**, *112*, 9059-9068.

48. Tanaka, T.; Tamatsukuri, S.; Ikehara, M. *Tetrahedron Lett.* **1986**, *27*, 199-202.

49. Bannwarth, W.; Trzeciak, A. *Helv. Chim. Acta.* **1987**, *70*, 175-186.

50. Hayakawa, Y.; Kataoka, M. *J. Am. Chem. Soc.* **1998**, *120*, 12395-12401.

51. Wada, T.; Morigchi, T.; Sekine, M. *J. Am. Chem. Soc.* **1994**, *116*, 9901-9911.

52. Zhu, X. F.; Williams, H. J.; Scott, A. I. *Tetrahedron Lett.* **2000**, *41*, 9541-9545.

53. Yu, K. L.; Fraserreid, B. *Tetrahedron Lett.* **1988**, *29*, 979-982.

54. Marwood, R. D.; Riley, A. M.; Jenkins, D. J.; Potter, B. V. L. *J. Chem. Soc., Perkin Trans. 1* **2000**, 1935-1947.

55. Hughes, N. A.; Kenner, G. W.; Todd, A. *J. Chem. Soc.* **1957**, 3733-3738.

56. Haynes, L. J.; Hughes, N. A.; Kenner, G. W.; Todd, A. *J. Chem. Soc.* **1957**, 3727-3732.

57. Wittmann, V.; Wong, C. H. *J. Org. Chem.* **1997**, *62*, 2144-2147.

58. Pendergast, W.; Yerxa, B. R.; Douglass, J. G.; Shaver, S. R.; Dougherty, R. W.; Redick, C. C.; Sims, I. F.; Rideout, J. L. *Bioorg. Med. Chem. Lett.* **2001**, *11*, 157-160.

59. Armstrong, J. I.; Verdugo, D. E.; Bertozzi, C. R. *J. Org. Chem.* **2003**, *68*, 170-173.

60. Marlow, A. L.; Kiessling, L. L. *Org. Lett.* **2001**, *3*, 2517-2519.

61. Imai, J.; Torrence, P. F. *J. Org. Chem.* **1985**, *50*, 1418-1426.

62. Ogilvie, K. K.; Beaucage, S. L.; Entwistle, D. W. *Tetrahedron Lett.* **1976**, *16*, 1255-1256.

63. Reddy, M. P.; Hanna, N. B.; Farooqui, F. *Tetrahedron Lett.* **1994**, *35*, 4311-4314.

64. Hsiung, H. M. *Tetrahedron Lett.* **1982**, *23*, 5119-5122.

65. Evans, D. A.; Gage, J. R.; Leighton, J. L. *J. Org. Chem.* **1992**, *57*, 1964-1966.

66. Gaffney, P. R. J.; Reese, C. B. *J. Chem. Soc., Perkin Trans. 1* **2001**, 192-205.

67. Kadokura, M.; Wada, T.; Seio, K.; Sekine, M. *J. Org. Chem.* **2000**, *65*, 5104-5113.

68. Kamber, M.; Just, G. *Can. J. Chem.* **1985**, *63*, 823-827.

69. Yashunsky, D. V.; Nikolaev, A. V. *J. Chem. Soc., Perkin Trans. 1* **2000**, *8*, 1195-1198.

70. Wada, T.; Mochizuki, A.; Sato, Y.; Sekine, M. *Tetrahedron Lett.* **1998**, *39*, 7123-7126.

71. Tian, Z. P.; Gu, C.; Roeske, R. W.; Zhou, M. M.; Vanetten, R. L. *Int. J. Pept. Prot. Res.* **1993**, *42*, 155-158.

72. Migaud, M. E.; Pederick, R. L.; Bailey, V. C.; Potter, B. V. L. *Biochemistry* **1999**, *38*, 9105-9114.

73. Dowden, J.; Moreau, C.; Brown, R. S.; Berridge, G.; Galione, A.; Potter, B. V. L. *Angew. Chem., Int. Ed. Eng.* **2004**, *43*, 4637-4640.

74. Tiazofurin is the generic name approved by the United States Adopted Name Council.

75. Ramasamy, K. S.; Bandaru, R.; Averett, D. *J. Org. Chem.* **2000**, *65*, 5849-5851.

Appendix

Pergamon

Tetrahedron Letters 43 (2002) 6561–6562

TETRAHEDRON LETTERS

A concise route to tiazofurin

Richard S. Brown, James Dowden,* Christelle Moreau and Barry V. L. Potter

Wolfson Laboratory of Medicinal Chemistry, Department of Pharmacy and Pharmacology, University of Bath, Claverton Down, Bath BA2 7AY, UK

Received 14 May 2002; accepted 16 July 2002

Abstract—Successful oxidation of a key thiazoline intermediate allows an efficient synthesis of tiazofurin in four steps from commercially available 1′-acetoxy-2′,3′,5′-tri-*O*-benzoyl-β-D-ribofuranose.

Tiazofurin **4**[1] is converted in vivo into the active metabolite thiazole-4-carboxamide adenine dinucleotide (TAD), an analogue of NAD that prevents de novo guanine nucleotide synthesis via inhibition of inosine monophosphate dehydrogenase (IMPDH, EC 1.1.1.205).[2] The consequent decrease in cellular GTP and deoxyGTP concentrations interrupts DNA and RNA synthesis in rapidly-dividing tumour cells. Tiazofurin proved effective in reducing the leukaemic cell burden in acute myelogenous leukaemia patients, but was found to be too toxic for general clinical application.[3–5] Subsequent discovery of two IMPDH isoforms, of which type II is up-regulated in human leukaemia cell lines,[6,7] has prompted studies to inform the design of isoform selective inhibitors[8] and has renewed interest in tiazofurin and its analogues.[9,10]

Several routes have been published toward this compound; of these the preparation reported by Ramasamy and co-workers[11] provides tiazofurin, while avoiding the use of hydrogen sulfide gas. These authors reported unsuccessful oxidation of thiazoline **1** with MnO_2, or a range of other conditions, observing elimination of the 2′,3′-benzoate esters to afford thiazole-furan **2** in each case (Scheme 1).

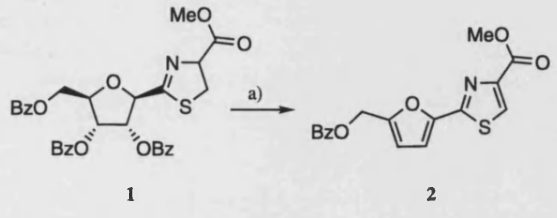

1 2

Scheme 1. *Reagents and conditions*:[11] (a) MnO_2/benzene/reflux.

Instead, isopropylidene **3** was converted into the target compound **4** with good reported yields, but the introduction and removal of the isopropylidene protecting group introduced an extra three steps from 1′-acetoxy-2′,3′,5′-tri-*O*-benzoyl-β-D-ribofuranose **5** (Scheme 2).

We now report the successful oxidation of thiazoline **1** that removes the need for this detour and reduces the synthesis of tiazofurin to a simple four-step procedure.

Thiazoline **1** was prepared by reaction of 1′-cyano-2′,3′,5′-tri-*O*-benzoyl-β-D-ribofuranose[12] with L-cysteine methyl ester in the presence of triethylamine according to an established protocol.[11] Complete epimerisation of the cysteine α-proton was observed by ^1H NMR, but this centre will become part of the aromatic thiazole. A number of oxidation conditions, including DDQ in toluene,[13] did not proceed to our satisfaction, but we were pleased to observe clean conversion of the thiazoline **1** in the presence of bromotrichloromethane and DBU.[14] Thiazole **6** was thus prepared from commer-

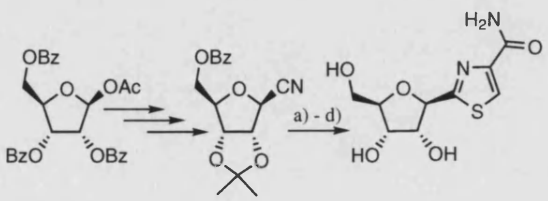

5 3 4

Scheme 2. *Reagents and conditions*:[11] (a) cysteine ethyl ester·HCl/Et_3N; (b) MnO_2/benzene/reflux; (c) 90% TFA; (d) NH_3/MeOH.

* Corresponding author. E-mail: j.dowden@bath.ac.uk

0040-4039/02/$ - see front matter
PII: S0040-4039(02)01470-3

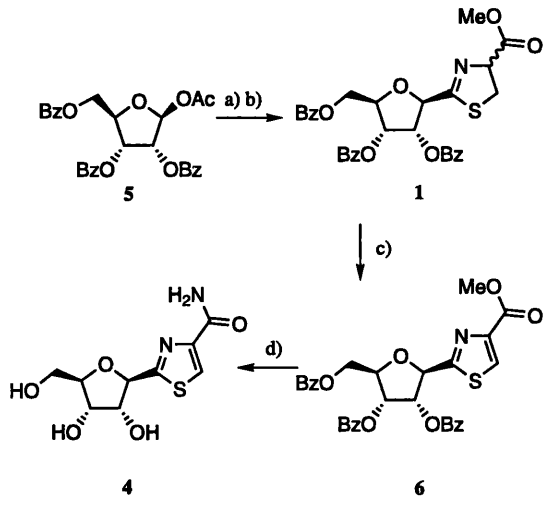

Scheme 3. *Reagents and conditions*: (a) TMSCN, $SnCl_4$, CH_2Cl_2, rt, 2 min; (b) L-cysteine methyl ester hydrochloride, Et_3N, CH_2Cl_2; (c) $BrCCl_3$, DBU, CH_2Cl_2, 0°C, 61% over three steps; (d) NH_3/MeOH, rt, 20 h, 86%.

cially available 1′-acetoxy-2′,3′,5′-tri-*O*-benzoyl-β-D-ribofuranose **5** in an unoptimised isolated yield of 61% over the three steps with just one chromatographic separation (Scheme 3).[15]

Ester aminolysis and global deprotection were effected by stirring **6** in methanolic ammonia.[16] Dissolution of the concentrated crude reaction mixture into water and extraction of all contaminants into ethyl acetate proved sufficient to afford pure tiazofurin **4** in 86% yield.

In summary, selective dehydrogenation of a thiazoline **1** in the presence of sensitive ribose 2′,3′,5′-tribenzoate ester protecting groups is described. The immediate benefit of this discovery is to improve the efficiency of tiazofurin synthesis in the absence of hydrogen sulfide affording a productive four-step protocol.

Acknowledgements

We thank the EPSRC for a studentship (to R.S.B.) and the BBSRC for a project grant, and we acknowledge the use of the EPSRC Chemical Database Service at Daresbury.

References

1. Tiazofurin is the generic name approved by the United States Adopted Name Council.
2. Lui, M. S.; Faderan, M. A.; Liepnieks, J. J.; Natsumeda, Y.; Olah, E.; Jayaram, H. N.; Weber, G. *J. Biol. Chem.* **1984**, *259*, 5078–5082.
3. Tricot, G.; Weber, G. *Anticancer Res.* **1996**, *16*, 3341–3347.
4. Tricot, G. J.; Jayaram, H. N.; Lapis, E.; Natsumeda, Y.; Nichols, C. R.; Kneebone, P.; Heerema, N.; Weber, G.; Hoffman, R. *Cancer Res.* **1989**, *49*, 3696–3701.
5. Wright, D. G.; Boosalis, M. S.; Waraska, K.; Oshry, L. J.; Weintraub, L. R.; Vosburgh, E. *Anticancer Res.* **1996**, *16*, 3349–3354.
6. Konno, Y.; Natsumeda, Y.; Nagai, M.; Yamaji, Y.; Ohno, S.; Suzuki, K.; Weber, G. *J. Biol. Chem.* **1991**, *266*, 506–509.
7. Natsumeda, Y.; Ohno, S.; Kawasaki, H.; Konno, Y.; Weber, G.; Suzuki, K. *J. Biol. Chem.* **1990**, *265*, 5292–5295.
8. Colby, T. D.; Vanderveen, K.; Strickler, M. D.; Markham, G. D.; Goldstein, B. M. *Proc. Natl. Acad. Sci. USA* **1999**, *96*, 3531–3536.
9. Franchetti, P.; Marchetti, S.; Cappellacci, L.; Jayaram, H. N.; Yalowitz, J. A.; Goldstein, B. M.; Barascut, J. L.; Dukhan, D.; Imbach, J. L.; Grifantini, M. *J. Med. Chem.* **2000**, *43*, 1264–1270.
10. Franchetti, P.; Grifantini, M. *Curr. Med. Chem.* **1999**, *6*, 599–614.
11. Ramasamy, K. S.; Bandaru, R.; Averett, D. *J. Org. Chem.* **2000**, *65*, 5849–5851.
12. Dudfield, P. J.; Le, V. D.; Lindell, S. D.; Rees, C. W. *J. Chem. Soc., Perkin Trans. 1* **1999**, 2937–2942.
13. Yoshino, K.; Kohno, T.; Morita, T.; Tsukamoto, G. *J. Med. Chem.* **1989**, *32*, 1528–1532.
14. Williams, D. R.; Lowder, P. D.; Gu, Y. G.; Brooks, D. A. *Tetrahedron Lett.* **1997**, *38*, 331–334.
15. **Preparation of methyl 2-(2′,3′,5′-tri-*O*-benzoyl-β-D-ribofuranosyl)thiazole-4-carboxylate 6.** 1,8-Diazabicyclo[5.4.0]-undec-7-ene (2.4 mL, 16 mmol, 2 equiv.) was added to a stirred solution of methyl 1′-(2′,3′,5′-tri-*O*-benzoyl-β-D-ribofuranosyl)thiazoline-4′-carboxylate **1** (4.7 g, 8 mmol) in CH_2Cl_2 (250 mL). The solution was cooled to 0°C and $BrCCl_3$ (1.9 g, 9 mmol, 1.0 mL) was added dropwise and the resulting mixture stirred overnight. The reaction mixture was then concentrated, dissolved into ethyl acetate and the solution washed 3× with satd aq. NH_4Cl. The organic layer was dried (Na_2SO_4), filtered, concentrated and subject to column chromatography on silica gel using a gradient of hexane:ethyl acetate from 9:1 to 7:3 as eluent to afford **6** as a light yellow foam. Yield 3.6 g, 6.1 mmol, 61% over three steps. $[\alpha]_D^{25}$ –43.3 (*c* 1, $CHCl_3$); IR (KBr) 1726, 1269, 1095, 710 cm^{-1}; ^1H NMR (400 MHz $CDCl_3$): δ 8.15 (1H, s, SCH) 8.09–8.07 (2H, m, Ar-H) 8.00–7.97 (2H, m, Ar-H) 7.92–7.87 (2H, m, Ar-H) 7.58–7.51 (3H, m, Ar-H) 7.45–7.33 (6H, m, Ar-H) 5.91–5.88 (2H, m, H-2′,3′) 5.75 (1H, d, J=4.7, H-1′) 4.89 (1H, dd, J=12.1, 3.1, H-5′a) 4.75–4.78 (1H, m, H-4′) 4.61 (1H, dd, J=12.1, 3.9, H-5′b) 3.91 (3H, s, $COOCH_3$); ^{13}C NMR (100 MHz (DEPT) $CDCl_3$): δ 169.6(0), 166.2(0), 165.3(0), 165.2(0), 161.6(0), 147.3(0), 133.8(1), 133.7(1), 133.5(1), 130.1(1), 129.92(1), 129.91(1), 129.6(0), 128.98(0), 128.92(0), 128.76(1), 128.7(1), 128.6(1), 80.9(1), 80.8(1), 76.9(1), 72.5(1), 64.0(2), 52.8(3). MS (FAB$^+$) *m*/*z* (M+H)$^+$ 588 (100). MS (FAB$^+$/HR) *m*/*z* (M+H)$^+$ calcd for $C_{31}H_{25}NO_9S$: 588.1329. Found: 588.1341.
16. Srivastava, P. C.; Pickering, M. V.; Allen, L. B.; Streeter, D. G.; Campbell, M. T.; Whitowski, J. T.; Sidwell, R. W.; Robins, R. K. *J. Med. Chem.* **1977**, *20*, 256–262.

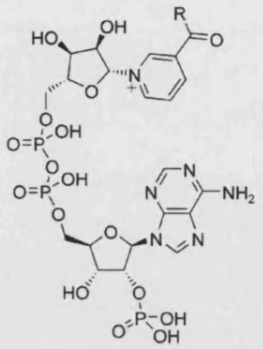

1 NAADP; R = OH
2 NADP; R = NH_2

Figure 1. Compounds **1** and **2**.

Natural Products Synthesis

Chemical Synthesis of the Second Messenger Nicotinic Acid Adenine Dinucleotide Phosphate by Total Synthesis of Nicotinamide Adenine Dinucleotide Phosphate**

James Dowden, Christelle Moreau, Richard S. Brown, Georgina Berridge, Antony Galione, and Barry V. L. Potter*

Modulation of intracellular calcium concentration creates signals that control a range of biological pathways. Orchestration of these signals by an array of small molecule second messengers provides the necessary complexity to complement multiple cellular responses, such as activation of the immune system or fertilization.[1] The discovery that nicotinic acid adenine dinucleotide phosphate (NAADP, **1**; Figure 1) potently induces intracellular calcium release in the eggs of sea urchins[2] raised its status, from minor contaminant of nicotinamide adenine dinucleotide phosphate (NADP, **2**), to an important novel second messenger.[3] Recent studies attest to the higher potency of this molecule than the well-known messengers for calcium release [i.e., inositol trisphosphate and cyclic adenosine diphosphoribose (cADPR)] and many of these extend its actions to a wide range of mammalian cells, including cardiac,[4a] skeletal,[4b] T cells,[4c] smooth muscle,[4d] pancreatic acinar[4e] and pancreatic beta cells.[3a,4f,4g]

Compound **1** also appears to play an important role in calcium signaling by triggering and coordinating calcium signals evoked by other calcium-mobilizing messengers. Sensitive radio-receptor assays for tissue measurements of this dinucleotide have been developed,[5] but it is clear that further understanding of its biology will draw heavily on the development of selective molecules to probe this novel signaling pathway and characterize its protein components. A chemo-enzymatic route has so far generated **1** and a small number of analogues from **2** by enzyme-mediated exchange of nicotinamide for nicotinic acid. Clearly, the chemistry that can be performed on this sensitive molecule and compatibility with the enzyme limits the range of available analogues. A synthetic route would provide a wider range of tailored derivatives, such as non-hydrolysable analogues, that could not be achieved by established methods.

We are currently exploring a range of strategies to generate chemical tools with which to interrogate this biological system, including the total synthesis of both dinucleotides. Whitesides and co-workers developed a semisynthetic route to β-nicotinamide adenine dinucleotide (NAD) by using NAD pyrophosphorylase immobilized on polyacrylamide gel, but this relied on a battery of enzymes and reagents to generate stoichiometric quantities of adenosine triphosphate (ATP).[6a] More recently, Lee et al.[6b] reported a practical total chemical synthesis of nicotinamide adenine dinucleotide (NAD) that built upon a much earlier synthesis by Todd and co-workers.[7] Indeed, a number of researchers have developed chemical approaches to NAD derivatives, not least for the preparation of cyclic adenosine 5′-diphosphate ribose.[8] However, the presence of a sensitive 2′-phosphate on a ribose makes the synthesis of **1** or **2** significantly more complex. During early studies Todd and co-workers reported an apparent preparation of **2** inferred from biological evaluation of the complex product mixture but did not successfully isolate the desired coenzyme from the mixture.[7b] Given that this dinucleotide is readily available from commercial sources, it is perhaps not surprising that further developments toward its chemical synthesis are not apparent

[*] Dr. J. Dowden, Dr. C. Moreau, R. S. Brown, Prof. B. V. L. Potter
Wolfson Laboratory of Medicinal Chemistry
Department of Pharmacy & Pharmacology
University of Bath
Claverton Down, Bath BA2 7AY (UK)
Fax: (+44) 1225-386-114
E-mail: j.dowden@bath.ac.uk
G. Berridge, Prof. A. Galione
Department of Pharmacology
University of Oxford (UK)

[**] This research was funded by the Biotechnology and Biology Sciences Research Council and an Engineering and Physical Sciences Research Council (EPSRC) studentship. We acknowledge the use of the EPSRC Chemical Database Service at Daresbury.

Supporting information for this article is available on the WWW under http://www.angewandte.org or from the author.

 DOI: 10.1002/anie.200460054

in the general literature. To the best of our knowledge therefore, we describe the first chemical synthesis of **2** as a single isomer, its enzymatic conversion to the potent second messenger **1**, and both chemical characterization and biological proof of the integrity of the latter dinucleotide.

The potentially fragile nature of **2** and its intermediates encouraged a conservative approach that involves the late construction of the pyrophosphate bond by activation of β-nicotinamide mononucleotide (β-NMN, **4**; Scheme 1) and reaction with a suitably decorated adenosine building block. It is known that the 2′-phosphate motif is critical for the activity of **1**[9] and may be involved in its degradation.[10] Structural modifications are likely to be informative and thus we designed a synthesis that was both robust and sufficiently flexible to accommodate future modifications at any position on the NAADP framework.

Compound **4** was generated from tetra-*O*-acetyl-β-D-ribose.[6,11] Reaction between adenosine and 1,3-dichloro-1,1,3,3,-tetraisopropyl disiloxane in pyridine proceeded without complication and lead to simultaneous tethering of the 3′- and 5′-hydroxyls of adenosine, thus permitting unambiguous phosphorylation of the 2′-alcohol. Subsequent elaboration of the 2′-alcohol **5** could be achieved with a range of phosphoramidites, including *bis*(benzyloxy)-*N,N*-diisopropylaminophosphane **6** (Scheme 1), to afford the respective phosphate **7** in high yield after oxidation of the intermediate phosphite with *m*-chloroperoxybenzoic acid (*m*CPBA). Imidazolium triflate[12] was used instead of tetrazole to produce a less reactive phosphytilating intermediate that does not react with the purinyl amine, thus saving two steps. Carefully controlled acidic conditions, as previously reported by Scott and co-workers afforded exclusive protodesilylation at the less hindered 5′-position in quantitative yield.[13]

Generally, phosphoramidite chemistry did not proceed in acceptable yields at the 5′-hydroxyl of the precursor, presumably because this position is somewhat crowded. Resorting to the reactive tetrazole-activated phosphoramidites required amine protection and actually led to incorporation of an unwelcome silanol phosphate. It was frustrating that a multitude of protection strategies failed due to unexpected incompatibility with the desired route. Although this chemistry might be optimized to provide acceptable yields of the desired compound, we found that *H*-phosphonate chemistry offered a very effective alternative. Selective 5′-protodesilylation of bis(benzyloxy)phosphate **7**, then treatment of the product with trisimidazolylphosphane, generated in situ from PCl_3 and imidazole, rapidly furnished **8** in quantitative yield (Scheme 1). Oxidation was best achieved by using conditions reported by Sekine and co-workers[14] in a process monitored by ^{31}P NMR spectroscopy, such that the *H*-phosphonate triethylammonium salt ($\delta(^{31}P) = 5.5$ ppm) was treated with *N,O*-bis(trimethylsilyl)acetamide (BSA) to afford the bis(trimethysilylphosphonate) ($\delta(^{31}P) = 116$ ppm) after approximately 1 h; the oxidant (1*R*)-(+)-(10-camphorsulfonyl)oxaziridine (CSO) was added to this to generate *bis*(trimethylsilyl)phosphate ($\delta(^{31}P) = -16$ ppm) in about 20 min, which

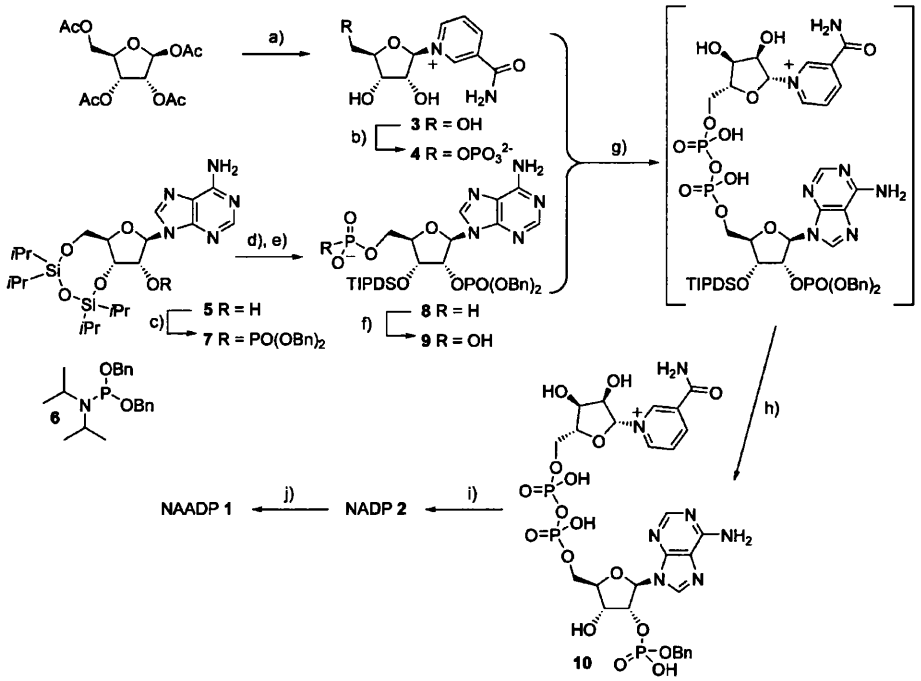

Scheme 1. a) Nicotinamide, CH_3CN, then TMSOTf, RT; 1.5 h, then MeOH, RT; 1 h; b) $POCl_3$, $PO(OMe)_3$, 0°C, 4 h; c) **6**, CH_2Cl_2, RT; 3 h, then *m*CPBA, −78°C, 0.5 h, 98%; d) TFA/H_2O/THF 1:1:4, 0°C, 3 h, 98%; e) PCl_3, imidazole, Et_3N, THF, 0°C, 15 mins, then 1 M TEAB aq. pH 7, RT, 15 mins, quant.; f) BSA, $CHCl_3$, RT, 1 h, then CSO, RT, 0.5 h, then MeOH/D_2O, RT, 15 mins, 72%; g) β-NMN, carbonyl diimidazole, Et_3N, DMF, RT, 3 h, then **9**, DMF, RT, 16 h; h) 1 M TBAF/THF, AcOH, 0°C, 1.5 h, 22% i) 10% Pd/C, cyclohexadiene, MeOH/H_2O, RT, 2 h, 77%; j) Nicotinic acid, *Aplysia* ADP-ribosyl cyclase, 1 M NaOAc aq. pH 4, RT, 5 h, 63%.

slowly hydrolyzed to give the phosphate **9** ($\delta(^{31}P) = 1$ ppm) upon addition of D_2O.

Successful repetition of the approach to NAD reported by Lee and co-workers[6b] encouraged initial exploration of morpholidate activation of the precursor **8**, but attempted conversions were not productive. Production and reaction of the β-NMN imidazolide could be monitored by using ^{31}P NMR spectroscopy ($\delta(^{31}P) = -10.6$ ppm).

Contrary to other reports,[6] we found that bisbenzylphosphate precursor **9** appeared to react with good conversion when monitored by ^{31}P NMR spectroscopy and offered an attractive protecting-group strategy (Scheme 1). Both benzyl groups remained intact during this reaction and the resulting product could not be purified by using our preferred ion-exchange chromatography method. Instead, the crude material was treated with 1M TBAF in THF/AcOH to effect simultaneous cleavage of the silanol ether and one of the benzyl protecting groups to yield monobenzyl NADP **10** after ion-exchange chromatography. Although there was no evidence of migration of the 2′-phosphate, the overall yield of around 22% for these two steps is modest, but is comparable to many literature reports as pyrophosphate bond formation and isolation of the resulting product is generally difficult and yields are highly variable. An alternative route that employs a bis(2-cyanoethyl) protected precursor related to **9** gave yields in the range of 60–80% for the pyrophosphate coupling and we are currently exploring improvements of this route to achieve useful conversion. Nonetheless, transfer hydrogenation of **10** yielded material that was identical to commercial preparations of β-NADP **2** in satisfactory (77%) yield.

With a wider objective in mind we chose to convert synthetic NADP **2** into the target NAADP **1** to test its behavior in a relevant biological system. Base exchange to replace nicotinamide with nicotinic acid was achieved by using an excess of the latter and crude *Aplysia* ADP-ribosyl cyclase [enzyme commission number E.C.3.2.2.5] prepared from *Aplysia* ovotestis[15] to provide NAADP **1** in 63% yield.

The ability of **1** to induce release of Ca^{2+} ions was tested by using a cell-free system derived from the eggs of sea urchins. Aliquots of homogenates of sea-urchin eggs comprise vesicles derived from the intracellular stores that sequester calcium when supplemented with an ATP-regenerating system. Concentration-dependent calcium release is observed when this mixture is challenged with second messengers, such as **1**, which can be measured by using cuvette-based fluorimetry and the calcium reporter dye fluo-3.[16] Synthetic NAADP, carefully quantified by using total phosphate assay prior to evaluation,[17] potently induced calcium release in an identical manner to "authentic" NAADP prepared from commercial NADP (Figure 2). Both preparations display an important characteristic of this signaling pathway that occurs at subthreshold concentrations of NAADP in homogenate of sea-urchin eggs. They both potently deactivate the calcium store in a time dependent manner, so that further challenge with NAADP does not lead to significant calcium release (Figure 3). This property allows competition binding experiments that measure the extent that nonlabeled NAADP displaces subthreshold concentrations of [^{32}P]NAADP (0.2 nM) from the putative receptor (Figure 4).

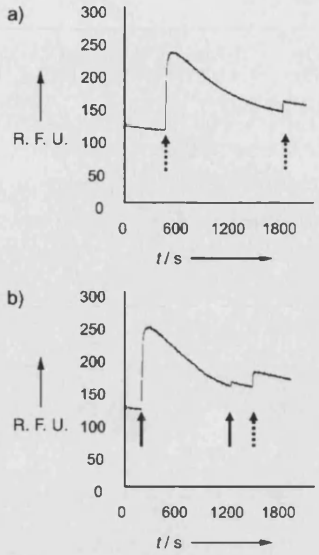

Figure 2. Ca^{2+}-ion release from homogenate of sea-urchin eggs by 100 nM authentic NAADP (dotted arrows) or 100 nM synthetic NAADP, **1** (solid arrows): Samples diluted to 2.5% in GluIM in the presence of regenerating system and kept at 17°C with agitation for 3 h to facilitate Ca^{2+}-ion uptake into stores. Ca^{2+}-ion release determined by an increase of Fluo-3 fluorescence at 526 nm; data expressed as released [Ca^{2+}], determined by fluorescence in arbritrary units; $n => 3$ for each point. R. F. U. = relative fluorescence units.

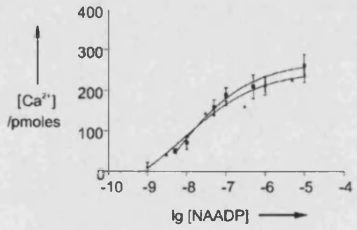

Figure 3. Inhibition of NAADP-induced Ca^{2+}-ion release by authentic NAADP (squares) or synthetic NAADP **1** (triangles) in the homogenate of sea-urchin eggs: Samples diluted to 2.5% in GluIM in the presence of a regenerating system and kept at 17°C with agitation for 3 h to facilitate Ca^{2+}-ion uptake into stores. Ca^{2+}-ion release determined by an increase of Fluo-3 fluorescence at 526 nm; data expressed as pmoles of Ca^{2+}-ions released; $n => 3$ for each point.

In summary, the strategy of using 1,1,3,3-tetraisopropyl disiloxane protecting groups offers a robust (70%, five steps from adenosine) route to 2′,5′-adenosine diphosphate precursors and the potential to incorporate a range of functionality at these positions. Pyrophosphate formation requires some further development, but affords benzyl protected precursor **10** that, after transfer hydrogenation, leads to the first total chemical synthesis of **2**. This flexible route to 2′-phosphate furnished dinucleotides will allow the development of new chemical tools that probe biological systems at the molecular level. Analogues of **1** are of immediate importance for dissecting this novel and important second

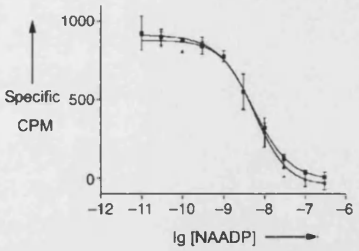

Figure 4. Competitive displacement of [^{32}P]NAADP (0.2 nM) with authentic NAADP (squares) or synthetic NAADP **1** (triangles) from sea-urchin homogenate: Samples diluted in GluIM, then 0.2 nM [^{32}P]NAADP in the presence of increasing NAADP added and incubated at room temperature for 20 mins. Samples filtered through Whatman GF/B filters to separate bound and free [^{32}P]NAADP ligand. Nonspecific binding is defined by incubation of the homogenate in the presence of 10 μM NAADP; $n = 3 \pm$ SEM; data expressed as specific cpm.

messenger pathway. Enzymatic conversion into **1** is confirmed both by identical behavior when evaluated for Ca^{2+}-release properties against sea-urchin-egg homogenate and spectroscopic characterization. Expansion of the route to include suitably protected beta-nicotinic acid mononucleotide (β-NAMN) towards the first total chemical synthesis of **1** and improved isolated yields of pyrophosphate will be reported in due course.

Experimental Section

2: Benzyl NADP **9** (15 mg, 0.018 mmol), 10% Pd/C (15 mg) and cyclohexadiene (100 μL) in a degassed mixture of H_2O:MeOH (3:1, v/v, 2 mL) were stirred at room temperature under an argon atmosphere for 3 h, after which the palladium was filtered and the resulting filtrate subject to ion-exchange chromatography (AG MP-1) by using a 150 mM aqueous TFA gradient. Fractions were combined and lyophilized to yield **2** as a white powder (10 mg, 77%): ^{1}H NMR (400 MHz, D_2O): $\delta = 9.29$ (s, 1H; H_N2), 9.11 (d, $J = 6.3$ Hz, 1H; H_N6), 8.78 (d, $J = 8.2$ Hz, 1H; H_N4), 8.41 (s, 1H; H_A8), 8.23 (s, 1H; H_A2), 8.13 (m, 1H; H_N5), 6.11 (d, $J = 5.9$ Hz, 1H; H_A1'), 6.01 (d, $J = 5.1$ Hz, 1H; H_N1'), 4.96 (m, 1H; H_A2'), 4.49 (m, 1H; H_A3'), 4.44 (br s, 1H; H_N4'), 4.40 (m, 1H; H_N2'), 4.31 (m, 1H; H_N3'), 4.27 (m, 1H; H_A4'), 4.26 (m, 1H; $H_A5'_a$), 4.12 ppm (m, 3H; $H_A5'_b$, H_N5'); ^{31}P NMR (162 MHz, D_2O): $\delta = -0.73$ and -11.42 to -11.84 ppm (br m); MS [FAB+]: *m/z* (%): 744.0 (50) [M^+−H]; found 744.0842 [M^+−H] $C_{21}H_{29}N_7O_{17}P_3$ requires 744.0833.

1: NADP **2** (4 mg 5 mM) and 100 mM nicotinic acid (12 mg) in a 100 mM aqueous AcOH/NaOH (pH 4, 1 mL) were incubated with 5 μL of ADP-ribosyl cyclase at room temperature. After 5 h, HPLC analysis (AG MP-1, aqueous TFA) showed complete consumption of NADP and formation of NAADP ($R_T = 16.8$ mins). The crude mixture was purified on an ion-exchange resin (AG MP-1) by using an aqueous TFA gradient (150 mM), the product eluted at 15% TFA. Combined fractions were evaporated under vacuum at room temperature and lyophilized overnight to afford **1** as a white powder (2.5 mg, 63%): ^{1}H NMR (400 MHz, D_2O): $\delta = 9.32$ (s, 1H; H_N2), 9.17 (d, $J =$ 5.9 Hz, 1H; H_N6), 8.87 (d, $J = 8.1$ Hz, 1H; H_N4), 8.45 (s, 1H; H_A8), 8.28 (s, 1H; H_A2), 8.14 (m, 1H; H_N5), 6.14 (d, $J = 5.5$ Hz, 1H; H_A1'), 6.03 (d, $J = 5.1$ Hz, 1H; H_N1'), 4.97 (m, 1H; H_A2'), 4.50 (m, 1H; H_A3'), 4.44 (br, 1H; H_N4'), 4.41 (m, 1H; H_N2'), 4.30 (m, 1H; H_N3'), 4.27–4.22 (m, 2H; H_A4' and $H_A5'_a$), 4.12–4.10 ppm (m, 3H; $H_A5'_b$, H_N5'); ^{13}C NMR (100 MHz, D_2O): $\delta = 165.4$ (CO_2H), 149.8 (C_A4), 148.3 (C_A6), 147.0 (CH_A2), 144.6 (CH_N6), 142.7 (CH_N4), 142.5(CH_A8) 141.8 (CH_N2), 133.8 (C_N3), 128.6 (CH_N5), 118.4 (C_A5), 99.7 (CH_N1'), 86.8 (CH_A4'), 83.9 (CH_A1'), 77.4 (CH_N2'), 76.8 (CH_A2'), 73.8 (CH_N4'), 70.3 (CH_N3'), 69.9 (CH_A3'), 65.1 and 64.8 ppm ($2 \times CH_2$); ^{31}P NMR (162 MHz, D_2O): $\delta = 1.47$ and -9.40 to -9.80 ppm (br m); MS [FAB+] 744.8 [M^+−H]; found 745.0658 [M^+−H $C_{21}H_{29}N_7O_{17}P_3$ requires 745.0673.

Received: March 19, 2004

Keywords: biological activity · calcium · intracellular signaling · nucleotides · total synthesis

[1] M. J. Berridge, M. D. Bootman, H. L. Roderick, *Nat. Rev. Mol. Cell Biol.* **2003**, *4*, 517–529.
[2] H. C. Lee, *Curr. Biol.* **2003**, *13*, R186-R188.
[3] a) R. Masgrau, G. C. Churchill, A. J. Morgan, S. J. H. Ashcroft, A. Galione, *Curr. Biol.* **2003**, *13*, 247–251; b) G. C. Churchill, J. S. O'Neill, R. Masgrau, S. Patel, J. M. Thomas, A. A. Genazzani, A. Galione, *Curr. Biol.* **2003**, *13*, 125–128.
[4] a) J. Bak, R. A. Billington, G. Timar, A. C. Dutton, A. A. Genazzani, *Curr. Biol.* **2001**, *11*, 987–990; b) M. Hohenegger, J. Suko, R. Gscheidlinger, H. Drobny, A. Zidar, *Biochem. J.* **2002**, *367*, 423–431; c) A. H. Guse, *Cyclic ADP-Ribose NAADP* **2002**, 301–318; d) F. X. Boittin, A. Galione, A. M. Evans, *Circ. Res.* **2002**, *91*, 1168–1175; e) J. M. Cancela, G. C. Churchill, A. Galione, *Nature* **1999**, *398*, 74–76; f) J. D. Johnson, S. Misler, *Proc. Natl. Acad. Sci. USA* **2002**, *99*, 14566–14571; g) K. J. Mitchell, F. A. Lai, G. A. Rutter, *J. Biol. Chem.* **2003**, *278*, 11057–11064.
[5] A. Galione, J. M. Cancela, G. C. Churchill, A. A. Genazzani, C. Lad, J. M. Thomas, H. L. Wilson, D. A. Terrar in *Methods in Calcium Signalling* (Ed.: J. W. J. Putney), CRC, Boca Raton, FL, **2000**, pp. 249–296.
[6] a) D. R. Walt, M. A. Findeis, V. M. Rios-Mercadillo, J. Auge, G. M. Whitesides, *J. Am. Chem. Soc.* **1984**, *106*, 234–239; b) J. Lee, H. Churchil, W. B. Choi, J. E. Lynch, F. E. Roberts, R. P. Volante, P. J. Reider, *Chem. Commun.* **1999**, 729–730.
[7] a) L. J. Haynes, N. A. Hughes, G. W. Kenner, A. Todd, *J. Chem. Soc.* **1957**, 3727–3732; b) N. A. Hughes, G. W. Kenner, A. Todd, *J. Chem. Soc.* **1957**, 3733–3738.
[8] V. C. Bailey, J. K. Sethi, S. M. Fortt, A. Galione, B. V. L. Potter, *Chem. Biol.* **1997**, *4*, 51–61.
[9] H. C. Lee, R. Aarhus, *J. Biol. Chem.* **1997**, *272*, 20378–20383.
[10] G. Berridge, R. Cramer, A. Galione, S. Patel, *Biochem. J.* **2002**, *365*, 295–301.
[11] S. Tanimori, T. Ohta, M. Kirihata, *Bioorg. Med. Chem. Lett.* **2002**, *12*, 1135–1137.
[12] Y. Hayakawa, M. Kataoka, *J. Am. Chem. Soc.* **1998**, *120*, 12395–12401.
[13] X. F. Zhu, H. J. Williams, A. I. Scott, *Tetrahedron Lett.* **2000**, *41*, 9541–9545.
[14] T. Wada, A. Mochizuki, Y. Sato, M. Sekine, *Tetrahedron Lett.* **1998**, *39*, 7123–7126.
[15] M. E. Migaud, R. L. Pederick, V. C. Bailey, B. V. L. Potter, *Biochemistry* **1999**, *38*, 9105–9114.
[16] A.Minta, J. P. Y. Kao, R. Y. Tsien, J. Biol. Chem. 1989, 264, 8171–8178
[17] D. Lampe, C. S. Liu, B. V. L. Potter, *J. Med. Chem.* **1994**, *37*, 907–912.

